1 2 9 0

UNIVERSIDADE Đ
COIMBRA

Tiago de Almeida Pinto da Cunha Leal

SEIZURE PREDICTION WITH SPECIALIZED CLASSIFIERS AND
IMAGE PROCESSING

VOLUME 1

Dissertação no âmbito do Mestrado em Engenharia Informática, especialização em
Sistemas Inteligentes orientada pelo Professor Doutor António Dourado e coorientada
pelo Professor Doutor César Teixeira e apresentada à Faculdade de Ciências e Tecnologia /
Departamento de Engenharia Informática.

Setembro de 2021

Faculdade de Ciências e Tecnologia

Departamento de Engenharia Informática

SEIZURE PREDICTION WITH SPECIALIZED CLASSIFIERS AND IMAGE PROCESSING

Tiago de Almeida Pinto da Cunha Leal

Dissertation in the context of the Master in Informatics Engineering, Specialization in Intelligent Systems advised by Prof. Dr. António Dourado and co-advised by Prof. Dr. César Teixeira and presented to the Faculty of Sciences and Technology / Department of Informatics Engineering.

September 2021

1 2 9 0

UNIVERSIDADE Ð
COIMBRA

Resumo

Em 30% das cerca de 70 milhões de pessoas que sofre de epilepsia, nem cirurgia nem medicação impede a ocorrência de crises epiléticas. Uma solução para melhorar a sua qualidade de vida passa pelo uso de dispositivos transportáveis que as prevejam.

Pretende-se desenvolver um algoritmo de previsão de crises com aprendizagem computacional, usando sinais EEG sem extração tradicional de caraterísticas ajudando na construção desses dispositivos.

A literatura mostrou que, apesar dos resultados promissores de estudos com abordagens semelhantes, nenhum foi capaz de os traduzir num funcionamento em tempo-real em ambiente clínico e, muito menos, em ambulatório. Tal ocorre, em grande medida, pela falta de acesso a um grande conjunto de dados essenciais. Também foi visto que nenhum trabalho utilizou várias CNNs a prever em conjunto, nem processamento de imagem.

Assim, a base de dados EPILEPSIAE foi usada para superar a necessidade de muitos dados contínuos e de longo prazo. Foram desenvolvidos vários algoritmos que usam sinal EEG bruto para treinar CNNs especializadas, e foram testados vários métodos para classificar, criar e processar imagens.

As experiências mostraram que processar a imagem ajudou a melhorar a performance numa arquitetura onde várias AlexNets especializadas foram usadas para prever, numa abordagem de "transfer learning". No entanto, os resultados obtidos de 62% de sensibilidade e 0.25 de FPR/h (False Positive Rate per Hour) estão ainda longe da aplicabilidade clínica e não são melhores do que outros publicados. No entanto, dado que nesses se usam dados substancialmente diferentes, não tem grande significado fazer comparações diretas.

Há ainda muitas variações do algoritmo que se podem testar. Devido à sua complexidade, o valor ideal para algumas variáveis não pode ser ainda encontrado e alguns métodos não puderam ser testados. No entanto, constatou-se que há potencial em prever as crises com métodos de aprendizagem computacional profunda e processamento de imagem.

Palavras-Chave - Previsão de crises epiléticas, aprendizagem computacional profunda, processamento de imagem, multi-classificadores profundos, Sinal EEG bruto

Abstract

For 30% of the 70 million people that suffer from epilepsy, neither surgery nor medication prevent seizures. A promising solution to improve their quality of life is the use of transportable devices that can predict them.

This thesis aims to develop a new seizure prediction algorithm based on deep learning techniques, using the raw EEG signal with no traditional feature extraction, helping in the construction of these devices.

Literature review showed that, even though various studies with similar approaches obtained good results, none could translate them into real-time operation in a clinical environment, much less in an outpatient setting. This happens due to a lack of a sizeable essential data for the predictor. Also, none neither tried several specialized CNNs working together nor applied image processing methods to improve performance.

So, EPILEPSIAE database is be used to overcome the need of a lot of continuous long-term data. Various algorithms using raw signal to train several specialized CNNs were trained along with several methods to classify, create and process images.

Results showed that image processing helped to improve performance on an architecture where several specialized AlexNets were used to predict seizures, in a transfer learning approach. However, the results obtained of 62% sensitivity and 0.25 FPR/h are still far away from clinical use are not better than other published works. However, because of substantially different data used in this work, it is not significant to make a direct comparison.

There are still variations of the algorithm created to be tried. Due to its complexity, the ideal value for most variables could not be found and other methods could not be tested. Nonetheless, there is potential in predicting seizures with deep learning methods and image processing.

Keywords

Agradecimentos

Contents

Acronyms

EEG - Electroencephalograms

ECG - Electrocardiogram

EMG - Electromyogram

ML - Machine Learning

DL - Deep Machine Learning

FPR/h - False-Positive Rate per Hour

SOP - Seizure Occurrence Period

SPH - Seizure Prediction Horizon

ICA - Independent Component Analysis

mDAD - Maximum Histogram Amplitude Distribution Difference

mRMR - Minimum Redundancy - Maximum Relevance

SVM - Support Vector Machines

ANN - Artificial Neural Networks

ANFIS - Adaptive Neuro-Fuzzy Inference System

LSTM - Long-Short Term Memory

Bi-LSTM - Bidirectional Long-Short Term Memory

CNN - Convolutional Neural Networks

CAE - Convolutional Autoencoder

CS - Channel Selection Algorithm

TSST - Time-Series Surrogate Test

LOOCV - Leave-One-Out Cross-Validation

MIDS - Merger of Increasing and Decreasing Sequence

List of Figures

List of Tables

Chapter 1
Introduction

1.1 - Motivation

Around 1% of the world population, about 70 million persons, suffer from epilepsy [3]. Of these, 30% suffer from refractory epilepsy, which means it is resistant to medication that tries to prevent or control epileptic seizures. The fact that these people can undergo an epileptic seizure at anytime and anywhere, with the possibility of causing accidents, injuries, stress, discrimination, or other problems, hampers them from living a comfortable life.

As such, it is important to find solutions that may help to improve the quality of life of those who have refractory epilepsy with methods other than medication or surgery. One of the most promising fields with that aim is epileptic seizure prediction. If one could predict when a seizure was about to happen, the patient would have time to act and position himself in a way that could prevent accidents or injuries. The fact that the patient would know that a seizure would only happen when the alarm is sounded, would substantially improve his quality of life.

1.2 - Contextualization

Since the 1970s, electroencephalograms (EEG) have been used to diagnose and monitor epileptic patients [3]. Over the years, and with the improvement of technology, these have also proven to be useful as the main source of data for seizure prediction methods. Thus, many prediction algorithms based on signals collected from the EEG have been developed, with the objective of creating a seizure predictor embedded in a transportable device, able to correctly predict a future seizure. But it has not yet been possible to find such predictor to work in real-time.

There are several steps usually followed in the building of a seizure prediction algorithm. Signal features extraction and selection, classification, regularization, and validation are the most common steps in works of this kind.

In the last couple of decades, prediction algorithms mainly used non-deep machine learning (ML) methods. Using EEG signal data collected from a group of epileptic patients and stored in a database, a set of features is extracted, and a model is trained to predict seizures.

Recently, there has been an increase in computational capabilities and an evolution in deep machine learning (DL) methods. The combination of these has proven useful in predicting epileptic seizures, especially because there is no need for manual feature engineering (extraction and selection). Therefore, these methods open the possibility to create predictors that work directly on the raw EEG signal and automatically construct a robust set of features to predict seizures.

But not all researchers in this area have access to a great set of complete, continuous, long-term, and quality data about this problem. Because of the great quantity of data needed by DL methods, that fact hampers a better development of this area.

This work had access to the *European Epilepsy Database* [34,37] developed in the EPILEPSIAE project [68]. For conciseness' sake, this database will be called EPILEPSIAE. This is the biggest and most complete database about this problem, composed of more than 45000 hours of recordings of 250 epileptic patients, and more than 2500 registered seizures.

1.3 - Objectives

The main objective of this work is the creation of an algorithm that employs DL to predict epileptic seizures using the raw EEG signal and image processing, with the hope that it can help improve the quality of life of patients suffering from refractory epilepsy. Thus, it is expected that it can contribute with:

- The use of EPILEPSIAE database, a long-term EEG database with a high number of patients

- A new method that uses the raw EEG signal, transformed into images, to train DL models to correctly predict epileptic seizures.

- The proof of the utility of this method by using state of the art validation techniques for different values of pre-ictal period.

1.4 - Structure

The rest of this document is organized as follows:

- Chapter 2 contains an introduction to the basic concepts of epilepsy and seizure prediction.
- Chapter 3 presents the state of the art and is split into two main sub-sections. In the first, an overview of the general state of the art of seizure prediction is shown, which describes the most used methods in the construction of a prediction algorithm. The second refers to works that employ approaches with some similarities with the present work.
- Chapter 4 describes the planned architecture, as well as tools and methodologies employed to realize it.
- Chapter 5 describes the different experiments done throughout the work, as well as the results that come from it.
- Chapter 6 contains an analysis to the results of the experiments, as well as some considerations about what can still be done to further explore this area of seizure prediction and continue this work.
- Chapter 7 presents the conclusions withdrawn from this work.

Chapter 2
Basic Concepts

This section will introduce the basic concepts associated with epilepsy and its prediction.

2.1 - Epilepsy

Epilepsy is a neurologic disease that affects about 1% (70 million) of people in the world. It is characterized by recurrent seizures caused by abnormal and excessive electric discharges in a group of neurons [1,2,5].

A person is considered to have epilepsy when they suffered one or more seizures unrelated to another clear cause, such as a head injury or drug use.

Epilepsy tends to cause other problems besides seizures. Discrimination, loss of productivity, financial impact, or injuries due to seizures that happened in less fortunate moments can all affect a patient's life.

As highlighted previously, in about 70% of epilepsy cases, medication or surgery is enough to prevent and control the seizures [2,4]. However, the remaining 30% need alternative methods, such as predict when a seizure might happen when such is possible.

To predict a seizure, it is first necessary to collect data that can describe any behaviors that the patient's body is having and that may, in some way, be relevant to determine the state of their brain activity.

Since 1970, there has been an interest in using the EEG signal [3] for this purpose. The EEG is used to record electrical activity in the brain; as an epileptic seizure results from an excessive electrical discharge in a group of brain cells [1,5], the EEG has become the major tool for monitoring it. Thus, this is the main tool used for diagnosing epilepsy (along with the patient's behavior, as a negative prognosis from the signal does not eliminate the possibility of epilepsy).

Because of that, EEG signal has also become the basis of seizure predictors research [5], though today, at a much smaller scale, some works also make use of other signals to the

same purpose, such as electrocardiogram (ECG) [21,22,23] or electromyogram (EMC) [22]. Figure 1 shows an example of EEG signal from various channels (electrodes) of the scalp of a patient from the CHB-MIT patient [8].
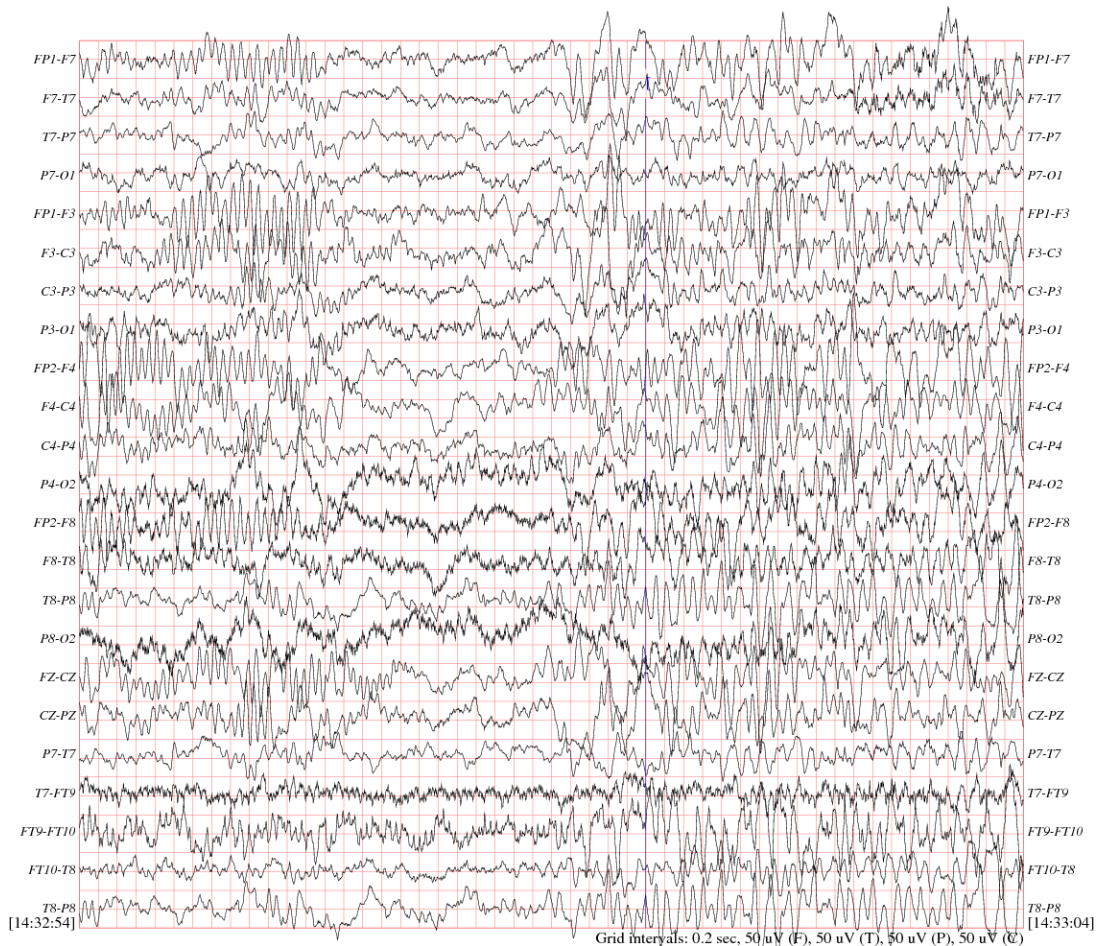
Figure 1 – Example of an EEG signal [8].

2.2 - EEG Signal Acquisition

Normally, EEG signal is acquired from electrodes placed in the scalp in predefined positions, dictated by international positioning systems, such as the 10-20 [6].

The international 10-20 system uses 21 reference points, all within 10 or 20% of the brain's distance from each other. The positions are determined using two reference points, called nasion (located on top of the nose) and inion (located on the base of the skull in the back of the head).

Figure 2 shows the placement of the electrodes according to this system. The nomenclature for each electrode is given according to the region where they are placed. Thus, those placed in the Frontal Polar region start with FP; those on the front start with F; in Temporal begin with T; in Parietal they start with P; in the Central region by C and in the Occipital region by O. Then, the electrodes placed on the line connecting the point nasion to inion end in z, while those placed on the left end in an odd number and on the right in an even number [6].
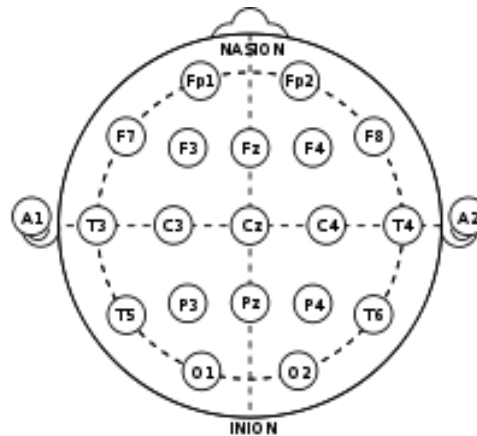
Figure 2 – Placement and nomenclature of electrodes in international 10-20 system [6].

There is also a higher resolution version of this system, in which there are also reference points between the ones in the 10-20 system. This version has been called 10-10 system [85].

There is, however, an invasive version, the Intracranial EEG. It is done by inserting the electrodes directly into the brain's surface or even in deep brain regions, preferably in the epileptogenic zone [7]. Thus, the effect of muscle movements or other events outside brain activity on the signal collected by the electrodes is lessened, increasing the signal-to-noise ratio, and improving quality. However, it should be noted that the patient's body may not react in the best way to this invasive method, and it is necessary to be extra careful when applying it. An example of this type of EEG is shown in Figure 3, where the electrodes are gridded.
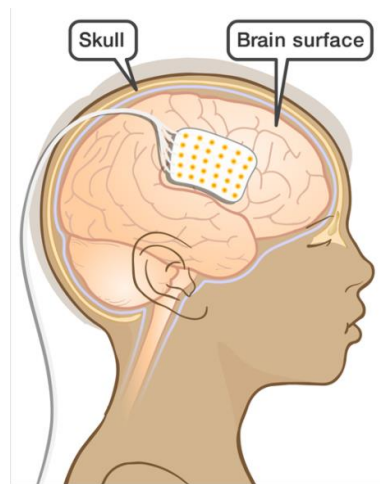
Figure 3 – Example of electrodes placed directly on the brain's surface. [9]

2.3 - Periods of the Epileptic Seizure Cycle in the EEG Signal

In the EEG signal, it is possible to identify various periods through which the patient's brain goes through during the seizure generation cycle. Figure 4 shows an example of these periods, which are usually divided into four types:

- Ictal: the period in the signal that corresponds to the seizure.
- Pre-ictal: the period before the seizure. The seizure prediction methods goal is the detection of this period, as it is in it that the seizure generation processes can be identified. The biggest problem with the detection of this period is that, despite its importance, it is the most difficult to detect. This difficulty comes from the fact that it varies a lot in duration, not only from patient to patient but also from seizure to seizure in the same patient. It is also not annotated by doctors, leading the researchers to try different values for its size to find the one that offers the best results.
- Post-Ictal: the period that follows the ictal period, where the brain is recovering from the seizure.
- Inter-ictal: normal state of the brain, between the end of post-ictal and the beginning of pre-ictal period.
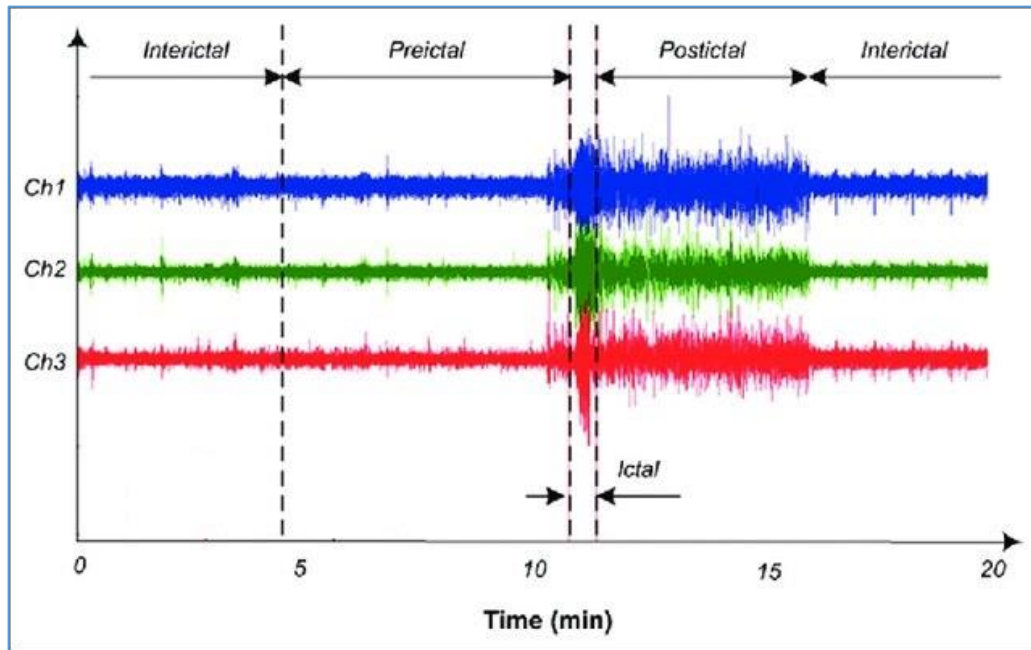
Figure 4 – Several periods of a seizure in various channels of a EEG signal. Adapted from [67].

2.4 - Epileptic Seizure Prediction

The development of seizure predictors goes through, in the first phase, the training of a model based on EEG signals. This model will then collect and classify, in real-time, the same indicators it was trained with so that an alert is given in case a seizure is expected to occur.

Winterhalder et al. [10] proposed in 2003 that the assessment of a predictor was based on two metrics: sensitivity and false-positive rate per hour (FPR/h). He also considered two important concepts for a predictor: the Seizure Prediction Horizon (SPH) and the Seizure Occurrence Period (SOP).

SPH is the period between the moment the alarm is given and the beginning of SOP. It must be enough to allow the patient to prepare for the occurrence of the seizure or to allow any automatic intervention, such as electrical brain stimulation [11].

SOP corresponds to the time interval in which it is expected that the seizure happens. If the patient does not have a seizure in that time interval, the alarm will be false. With the occurrence of the seizure during the SPH period, the alarm is also considered false.

In the approach of Winterhalder et al. [10], illustrated in Figure 5, an alarm is only considered true (C) if the onset of the seizure occurs during the Seizure Occurrence Period. Otherwise, as exemplified in A and B, false predictions occur. The time that the system spends on false alarm (SPH + SOP) must then be considered in the calculation of the FPR/h metric.

Case B can, however, be the subject of debate. If a seizure occurs a few minutes after the alert is given, the effect is not too negative. The important thing is for the patient to have time to react and avoid accidents and possible injuries.
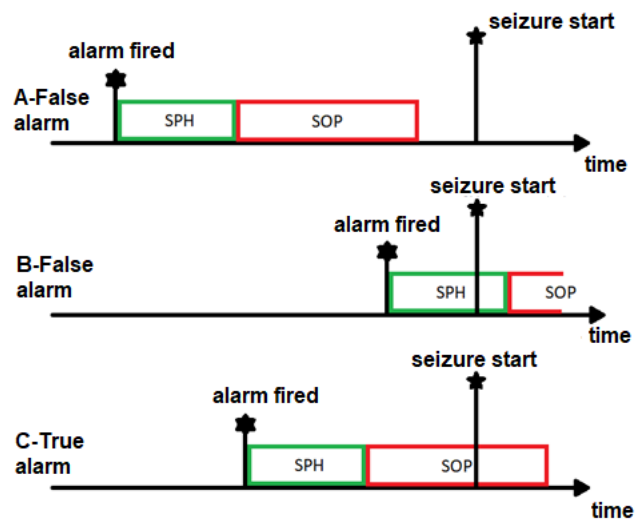
Figure 5 - Conditions for false and true alarms. Adapted from [10].

These parameters are adjusted during the construction of the predictor, as will be explained in the state of art chapter.

Too many false alarms can have more disadvantages than advantages. A patient may, for example, lose confidence in the predictor and ignore it if he sees that many of the past alarms were false. Even if the patient never ignores them, too many false alarms can further impede the patient's life or cause increased stress.

After training and testing the predictor, a performance evaluation must be done. As explained above, this evaluation is done by calculating the sensitivity and the FPR/h (1) of the same. Sensitivity can be calculated using the confusion matrix, but in this problem, equation (2) is the preferred method to evaluate it.

$$FPR/h = \frac{\text{Number of alarms fired} * (1 + \text{time under false alarm})}{\text{inter-ictal period duration}} \quad (1)$$

$$Sensitivity = \frac{\text{N}^\text{o} \text{ of correctly predicted seizures}}{\text{total number of seizures}} \quad (2)$$

Sensitivity is calculated by obtaining the percentage of correctly predicted seizures against the total. A seizure is considered correctly predicted if its onset occurs during a SOP, as described above.

FPR/h is calculated using the number of false alarms originated by the predictor, the time under false alarm, and the inter-ictal duration. The inter-ictal period duration is obtained by removing from the total recording time the periods in which the system was inhibited from generating alarms. This happens when the predictor generates an alarm and automatically inhibits the generation of new alarms for a certain time. Typically, this time is equal to SOP + SPH.

Another important concept about the construction of epileptic seizure predictors is how they are validated. For a predictor to be statistically accepted, it must show better performance than a random predictor, as proposed by Winterhalder et al. [10]. It triggers alarms randomly, without using any information from the EEG signal. It was used, for example, in [15,16].

Another validation method widely used in the construction of epileptic seizure predictors is Surrogate time-series validation. It was used, for example, by [13,14]. In this, the periods of seizures are shuffled to generate new artificial ones. If the proposed predictor has a better performance in the original data than in the new one, it is considered to have a better performance than a random predictor.

2.5 – Prediction Difficulties

The prediction of epileptic seizures is affected by several difficulties caused, namely, by the complexity of the EEG signal.

Epileptic seizures and the periods that precede them vary, not only from patient to patient but also from seizure to seizure. This makes each predictor to be trained specifically for a patient. Even so, it is hard to create a good enough one for constant use without retraining.

Furthermore, there is still the problem of class imbalance. Typically, there are many more inter-ictal samples than in other states. This means that, if the proper precautions are not taken, predictors may not have such good accuracy for less frequent classes. This problem and its solutions will be addressed in the state of art chapter.

There is also a problem created by the fact that the patient's physiology can change over time. This can happen, for example, due to stress or changes in their routine. As a predictor is trained with signals and features of these signals collected from a patient, if there are changes over time in the brain activity of that patient, these may no longer be the most suitable for predicting epileptic seizures in that patient. This problem of Concept Drift can lead, over time, to a predictor losing its initial ability to predict seizures in the patient it was trained for, thus requiring a new training phase.

Chapter 3
State of the Art

Artificial intelligence studies around epileptic seizures focus on detecting and predicting them. The first aims to alert to the present onset of an epileptic seizure, trying to identify the moment it starts [17,18,19]. The latter aims to alert for a future coming seizure, trying, based on various indicators, to identify that the patient is in the pre-ictal period [10,11,12,13].

In the following sections, the steps that make up a predictor of epileptic seizures based on computational learning will be presented. For each step, techniques used successfully, according to its authors, in the construction of a predictor will be presented.

Comparative tables of various works developed over the years intending to predict epileptic seizures will also be presented. They aim to show which types of algorithms were used for each step, giving an idea of the great diversity of prediction models found in the literature.

Some studies that used the raw EEG signal without any feature extraction as a base to deep learning (DL) models will also be presented.

3.1 - Basic Predictor Architecture

A ML based seizure predictor is usually built through the following steps:

1. Signal Acquisition
2. Signal preprocessing
3. Signal Feature Extraction
4. Signal Feature Selection
5. Classification
6. Regularization
7. Performance Evaluation

With steps 1 to 3 being for data preparation, 4 and 5 dedicated to model development including training and 6 post-processing, as can be seen in Figure 6.

Each step will be described in detail, as well as some techniques used in each of them and works that focused on them.
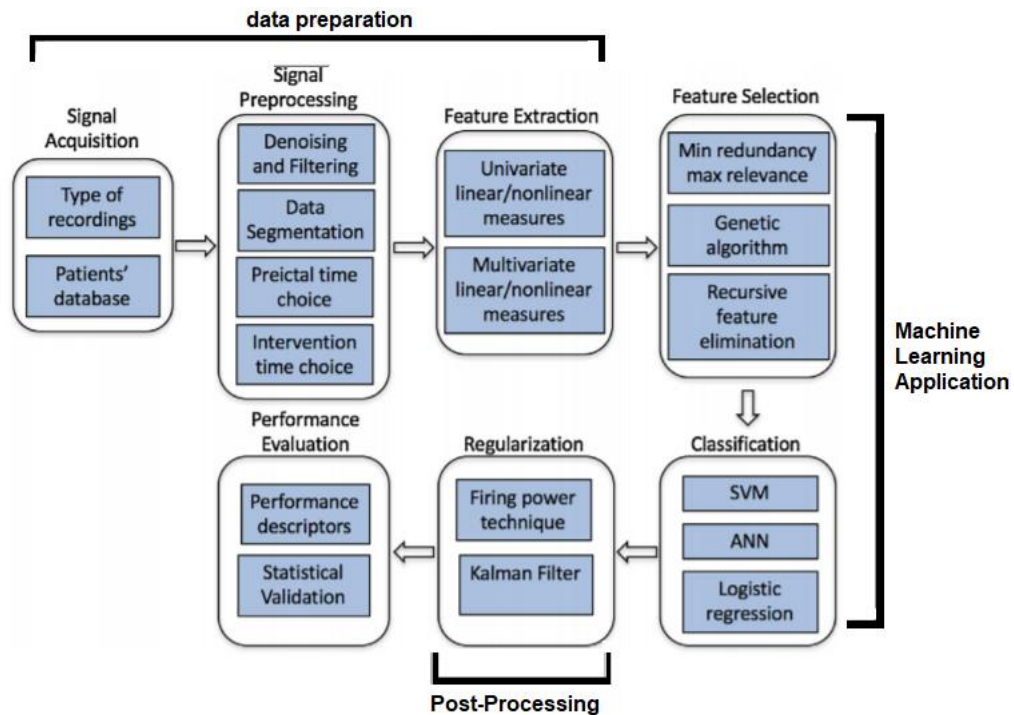
Figure 6 - Steps of a ML based seizure predictor. Adapted from [12].

3.1.1 - Signal Acquisition

The most commonly used signals as input for ML approaches in predicting seizures are EEG signals [14,15,16], but some approaches use EMG signals [20] and others ECG signals [21,22,23].

As previously stated, even within the EEG signals there are two types: intracranial [13,14,24,25,26] – where the signals are collected with electrodes placed directly on the brain's surface or even in-depth – and Scalp EEG [13,27,28,29] – where the electrodes are placed in the scalp of the patient. Usually, intracranial signals are more effective due to the direct contact with the brain, which reduces the disturbances normally caused by noise and other artifacts. However, because electrodes are placed on the brain's surface, this method is invasive and more likely to cause side effects.

These data have been collected and stored in databases [8,30,31,32,33,34,35,37]. The quality of the data has a great influence on the performance of a predictor, as the greater the number of epileptic seizures recorded, the total recording time, and the number of patients, the more data one will have to train a predictor.

Table 1 presents information from some of these databases, as well as their characteristics. As can be seen in Table 1, the EPILEPSIAE database [34,37] is the largest. It contains not only a large amount of long-term EEG and ECG records from many patients but also a vast number of seizures. It was created through the collaboration of several hospitals: the Epilepsy Center of the Medical Center of the University of Freiburg (Germany), Centro Hospitalar e Universitário de Coimbra (Portugal), and University Hospital Pitié Salpêtrière (France).

Table 1 – Summary of some epilepsy databases.

Database	Number of Patients	Register Type	Recorded Seizures	Recording Hours	Frequency (Hz)
MSSM [30]	28	Scalp	61	48-192	256
CHB-MIT [8]	24	Scalp	198	1-4	256
Flint Hills [31]	10	Intracranial	49	1400	239.74
Bonn [32]	5	Scalp/ Intracranial	5	35	173
Freiburg [33]	21	Intracranial	88	509	256
EPILEPSIAE [34, 37]	275	Scalp/ Intracranial	2400	More than 45000	250-2500

3.1.2 - Signal Pre-processing

With the signal collected and ready to use, a series of steps are sometimes carried out to improve its quality and prepare it for the next phases.

Typically, this step consists of splitting the signal into time windows, removing artifacts (perturbations in the signal caused by extra-cerebral effects – like muscle movement), and increasing the signal-to-noise ratio.

The signal must be segmented into small windows to extract the characteristics of the signal. The length of this varies between studies. Looking at Table II, the most common length has been the 5-second window, but various values have been used. The choice of this size must take into account the number of electrodes, the sampling frequency, and the duration of the recordings so that we can have time windows that can capture changes in the signal without taking too much time or computational power.

Additionally, several EEG analysis methodologies assume that the signal is stationary. This window size should at a certain level ensure this aspect.

Denoising, filtering, and artifact removal are used to remove interference and artifacts from the signal. First, a bandpass filter (which attenuates frequencies outside a determined band) is applied. Then another filter, a notch filter, is used to remove interference from the electric power network (which, for example, in Europe is 50 Hz).

In this step, the various pre-ictal periods, SOP, and SPH to be considered are chosen. To get a better idea of the performance of the created method, several SOP, SPH, and pre-ictal time values should be tested, as will be discussed in the performance evaluation section.

Another useful method for signal pre-processing is the Independent Component Analysis (ICA) [51, 52]. The signal is assumed to be a linear combination of several independent signals and so, it is decomposed into several independent components. The signal can then be rebuilt without the independent components that represent noise or artifacts, forming another signal with higher quality.

Table 2 - Summary of some studies, with the databases and pre-processing methods used.

Work	Database	Sliding Window (seconds)	*Denoising* and *Filtering*	Artifact Removal	Pre-ictal Size (minutes)	SPH Time
D'Alessandro et al. [38]	Private	0.25, 5, 10 and 60, no overlap	60 Hz Notch Filter. 0.1 – 100 Hz Bandpass Filter.	-	10	10 minutes
Mormann et al. [13]	Bonn	17 a 20.5, no overlap	0.5 – 85 Hz Bandpass Filter.	-	5, 30, 120 e 240	10 minutes
Schelter et al. [39]	Freiburg	Yes, but does not say size nor overlap	50 Hz Notch Filter. 0.5 - 120 Hz Bandpass Filter.	-	50	2 to 40 minutes
Mirowski et al. [14]	Freiburg	5, no overlap	60 Hz Notch Filter. 0.5 – 120 Hz Bandpass Filter.	-	50	-
Park et al. [40]	Freiburg	10, 50% overlap	50 Hz e 100 Hz Notch Filter.	Yes	30	-
Teixeira et al. [27]	EPILEPSIAE	5, no overlap	50 Hz Notch Filter.	-	10, 20, 30 and 40	-
Valderrama et al. [41]	EPILEPSIAE	5, no overlap	-	-	5, 10, 20, 30, 45 and 60	-
Moghim et al. [42]	Freiburg	5 and 9, no overlap	-	Yes	5	0, 1, 8 and 14 minutes

Bou Assi et al. [25]	iEEG Kaggle [37]	5, no overlap	50 Hz Notch Filter. 0.5 – 180 Hz Bandpass Filter;	-	60	5 minutes
Bandarabadi et al. [16]	EPILEPSIAE	8, 50% de overlap	-	Sim	10, 30, 50 e 70	-
Direito et al. [43]	EPILEPSIAE	5, no overlap	50 Hz Notch Filters;	-	10, 20, 30 e 40	10 seconds

3.1.3 - Signal Feature Extraction

Once divided into windows, and with its quality improved, it is necessary to extract characteristics of the signal that can describe its behavior in that temporal window.

Several characteristics can be extracted from the signal, with this step being the one in which works on prediction (and even seizure detection) vary the most.

The different approaches start with some considering characteristics based only on one electrode, while others consider characteristics dependent on several ones. The first ones are called univariate features and the latter multivariate. The multivariate measurements try, from the extraction of features involving several electrodes, to capture more complex processes in the brain and complement the univariate measurements. So, features of both types can be used at the same time.

In addition to the classification into univariate and multivariate, there is also classification into linear and non-linear features.

Mormann et al. [13] presented a study comparing 30 multivariate and univariate features. They concluded that the multivariate ones have greater statistical significance, managing to reveal preictal changes 240 minutes before the seizure. Univariate measures could only do it 30 minutes in advance.

Furthermore, they concluded that the linear features performed so well, or even better, compared to the non-linear ones. In another work, McSharry et al. [44] concluded that non-linear measurements should only be used if they have better performance than linear ones.

A useful tool developed for the extraction and computation of the most used features in seizure prediction is EPILAB [45], a public application in MATLAB environment [46].

Linear Univariate Measures

Mathematical techniques that use the signal's amplitude and phase/frequency information and that obey the linearity property. The most used include:

- Statistical moments [13, 27, 28, 29, 41, 42, 43] – statistical measurements such as variance, skewness, and kurtosis. For example, Aarabi et al. [47] noticed greater kurtosis and lesser variance during the preictal state.

- Accumulated Energy [27, 29, 41, 42] – The seizure generation process leads to an intensification of brain activity. The accumulation of that energy can thus be used as a metric to help predict a crisis.

- Spectral Band Power [13, 25, 40] – The division of the EEG signal into different frequency bands - Delta, Theta, Alpha, Beta, and Gamma - has also been used in several works. For example, Mormann et al. [13] detected a transfer of power from the lower to the higher ranges during the pre-ictal period. Compared to other bands, frequencies in the Gamma band have shown better ability to predict seizures [40].

- Decorrelation Time [13, 25, 27, 28, 29, 41] – tries to find repeating patterns that may be overshadowed by noise. It also tries to identify the fundamental frequency behind the harmonic frequencies. If brain activity changes with the seizure generation process, it can be detected through changes in this metric. Teixeira et al. [28] and Mormann et al. [13] concluded that this metric decreases before the epileptic seizure starts.

- Energy of Wavelet Coefficients [13, 28, 43] – through the discrete wavelet transform, the signal is decomposed into subbands. For each, there is a coefficient whose amplitude represents the relative importance of a given subband. The amplitude of each subband is quantified by its energy. These types of characteristics tend to be equivalent to Spectral Band Powers.

- Hjörth parameters [13, 28, 29, 41] – are three time-domain activity measures – the activity, mobility, and complexity of Hjörth. The Hjörth activity corresponds to the signal variation, while the Hjörth mobility corresponds to the square root of the variance of the derivative of the signal over the variance of the same. Hjörth complexity corresponds to the Hjörth mobility of the derivative of the signal, over the Hjörth mobility of the same. In the study that compared 30 characteristics,

Mormann et al. [13] noticed that Hjörth complexity and Hjörth mobility were the best univariate measures.

- AR Coefficients [28, 41] – modeling of the EEG signal according to autoregressive models. The parameters of the autoregressive models translate the frequency information and are, therefore, useful for seizure prediction.

Non-linear Univariate Measures

These measures are based on the fact that the brain goes through various dynamic states. As such, and as the EEG signal is quite noisy, measures derived from Dynamical Systems Theory have been proposed to help better explain these brain dynamics. They are usually more computationally demanding. In the study by Mormann et al. [13], it is concluded that they are not able to perform significantly better than chance. Some of the proposed measures of this type are:

- Correlation Dimension/Sum [13, 42, 48] – the correlation dimension is a measure of the dimensionality of the space occupied by a set of random points. The correlation sum is the measure that reflects the mean probability that the states at two different times are close. It is used to estimate the correlation dimension. Mormann et al. [13] observed an increase in the correlation dimension before the onset of the seizure, while Lehnertz & Elger [48] report a decrease 5 to 25 minutes earlier.

- Lyapunov Exponent [13, 42, 49] – quantifies the speed at which two points starting close in phasic space move apart. Iasemidis et al. [49] noted a significant reduction in this indicator during the pre-ictal period.

- Dynamic Similarity Index [13, 50] – measures the similarity between segments of the EEG signal, taking a reference segment of the inter-ictal state and a movable window over the signal. Thus, it quantifies the dynamics' difference between the reference and other windows, hoping that it will change in the pre-ictal period.

- Entropy [26, 27, 38] – measures the regularity and unpredictability of fluctuations on EEG signal data. Because a seizure is characterized by brain synchronization, entropy has served to detect changes from the inter-ictal to the pre-ictal period. Various types of entropy have been used.

Linear Multivariate Measures

Measures whose main objective is to capture how interactions between several brain regions modulate epileptic seizure activity.

As the pre-ictal period is complex, and epileptic seizures are electrical discharges due to a group of neurons that start firing abnormally, excessively, and synchronously, multivariate measures can capture and quantify these behaviors.

A popular measure of this kind is the Maximum Cross-Correlation [13, 14, 28]. It measures the linear synchronization between two electrodes to quantify the similarity. In the study comparing several measures, Mormann et al. [13] saw that this is one of the most discriminating.

Non-linear Multivariate Measures

Measures based on the similarity and mutual information between channels, which characterize the synchrony between them. Within this category, measures such as:

- Dynamical Entrainment [14, 53] – version of Lyapunov's exponent for multi-channels. In the work where it is proposed, Iasemidis et al. [53] also noted that it demonstrates good predictive power with a relatively low FPR/h.

- Mean Phase Coherence [13, 15, 16] – measure whose objective is to quantify the phase synchronization between two channels. It is one of the most used measurements. Mormann et al. [13] noted that it exposes a drop in synchronization during the preictal state.

3.1.4 - Signal Feature Selection/Reduction

Feature Selection is done to reduce the total number of those that will feed the classifier. If a vast number of features are extracted from the signal, a high dimensional space is created, leading to the so-called curse of dimensionality.

So, in summary, this step serves to select the most discriminating ones while removing those that are redundant or worsen the classifier performance. It also helps reduce the computational cost, improve classification, and avoid overfitting.

Several techniques have been applied to carry out this reduction, including:

* RelieF [21, 42], Minimum Normalized Percentile Difference [54], Maximum Histogram Amplitude Distribution Difference (mDAD) [16, 54], and Minimum Redundancy - Maximum Relevance (mRMR) [25, 54, 55] all have the same principle of maximizing relevance and minimizing similarity so that a diverse and relevant set of signal features are selected.

* Genetic algorithms [25, 29] have also been employed. These are based on the principles of natural selection to select a more robust set of features adapted to the environment.

* Principal Component Analysis (PCA) [14, 56, 57] has also been used, as it can transform sizeable dimensional data into a smaller orthogonal dimensional subspace. So, it is used to reduce the number of features rather than selecting them.

Direito et al. [29] compared several methods (mRMR, genetic algorithms, and recursive feature elimination) and concluded that dimensionality reduction improves performance. However, they also noticed that the best technique varies from patient to patient, with mRMR and genetic algorithms being the best performers.

Both the signal feature extraction and selection are automatically done by DL methods. This makes so that there isn't a need to manually apply these to steps.

3.1.5 - Classification

For short, one can sau that there are two types of main approaches to prediction: one based on thresholds [13, 58] (if a certain threshold is passed, the warning is given that a seizure might happen) and another based on ML techniques. Even within each of these types of approaches, there is a wide variety of methods used by different works.

As this work is focused on ML, the emphasis of this state of art research is given to classifiers of this type. Within this type, the Support Vector Machines (SVM) [25, 28, 43, 54] have proven to have better performance than the other classifiers in terms of sensitivity and specificity, but Artificial Neural Networks (ANN) [27, 28] also stand out. There are also other methods such as the Adaptive Neuro-Fuzzy Inference System (ANFIS) [27] and DL methods [14, 59, 60, 65].

SVMs can transform a non-linear feature space into a higher-order problem to make the data more linearly separable. The fact that they can produce linear boundaries makes them more easily interpretable.

ANNs are known as universal approximants because of their ability to approximate any continuous function if a sufficient number of neurons and layers are used. However, they can be too sensitive to training data and can fail if trained with less adequate signal characteristics.

Teixeira et al. [28] compared the performance of 3 types of classifiers: SVM, ANN with a Multilayer Perceptron (MLP) structure, and another ANN with a Radial Basis Function (RBF) structure. They concluded that SVM had better performance in terms of FPR/h. As for the two ANNs, the MLP structure showed the best result concerning FPR/h, but with no significant difference in sensitivity.

With the increase in the amount of data and computational power, several DL models, based on ANNs, have been applied in this issue. Neural Networks with memory (especially the Long-Short Term Memory - LSTM) and Convolutional Neural Networks (CNN) are two deep computational learning models widely adopted to predict epileptic seizures [59, 60, 65].

CNNs were originally built for image classification, but have been successfully applied to time series. They will be addressed in more detail in chapter 3, as it will be the classifier used in this work.

To use DL methods, it is necessary to change the way you look at the normal architecture of a predictor. While the phases of signal acquisition, pre-processing, regularization, and performance evaluation may not change, the phases of feature extraction and selection can be included in the used classifier. This eliminates the need to perform these phases manually before giving data to the classifier. These methods can handle raw data well and are able to train feature selection mechanisms capable of improving classification. However, it is also possible to use these deep methods with the normally applied feature extraction and selection algorithms.

A major difficulty with seizure prediction classification is that there are many more interictal instances than in other periods. This class imbalance problem is usually addressed by ignoring some instances of periods with the greatest amount of data or by adapting classifiers, attributing different costs to different classes. Park et al. [40], for

example, used an SVM with two costs, with a heavier penalization of wrong classifications of the pre-ictal instances.

Table 3 shows the used/studied classifiers on some works, as well as some of the features on which they were applied. It can be seen that the use of many features is, in most cases, in conjunction with others.

Table 3 - Summary of some works, with features and classifiers used.

Work	Database	Some used features	Classifier/s Used
D'Alessandro et al. [38]	Private	Spectral Band	Probabilistic Neural Network
		Wavelet Coefficients	
		Linear Modelling	
		Entropy	
Mormann et al. [13]	Freiburg	Statistical Moments	Threshold based
		Wavelet Coefficients	
		Hjörth Parameters	
		Lyapunov Exponent	
		DSI	
		MPC	
		Entropy	
Mirowski et al. [14]	Freiburg	Cross-Correlation	CNN, SVM and Logistic Regression.
		Wavelet Coefficients	
		Dynamical Entrainment	
		Other non-linear multivariate features	
Direito et al. [29]	EPILEPSIAE	Statistical Moments	SVM
		Spectral Band	
		Wavelet Coefficients	
		Linear Modelling	
		Accumulated Energy	
		Hjörth Parameters	
		Decorrelation time	
Moghim et al. [42]	Freiburg	Statistical Moments	SVM
		Spectral Band	
		Wavelet Coefficients	
		Accumulated Energy	
		Correlation sum/dimension	
		Lyapunov Exponent	

3.1.6 - Regularization

After classification, it is convenient to regularize the output of the classifiers to mitigate the number of false alarms. The goal is to improve specificity and attenuate the FPR/h that, if too high, can harm the patient's life.

Regularization is usually done with the Firing Power technique [16, 27, 28, 29, 45] or using the Kalman filter [40, 61].

The Firing Power technique quantifies the number of instances classified as pre-ictal during a time window of the same size as the SOP + SPH period. If that number exceeds a threshold, the seizure alarm is raised. As the time window is equal to SOP + SPH duration, only one crisis alarm can be triggered. The threshold that must be exceeded to raise the alert is a value that can be adjusted. Teixeira et al. [27] compared several threshold values and showed that, in general, lower FPR/h were achieved with lower threshold values, but no optimal value was found.

The Kalman Filter is an approach that was first used by Chisci et al. [61], to smooth the output of an SVM classifier.

Teixeira et al. [27] compared both regularization measures and concluded that the firing power method is more conservative in issuing alerts. They also saw that the Kalman filter, despite producing better sensitivities, raised too many false alarms in many patients.

3.1.7 - Performance Evaluation

For a seizure predictor to be evaluated, it is necessary to use metrics such as sensitivity and FPR/h for various SOP, SPH, and pre-ictal time values [10]. However, not all works report FPR/h. It is also necessary that these values are obtained in tests on data that the classifier did not have access to during its training or optimization.

In addition, for a study to be validated, it is necessary to carry out at least one of the following:

- Test against a random predictor [10, 62, 42].
- Time-Series Surrogate Test (TSST) [13, 14, 42].
- Classical Statistical Tests [28].

Table 4 shows several works developed over the years and some classification, regularization, and performance evaluation methods used in them. The SVM classifier is the most utilized and, recently, DL methods have also been used. It is also a visible fact that not all authors use regularization or validation methods, making the comparison between all works harder.

Although several authors claim good results for their classifiers, some even very good, the truth is that they are not replicable in real-time data. Thus, there is not yet (nor are we close to) a patient-carryable device capable of predicting seizures in a clinically acceptable way. There is still a long way to go, and this dissertation aims to help take a small step forward in that direction.

Table 4 - Some works and the database, classifiers, regularization, performance, and validation used in them.

Work	Database	Used Classifier/s	Regularization	Sensitivity	FPR/h	Validation Technique
D'Alessandro et al. [38]	Private	Probabilistic Neural Network	-	62.5%	0.28	-
Mirowski et al. [14]	Freiburg	CNN	-	71%	0	Yes
		Logistic Regression		52%	0	
		SVM		38%	-	
Park et al. [40]	Freiburg	SVM	*Kalman Filter*	97.5%	0.27	-
Direito et al. [29]	EPILEPSIAE	SVM	-	89.5%	-	-
Acharya et al. [26]	Freiburg	SVM	-	97.2 %	-	-
		Decision Tree		98.3%		
		Gaussian Mixture Model		98.3%		
		Probabilistic Neural Network		97.8%		
		Fuzzy Sugeno Classifier		99.4%		
		K-Nearest Neighbours		97.8%		
		Naive Bayes Classifier		94.4%		
Teixeira et al. [27]	EPILEPSIAE	SVM	*Kalman Filter Firing Power*	73.7%	0.19	Statistical Test
		RBF		69.1%	0.42	
		MLP		71.2%	0.29	
Valderrama et al. [41]	EPILEPSIAE	SVM	-	94.5%	-	TSST
Moghim et al. [42]	Freiburg	SVM	-	91%	-	Random Predictor
Bou Assi et al. [25]	iEEG Kaggle	SVM	-	85.5%	-	-
		ANFIS		75.8%		
Khan et al. [59]	MSSM e CHB-MIT	CNN	-	87.8%	0.14	Random Predictor
Daoud et al. [64]	CHB-MIT	Bi-LSTM	-	99.72%	0.004	Statistical Test
Abdelhameed et al. [60]	Bonn	LSTM	-	93.3%	-	-
		Bi-LSTM		99%		

3.2 - Works Using DL Methods on the Raw EEG Signal

This dissertation aims to use the raw EEG data as inputs to the CNN classifiers, without previous feature extraction.

There is, however, a scarcity of works that study epileptic seizure prediction with approaches of this type. This is mainly because DL methods require large amounts of data to train. Most of the databases currently available have non-continuous and short-term EEG recordings, making it difficult to properly apply this approach. Furthermore, this approach is based on using the raw EEG signal, which is quite complex and, especially if collected from the scalp, susceptible to noise and artifacts.

Works that use deep learning methods to classify have already been referred here [14, 59, 60]. However, all of these used some other pre-processing method (either deep or manual) to extract characteristics from the signal and feed the deep learning algorithm. This section presents the known works that have directly fed the raw EEG signal to some DL algorithm.

Zhou et al. [63] compared performances in the detection and prediction of epileptic seizures using CNNs fed with raw EEG signals, without manual feature extraction. They also compared the performances of time and frequency domain signals in the prediction. The first used the raw EEG signal, and the latter was obtained from the transformation of the time signal with the Fourier Transform (which is already feature extraction).

CNNs were developed, using data from two different databases (Freiburg and CHB-MIT), and concluded that frequency-domain signals performed better than time-domain signals, as shown in Table 5.

It should be noted, however, that validation was not carried out and FPR/h was not reported. Only the sensitivity and specificity of the various tests were.

The authors also recognized that the study was limited by the lack of access to a large quantity of data, needed to properly implement DL methods.

Table 5 – Results of the study carried out by Zhou et al.

Database	Time-domain		Frequency-domain	
	Sensitivity	Specificity	Sensitivity	Specificity
Freiburg [33]	0.91	0.91	0.97	0.97
CHB-MIT [8]	0.62	0.57	0.94	0.97

As can be seen from Table 5, there is a large discrepancy between the results obtained by Zhou et al. [63] in the time domain (in which the images given to CNN were the EEG signal itself) from one database to another. The authors note that a potential explanation for this is because the Freiburg database (which had better results) is composed of intracranial records, while those in the CHB-MIT database have data collected from the scalp.

Daoud et al. [64] also dispensed pre-processing, giving the raw EEG signal collected from the scalp of 8 patients from the CHB-MIT database directly to 5 deep learning models. These models were:

- MLP

- CNN + MLP

- CNN + Bidirectional LSTM (Bi-LSTM)

- Convolutional Autoencoder (CAE) + Bi-LSTM

- CAE + Bi-LSTM + Channel Selection Algorithm (CS)

The models were tested using the exhaustive Leave-One-Out Cross-Validation (LOOCV) method, and class balancing was applied, considering the same number of instances for each class in the training.

For statistical validation, a non-parametric Kruskal-Wallis statistical test was performed. The results for each model can be found in Table 6. The CS was implemented for the system to be suitable for real-time use, reducing training time and computational cost.

Table 6 – Results of the methods implemented by Daoud et al.

Model	Sensitivity	FPR/h	Training Time (minutes)
MLP	84.67%	0.174	7.3
CNN + MLP	95.41%	0.072	12.5
CNN + Bi-LSTM	99.72%	0.004	14.2
CAE + Bi-LSTM	99.72%	0.004	4.25
CAE + Bi-LSTM + CS	99.72%	0.004	2.2

Wei et al. [65] also used the raw EEG signals to train a CNN and evaluate its performance, applying Merger of Increasing and Decreasing Sequence (MIDS) to improve it. They achieved a sensitivity of only 74% and specificity of 92.46% for some patients in the CHB-MIT database, but they did not present FPR/h.

More recently, Catalina et al. [67] transformed the raw EEG signal into images to train and test a CNN to detect epileptic seizures. They achieved an average of 99.3% accuracy and 58.3% sensitivity for their best model, in patients from the CHB-MIT database. In patients of the EPILEPSIAE database, they reached a high accuracy of 99.6%, but the other metrics showed low values, with an average of around 25%. They explain that this disparity is due to the imbalance in the amount of data in each class. By incorporating intracranial electrodes along with those on the scalp, they concluded that both types of recording complement each other and can provide better detection when used in this way.

3.3 - Summary

Even though there is already a great variety of studies in several areas of seizure prediction, the usage of DL methods with the raw EEG signal is still in its early days.

There is a clear lack of studies that focus on predicting (and even detecting) epileptic seizures directly from the raw EEG signal; those that do, admit that they had a limitation in the amount of data they had access to train and test the algorithm. This limitation means that, when applied to real data, with many hours or even days of continuous EEG recording, it has not been possible to reproduce the published performances so far.

The availability of the EPILEPSIAE database now creates an opportunity for more realistic studies using this approach.

Also, the fact that the raw EEG signal is being transformed into an image before being processed by the DL algorithm, opens the doors to experiments applying image processing methods. This is something not yet tried in DL based seizure prediction, but that could be useful to improve classifying performance.

There aren't any works that also try to improve the classifiers' performance by making several specialized ones working together.

As such, this work tries to explore these techniques that were successful in other areas [89, 90], and test if they can help seizure prediction to make a step forward in its objective of building a carriable device that can predict in real-time.

Chapter 4
Methodology

This works aims to use the raw EEG signal as the main source of data to train and test a DL model. This should be able of predicting epileptic seizures in real-time, without manually extracting any features. The DL model itself won't be as simple as it was in other works, as it will consist of a set of specialized CNNs working together to predict. Furthermore, the images formed from the signal that will be used to train and test the models will be processed using image processing methods, something not done before in this area.

To achieve such an objective, several techniques and programs will be used as a base to develop it.

MATLAB was used as an environment to develop scripts to process everything in training and testing. Extensions like the Deep Learning Toolbox [69], Signal Processing Toolbox [70], and Image Processing Toolbox [71] were very useful since the most popular methods for those tasks can be found there.

So, in this chapter, the techniques used throughout the work and the used architecture will be explained and described. It is divided into four sections. In the first, the database and patients used as a base for these experiments will be presented. Then, in the second, the modified architecture will be shown, separated in training and testing. After that, the techniques used in training will be explained, followed by the last section where the same will be done for the techniques used in the testing of the constructed predictor.

4.1 - Signal

As it was said before, the database is very important in the construction of a seizure predictor. It is important that the data is complete and has recordings over a long and continuous period.

In this thesis, recordings from patients from the EPILEPSIAE database will be used as a base to train and test the prediction algorithm.

The EPILEPSIAE database is the most complete seizure-oriented database, containing more than 45000 hours of continuous EEG recordings from more than 250 patients, and more than 2400 recorded seizures.

In total, recordings from 6 patients were used for these experiments. Ideally, more patients would be used, but the complexity of the created algorithms made it hard to apply them over more patients inside the temporal window of delivery for this work.

All the recordings had a sampling frequency of 1024 Hz, so that images can have a good horizontal definition, while still capturing small windows of time. Additionally, all the patients have at least 10 recorded seizures. In this way, there are always at least 3 seizures for testing.

To prepare the signals to be used in training and testing, they were firstly divided into two portions – the training signal and the testing signal. The division was made using 70% of the total recorded seizures for training, and the remaining 30% for testing.

Any 30% of recorded seizures can be used in testing. It doesn't matter if they are the first, middle or last recorded seizures. What is important is that the continuous set used for testing has at least 3 seizures and a considerable amount of interictal period, to assess the FPR/h.

The separation is always done in the middle point between the end of a post ictal period of a seizure, and the beginning of the pre-ictal of the next seizure. As the pre-ictal duration is not clinically annotated, it is needed to test a prediction algorithm for different preictal sizes.

So, if there are 10 recorded seizures for a certain patient, 7 would be used to train, and 3 to test. Ideally, the testing would be a continuous set, so that the interictal period in between the testing seizures will also be part of the testing set. In Figure 7, an example of that separation can be seen. Interictal instances are represented in blue, while preictal are in green. Postictal instances are in yellow, and red represents ictal periods. In this case, there are a total of 5 seizures (thus, this recording was not used for the experiments, it is merely used as an illustrative example). Because 70% of 5 seizures is 3 rounded down, 3 seizures are being used to train, and 2 (approximately 30% of 5,

rounded up) for testing. The division is made in the middle interictal point between the 2nd and the 3rd recorded seizures.
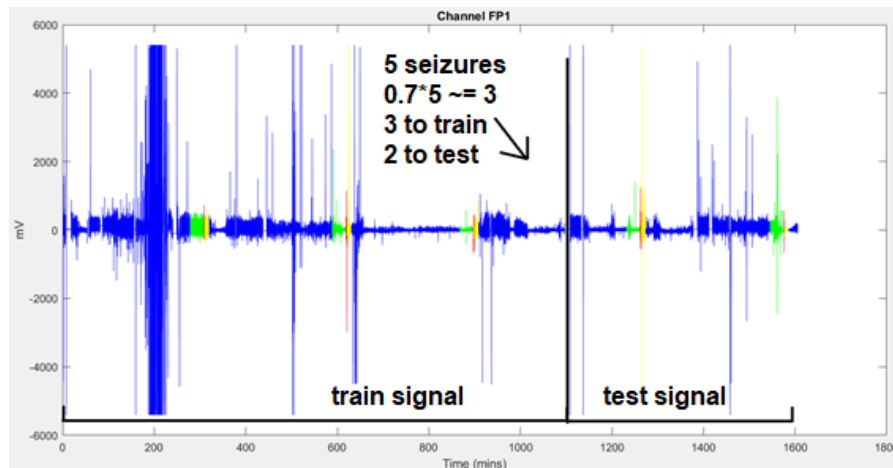
Figure 7 - Division of the signal recorded by FP1 electrode of a patient from EPILEPSIAE database.

4.2 - Training and Testing Architectures

The architecture used as a basis for the algorithms created in this work, is based on most of the steps shown in the state of art. However, as there will be no manual extraction of signal features, the extraction and selection of signal features steps are not used - they are done automatically by the CNNs.

Because this work will focus on the cooperation of several specialized CNNs, there is also a need to add an extra step to the normal testing architecture. Each specialized CNN will produce an output, indicating if the given image is or is not from the class they are specialized in. As such, a mechanism that considers the outputs from all CNNs and decides on one state for the current condition of the patient is needed.

Furthermore, after the division of the signal in images, there will be an extra step where processing can be applied to them.

In the following subsections, both the training and testing architectures will be explained.

It is important to note that, due to the nature of epileptic seizures, each may vary from patient to patient. So, when it comes to apply these training and testing architectures, it needs to be done for each patient individually.

4.2.1 - Training Architecture

The high-level architecture planned for the training can be seen in Figure 8. In this subsection, only the general steps will be explained. A deeper explanation of the techniques used in each step can be found in section 4.3.
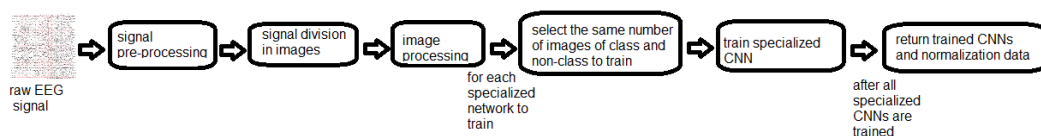
Figure 8 - High-level architectures planned for training each prediction algorithm.

First, some signal processing operations are applied to the signal, to improve its quality and reduce the effects of noise and artifacts. Normalization is also applied after that, so that all channels can be in the same range of 0 to 1.

Then, the signal is segmented. This window size of the segmentation depends on the used classifier. The segmentation creates images, and to those images, some processing may be applied to them, again, aiming to improve their quality.

With the images created and ready, to circumvent the problem of class imbalance, the same number of images are selected for each specialized CNN.

The selected images are then used to train each CNN that, when fully trained, will be returned. The normalization data obtained from the training signal will also be returned. Both the trained networks and the normalization data will be used in the testing phase of the predictor.

4.2.2 - Testing Architecture

The high-level architecture planned for the testing can be seen in Figure 9. Again, deeper explanation of the techniques used in each step are given in section 4.4, as this subsection only serves to present the testing high-level architecture.
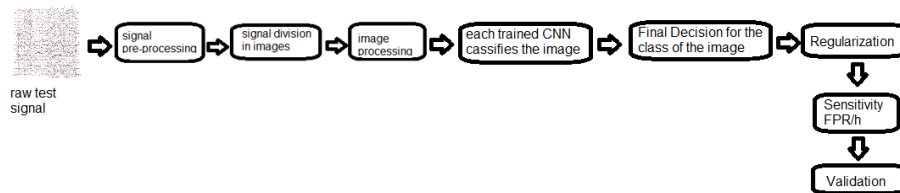
Figure 9 - High-level architectures planned for testing each prediction algorithm.

First, normalization with the data obtained from training signal is applied, so artifacts and noise are removed, and the range of all channels stays the same, 0 to 1. If any value goes above 1, it is limited to 1. The same happens if any value goes below 0, staying limited to 0.

The signal is then segmented, and images created from those segments. If any processing was applied to the images in training, the same will be applied in testing. Images are then given to the set of classifiers trained before. They will, then, return a decision wheter the image is from the class they are specialized in or not. As the result will be different for each one, a decision mechanism is needed to make a final decision based on these.

After this, basic architecture steps are followed. The output of the decision maker is then regularized, its performance evaluated and validated.

4.3 - Techniques Used in the Training of the Predictor

In this section, the techniques used in each step of the training architecture will be explained in detail. Each technique here explained will be used, at least, in one of the experiments that will be presented in future chapters of this work.

4.3.1 - Signal Acquisition and Processing

As said before, recordings from 6 patients from the EPILEPSIAE database were used to train and test several prediction algorithms.

To improve the quality of each signal, in all the experiments done in this work a bandpass filter of 1 to 256 Hz was applied. A bandpass filter is a device that passes frequencies within a certain range and attenuates frequencies outside that range. So, all frequencies outside the range 1 to 256 Hz were attenuated, reducing artifacts and effects of noise.

Furthermore, to remove the influence of the electric power current from the signal, a notch filter was also used. Because all these recordings were from Europe, the notch filter was of 50 Hz.

After removing artifacts and noise, normalization was applied to reduce every channel to the same range 0-1. The normalization consisted in dividing the whole signal by a maximum value, centered in the mean of the signal. That maximum was different from patient to patient.

To obtain the maximum for each patient, first the mean and standard deviation of the whole training signal was calculated.

With those two values in hand, a multiplier value was found so that the sum of *mean + multiplier * standard deviation* would be a value bigger than the non-noise portion of the signal, but smaller than the noise spikes.

In Figure 10, we can see an example of a recording obtained from a seizure of a patient. In it, it can be seen the line that represents the maximum obtained by summing the mean to the multiplier times the standard deviation. In this case, the multiplier was 18. The two lines above and beneath the signal are the value of the maximum and minimum. Those lines cut the signal in some parts that may seem important, but it only limits very few values in total on those areas (mainly pre-ictal). This happens because when spikes happen there, they only take very few instances, that won't make a difference even in the construction of the image.
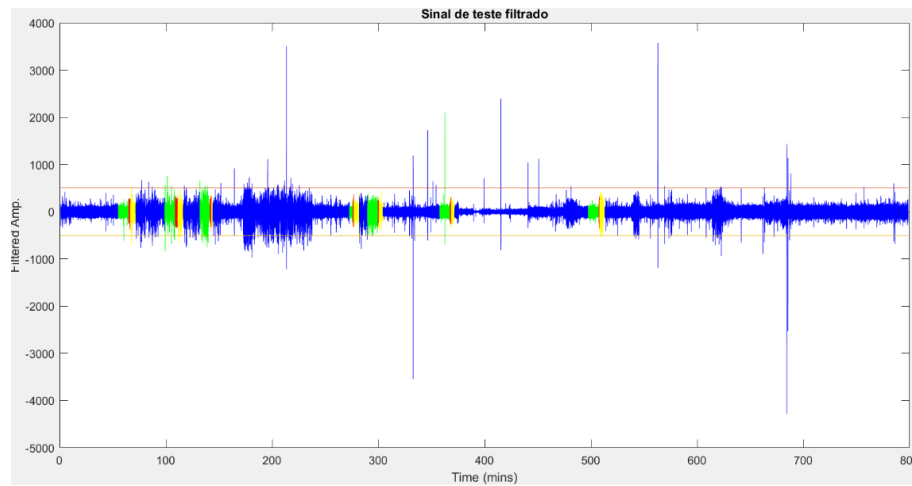
Figure 10 – Signal of a patient with lines that will define the maximum and minimum.

This kind of normalization makes it so that the noise spikes don't have a lot of influence on the division of the signal by the maximum. This will allow the signal to be reduced to the range 0 to 1 without losing a lot of information.

4.3.2 - Signal Segmentation and Image Creation

The EEG signal is collected and stored as a matrix, with the number of lines being the number of electrodes the signal is collected from, and the columns representing the instances collected.

As it is a matrix, it is simple to transform the signal into images. After the signal pre-processing techniques explained above are applied to the signal, each element of the matrix will be in the range 0-1, just as a pixel. Now, depending on the CNN input size needed, the signal will be divided into a sequence of matrixes, each with the number of columns being the column size of the CNN input.

For the ictal periods, data augmentation was applied. The step with which the smaller matrixes are created is of half the length of the other periods, so images created are 50% superposed. So, if, for example, images need to be of 27x227, in the inter-ictal, pre-ictal and post-ictal periods, each sequential 27x227 sub-matrix is an image. But for the ictal period, the first 27x227 would be an image, then a step of half of 227 rounded down would be done, and the next image was created from the instance 113 to the instance 340. Next, as it is an even number step (second step), the step would be of 114 (half of

the 277-step rounded up). So, the next image would begin from instance 227, and stop at instance 454. Again, as the next step is an uneven one (third step), a step of half of 227 rounded down would be done, so the next image would start on the 340th instance. This process was repeated until the ictal period sequence would be over.

This is done so that almost double the original number of ictal images are created with the objective of helping in a better detection of images of such period (with the normal step, very few images would be created).

With the original matrix divided, the number of lines of each sub-matrix is the same as the original. The order of the sub-matrices is the same as the order in the original sequence, so that no information about the signal is lost. As such, it can be reconstructed simply by putting the individual matrixes together. Each individual sub-matrix can, at this stage, be considered an image. The process is shown in Figure 11.
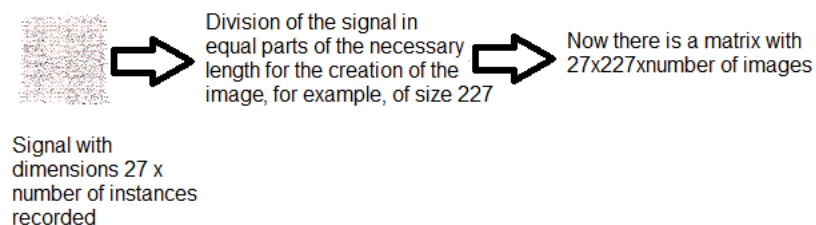
Figure 11 – Division of signal in tensors (tri-dimensional images).

As said before, the dimension of the image used to train, depends on the classifier input dimension. In this work, two types of CNN were used. The first one, used mainly for preliminary experiments needed an input size of 81x81 (number of lines x number of columns). The second one needed image with a size of 227x227.

In this work, the considered signal of each patient was collected from 27 electrodes. This happens because not all recordings were collected from the same electrodes, even for the same patient (a patient has several recordings). However, the first 27 electrodes in each recording were all the same. So, to have more data to use, only the first 27 channels of each patient's signal were considered.

81x81 Images

As the signal has 27 channels (lines), to create a squared image, 27x27 would be enough. But only 27 instances (in the columns) per image wouldn't provide enough information to be distinguishable. So, it was decided to try creating 81x81 images, by putting three 27x81 images on top of each other.

For that, the pre-processed EEG signal was separated into 27x243 matrixes. To adapt them to the 81x81 CNN input, those matrixes were divided into three 27x81 matrixes. The first 27 lines of the final 81x81 image were formed by the first 27x81 matrix, with the second 27 lines being filled with the second 27x81 matrix and, finally, the last 27 lines were filled with the third 27x81 matrix.

As such, an 81x81 image representing about 0.24 seconds (because of the sampling frequency of 1024 Hz of all patients – 243/1024) of the patient brain state was formed and used to train/test the classifier. The process can be seen in Figure 12.
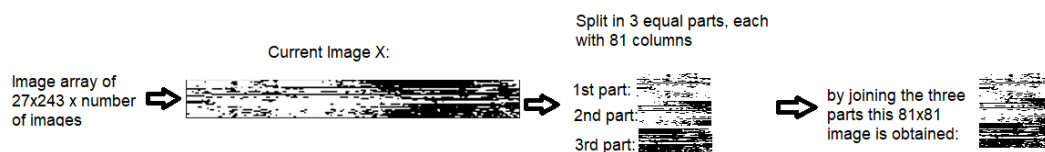
Figure 12 – Creation of 81x81 images.

227x227 Images

The second type of classifier used in this work, AlexNet, needed an 227x227 image input. As such, the pre-processed signal was divided into sequential 27x227 matrixes.

As this type of classifier was used to more final experiments, various ways of building the 227x227 images were tried.

The first way involved simply padding the image with lines of zeros, until it became the required size. So, the first 100 lines of the image contained only zeros. The following 27 lines contained the matrix used to create the image, and the last 100 lines contained, again, only zeros. In this way, approximately 0.22 seconds (227/1024) of the patient brain state were recorded in the image, which was less than the 81x81 images. In Figure 13, the formation of the images with this technique can be seen.
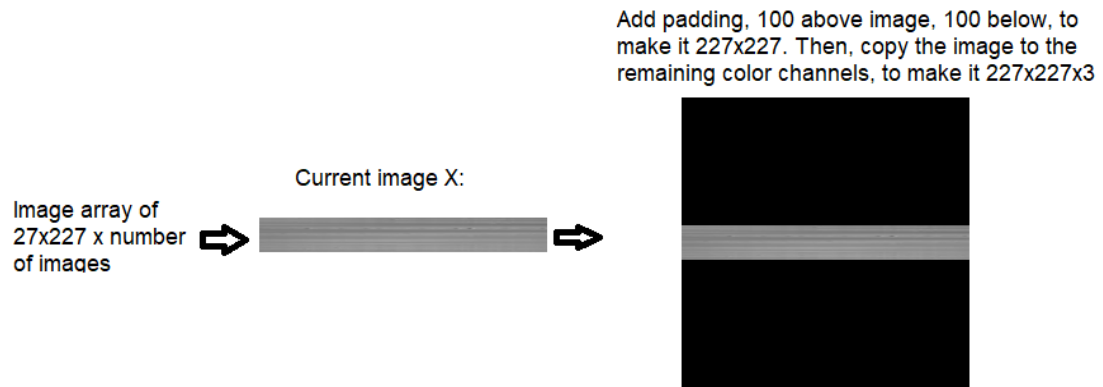
Figure 13 – Creation of padded 227x227 images.

But creating images in this way was a waste of perfectly usable space in the image (only 27 lines out of 227 were useful to the classifier) and would create images hard to distinguish.

One solution could be to adapt the AlexNet to accept rectangular images. But, fearing that doing so would lower its performance in relation to the original AlexNet, it was decided to simply adapt the current images to the input size.

For this, and because individual matrixes only had 27 lines, not only the last matrix recorded, but also the 7 before it (8 times 27 is 216, so only 11 lines will have no information) will be in the final image. So, in the last 27 lines would be the current matrix, the 27 before will be the last image recorded before the current one, and so on. This way, the last 1.77 seconds (227 * 8 / 1024) of the patient brain activity were registered in an image, providing a lot more information. These types of images were called '*dynamic images*' and in Figure 14, their creation can be seen.
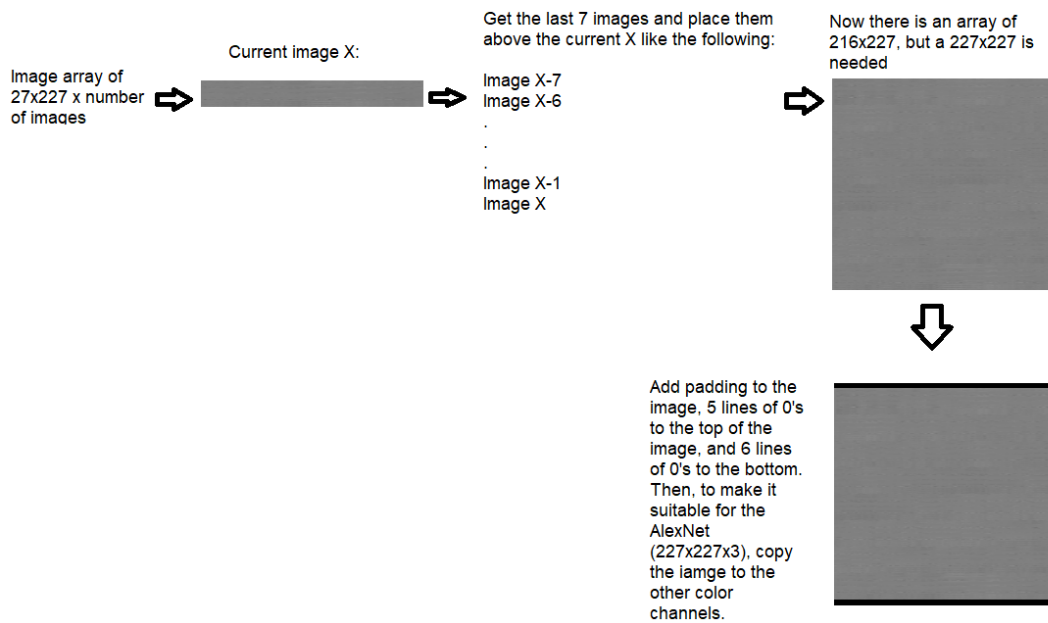
Figure 14 – Creation of the dynamic 227x227 images.

Finally, the last type of images experimented occupied all the 227 lines with useful information. Each line contained the mean of every channel of a matrix 27x227. So, the current image would be in the last line, with each column being the mean value of all the values on that column in the matrix. Above it, in the 226th line, would be the matrix before the current one and, in the same way, each column in that line would be the mean by column of all the values of the 27x227 matrix. This was done for each line, which meant that not only the current image was used, but also the last 226 images. This means that approximately 50.3 seconds (227*227/1024) were recorded in this type of image. In Figure 15, the formation of this type of image can be seen. These types of images were called '*mean images*'.
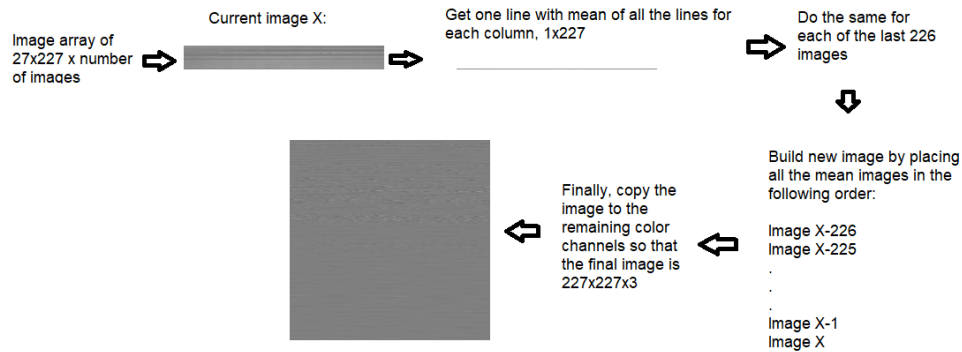
Figure 15 – Creation of the mean 227x227 images.

Having images composed by the current and the preceding ones means that some images will have parts of different stages (for example, the current image can be pre-ictal, while all the others from inter-ictal). In training, this is not a problem, since the only images selected to train are composed by images all from the same stage. It's in testing that doubts may arise. As the prediction is done by raising an alarm that will stop the predictor for the SPH+SOP period, the small number of images it takes for a composed image to start being fully from a stage does not matter. What matters is that the predictor can classify the necessary number of images to raise the alarm at least SPH minutes before the actual seizure.

4.3.3 - Image Selection for Training

Image selection is used in this work to solve the class imbalance problem and ensure that each classifier is trained with the same number of images from each class.

As there are much more inter-ictal samples than any other class, an algorithm is needed to balance those numbers and guarantee that a classifier does not have a worse performance for the less frequent classes.

Throughout this work, three types of networks will be trained. The first will distinguish between inter-ictal and non-inter-ictal images. The second, between pre-ictal and non-pre-ictal and the last between inter-ictal and pre-ictal. All these will be better explained further ahead.

Inter-ictal vs non-inter-ictal

For this problem, it is needed to guarantee that the classifier gets the same number of inter-ictal and non-inter-ictal images. As such, if the inter-ictal class has more images than all the other classes (pre-ictal, ictal, and post-ictal) together, the number of inter-ictal images that will be selected is the same as the total amount of non-inter-ictal samples. As for non-inter-ictal images, because its number is smaller than the inter-ictal, all of them are selected for training. This case can be seen in Figure 16.

Figure 16 – Example of image selection for the training of the inter-ictal vs non-inter-ictal CNN.

If the inter-ictal class doesn't have more images than non-inter-ictal classes, then it simply selects every inter-ictal image, and the same amount of non-inter-ictal images (again, trying to get the same number for each of the non-inter-ictal classes).

Selecting the non-inter-ictal classes is now also a complex problem. The algorithm tries to select the same number of images from each of the three classes, so 1/3 of the total non-inter-ictal images to be selected. But it is not always possible, because ictal and post-ictal classes normally aren't enough to fulfil that 1/3 of the number of non-inter-ictal images. In that case, if the ictal stage doesn't have enough images, all the ictal images are selected, and the remaining images are taken from the inter-ictal and post-ictal periods, 1/2 of the remaining to be selected for each. Then, if the post-ictal period doesn't have enough images to comply with that demand, all post-ictal images are selected, with all the remaining images being selected from the pre-ictal pool. In Figure 17, this process is better explained.

Example of image selection for training of inter vs non-inter CNN non-inter-ictal with more images

Example conditions:
70000 inter-ictal images
50000 pre-ictal images
7000 ictal images
20000 post-ictal images

inter-ictal   vs   non-inter-ictal

70000 images   vs   77000 images

70000 images will be selected from each group.

All the inter-ictal images are selected for training.

Try to get the same number of non-ictal images, 1/3 of the maximum 70000 for each. So, 23333 ictal iamges, 23333 post-ictal images and 23334 inter-ictal ones.

Because ictal images have the smallst number, they are selected first.
23333 are needed but there are only 7000. All the 7000 are selected and we add the remaining 16333 to the number of images to be selected from pre-ictal and post-ictal pools.

So, now it is needed to select 63000 from pre-ictal and post-ictal images. To balance, 63000/2 = 31500 should be selected from each.

But, there are only 20000 post-ictal images. In that case, all of them are selected.

So now, 63000-20000 = 43000 images are needed from the pre-ictal pool.

Because the number of pre-ictal images is 50000, 43000 can be selected without any problem. So, to finish, 43000 are randomly selected from the entirity of the pre-ictal pool.

Figure 17 – Example of image selection for training of inter-ictal vs non-inter-ictal CNN, in the case the non-inter-ictal group has more images.

Pre-ictal vs non-pre-ictal

Because the number of pre-ictal and ictal is always smaller than non-pre-ictal and non-ictal images, respectively, all pre-ictal and ictal images are selected.

As for the non-class (depending on the case, non-pre-ictal or non-ictal), the same technique used for the non-inter-ictal images is used, but instead of pre-ictal, the predominant class from which remaining images are selected is the biggest available, always inter-ictal. This is basically the same process as shown in Figure 17.

Inter-ictal vs pre-ictal

This problem is the most easily solved. If the inter-ictal class has more images than the pre-ictal, then all pre-ictal images are selected for training and the same amount of inter-ictal images are randomly sampled and selected.

If the opposite happens, then the roles are simply inverted, and all inter-ictal images are selected, while the same amount of pre-ictal images are sampled and selected.

4.3.4 - Image Processing

Throughout the experiments, not only the way images were built varied. In some experiments, some processing was added to those images.

From the state of the art, it was concluded that applying image processing to seizure prediction was a possibility that to the best of our knowledge was not yet tried. While some experiments in this work did not have any kind of image processing, others used a combination of several methods to try and get the most out of each image. With this, this work tried to explore the possibilities of applying these methods to seizure prediction.

In the following paragraphs, the techniques used throughout this work's experiments will be explained. All the used techniques can be found in the Image Processing Toolbox for MATLAB.

In Figure 18, Figure 19 and Figure 20, some non-processed images of each important state of the epileptic cycle are presented. It should be noted that these are only some images, and that a lot of the rest can, and will, be very different from these.
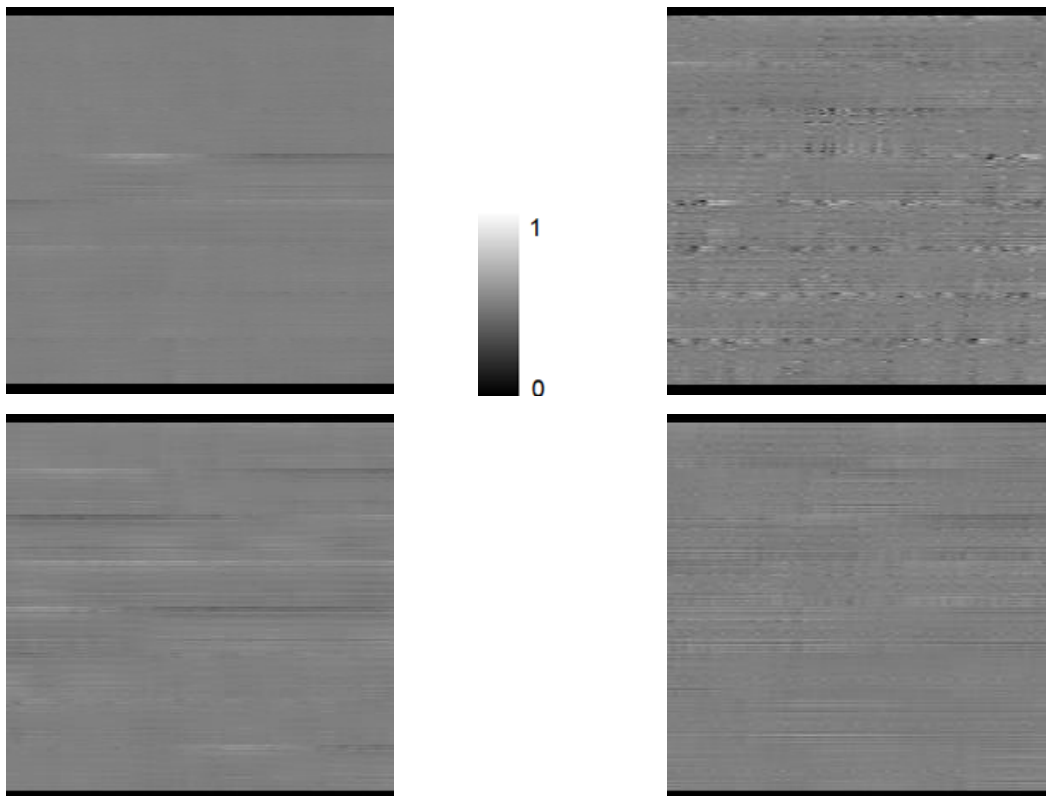
Figure 18 – Some normal dynamic 227x227 inter-ictal images.
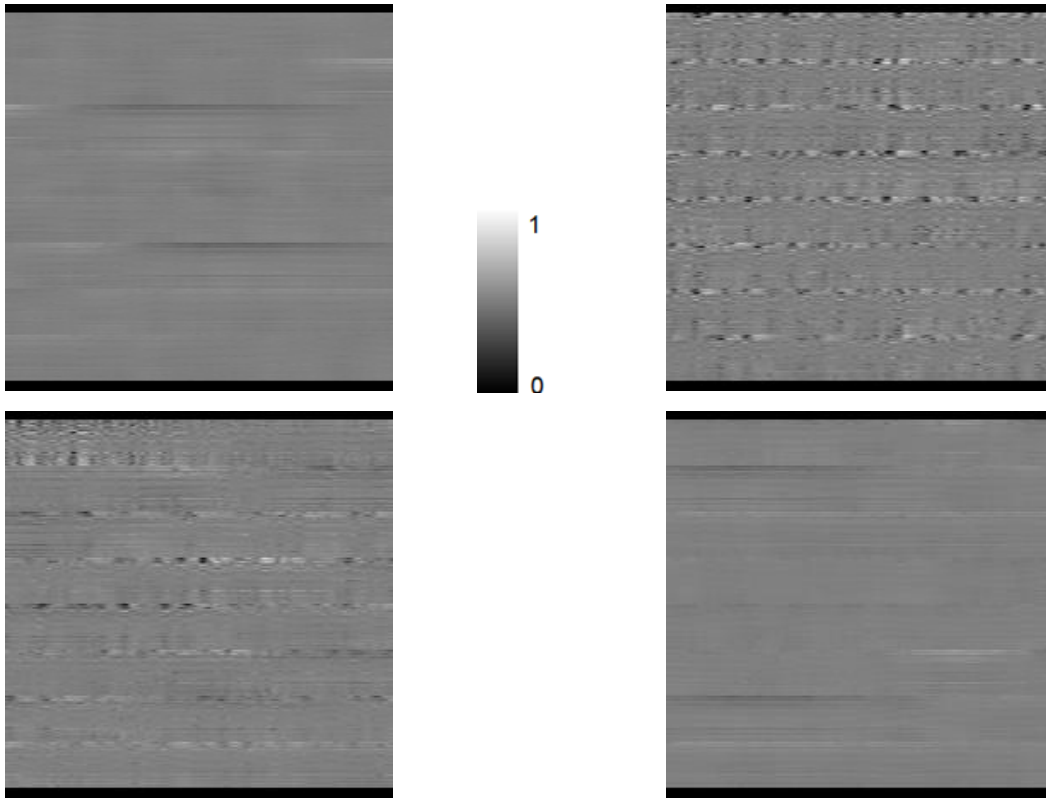
Figure 19 – Some normal dynamic 227x227 pre-ictal images.
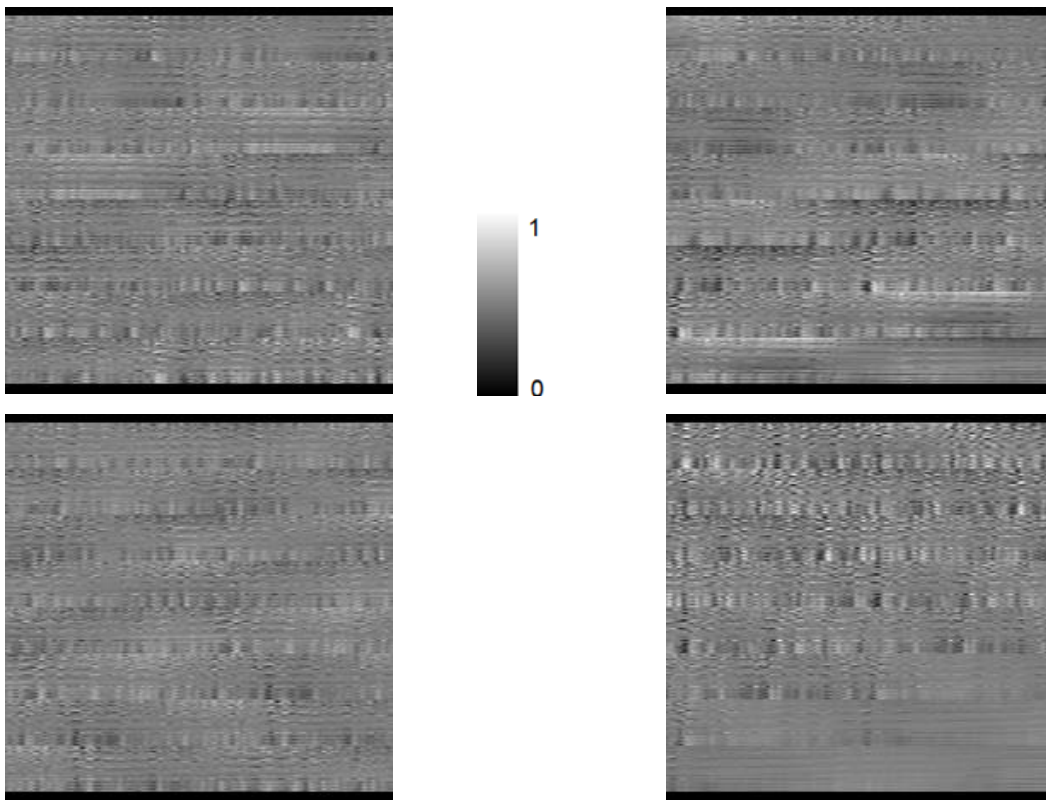
Figure 20 – Some normal dynamic 227x227 ictal images.

Contrast enhancement

As the formed image is grayscale, it was first experimented to add a method that could increase the difference between black and white in the image contrast.

A contrast enhancement method from MATLAB, imadjust [72], was used. It maps the intensity values in the original grayscale image to new values in the output image. By default, this method saturates the bottom 1% and the top 1% of all pixel values, thus, increasing the contrast of the output image.

In Figure 21, Figure 22 and Figure 23, some images where this method was applied can be seen. Compared to the same images without contrast enhancement shown in Figure 18, Figure 19 and Figure 20, it's visible how much whiter the images are, and how now, the darker points present in each image, are more distinguishable against the background.
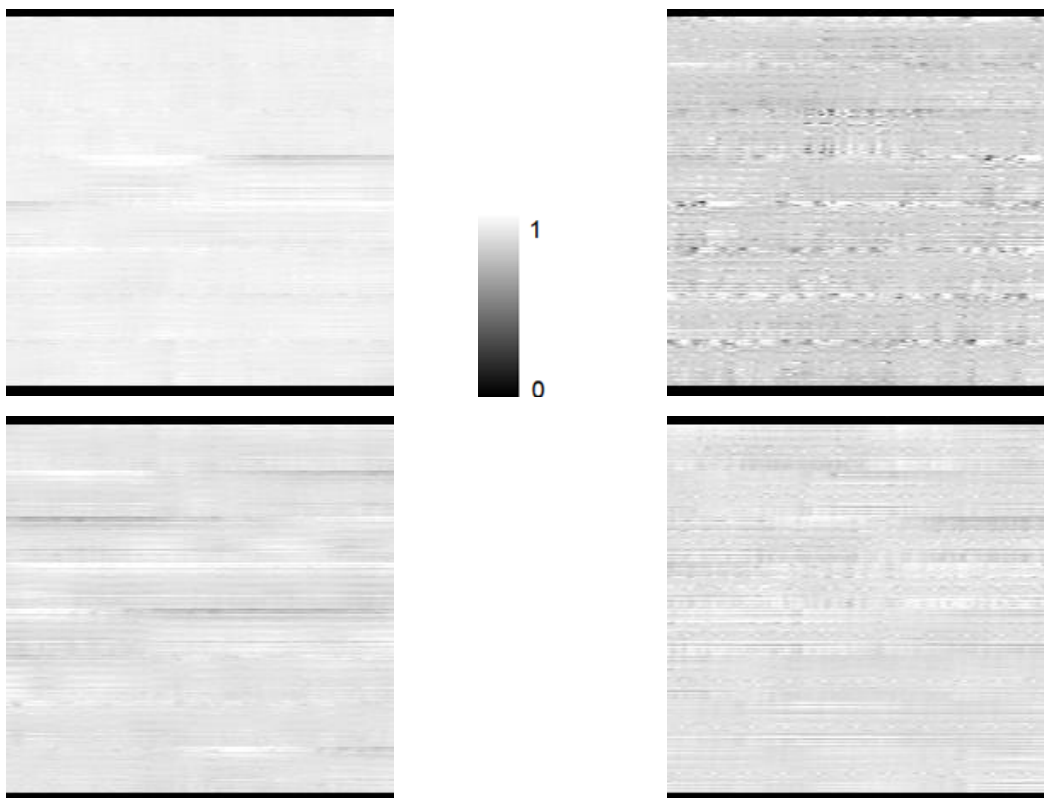
Figure 21 - Some dynamic 227x227 inter-ictal images with contrast applied. The original images are in Figure 18.
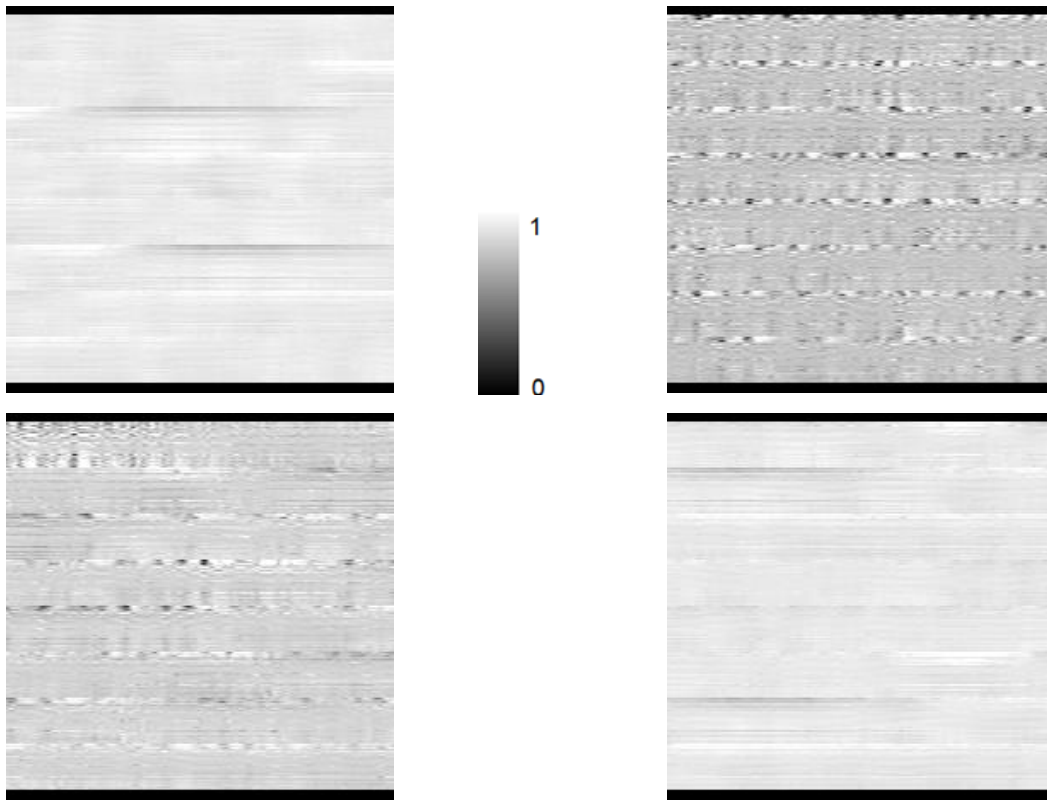
Figure 22 – Some dynamic 227x227 pre-ictal images with contrast applied. The original images are in Figure 19.
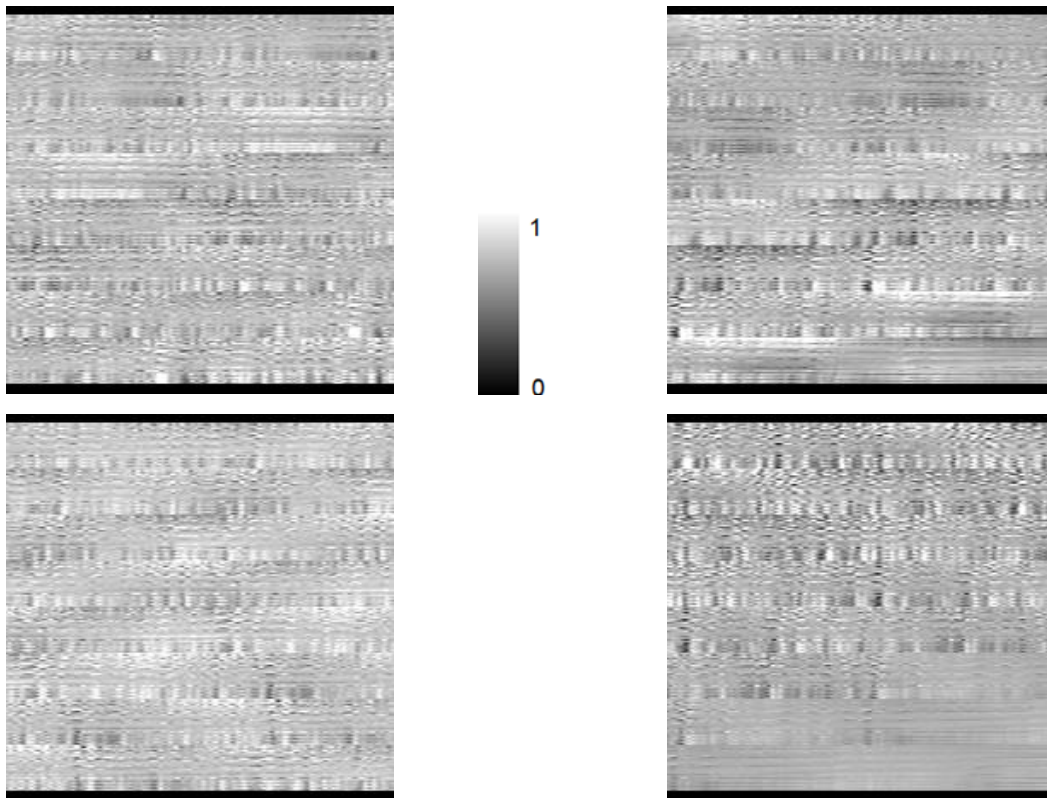
Figure 23 - Some dynamic 227x227 ictal images with contrast applied. The original images are in Figure 20.

Sharpening

Sometimes transition between black and white in the formed image is gradual. Such an aspect makes it look blurry. By subtracting a blurred version of the original image from itself, in a technique called unsharp masking, imsharpen [73] from MATLAB, can sharpen an image, turning the before gradual transition from black to white quicker, and so, sharper.

It was used in some of the experiments to try and enhance the quality of the edges of black points in the formed images.

Dilation

Image Dilation is a morphological operation that enhances the white against the black in an image. This is done by increasing the border, so white objects become more visible. The imdilate [74, 75] method from MATLAB was used to apply this technique. Along the image, an array of structuring element objects is also provided to the method. Dilation works by performing multiple dilations to the input image using each structuring element in the array in succession. That array, in this work, was always created using the strel [76, 77] function to create a disk with a radius of 2.

This method was used as a helper to the reconstruction technique. So, in that subsection, it will be explained why a disk with a radius of 2 was used.

Reconstruction

Image reconstruction [78, 79] is an operation that performs a morphological reconstruction of an image, using another mask image.

To apply it, a mask image was created by applying contrast to the original image. Then, a marker image is created by applying dilation to the mask. This marker image identifies the high-intensity objects. Then, image reconstruction is applied to the mask image, using the marker image to identify the high-intensity objects.

This method helps to differentiate better objects in the image. In Figure 24, Figure 25 and Figure 26, some images used for the last experiment can be seen (the same images presented in the images shown before). They are built not only with reconstruction with dilation, but also with contrast, sharpening and complement (inverting the colors in the image). In section 5.3.3, the creation of this images will be explained.
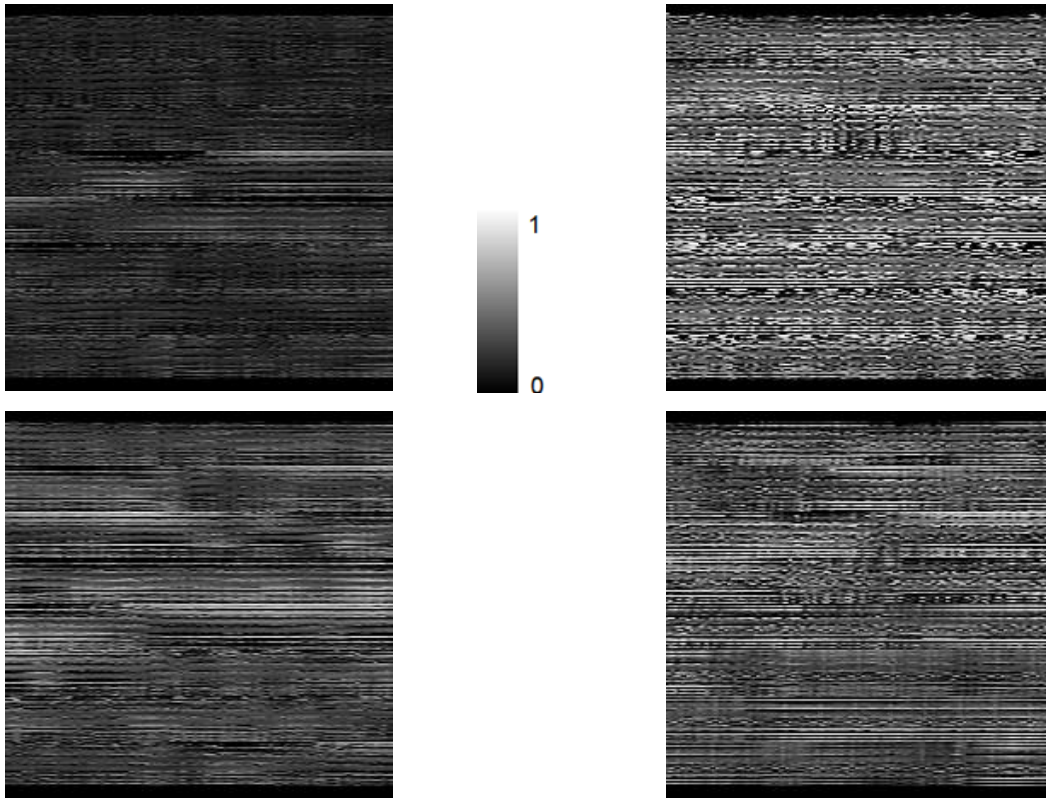
Figure 24 - Some dynamic 227x227 inter-ictal images with contrast, sharpening, reconstruction by dilation applied. The original images are in Figure 18.
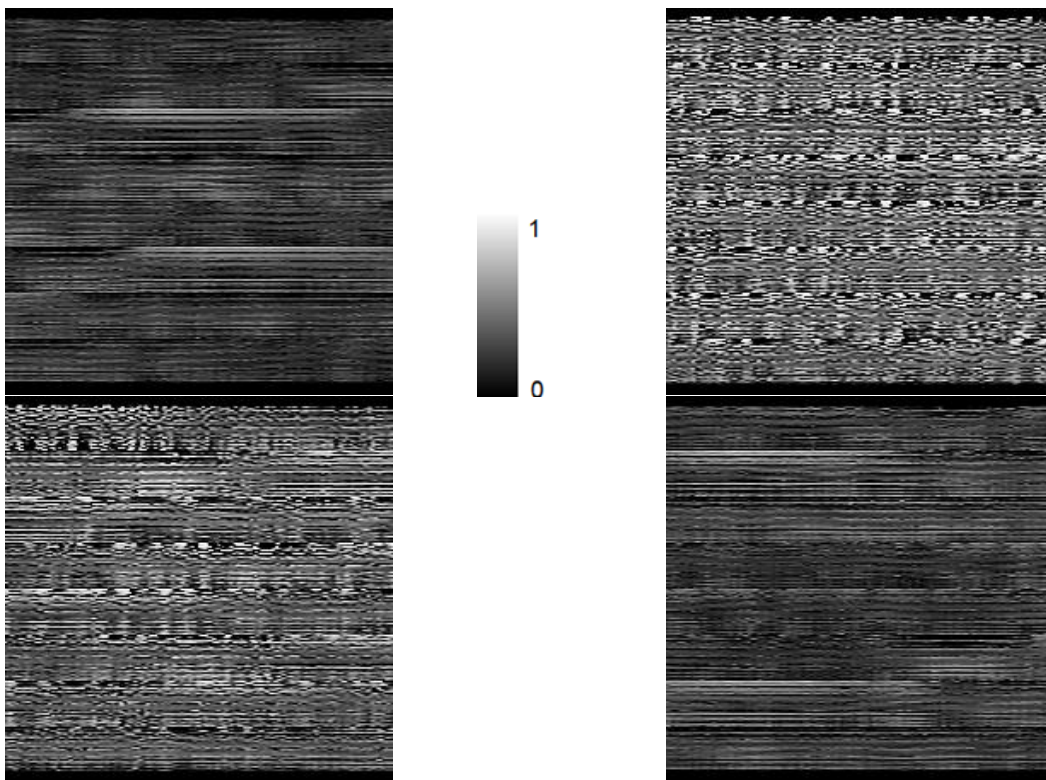
Figure 25 - Some dynamic 227x227 pre-ictal images with contrast, sharpening, reconstruction by dilation applied. The original images are in Figure 19.
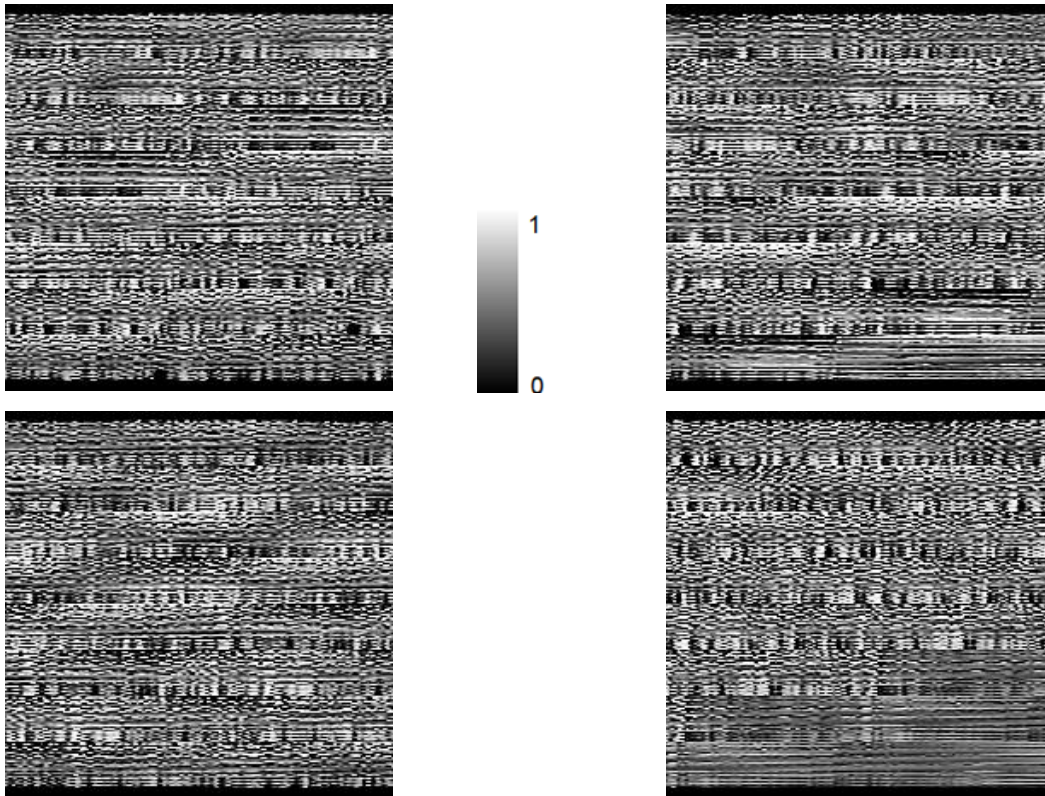
Figure 26 - Some dynamic 227x227 ictal images with contrast, sharpening, reconstruction by dilation applied. The original images are in Figure 20.

The application of these methods in this work is similar to the 'Perform Opening-by-Reconstruction to Identify High-Intensity Objects' example in the MATLAB imreconstruct method page [78], but instead of using erosion, this work used dilation. This is because the images used at the stage of the reconstruction are mainly white. So, applying a dilation to white with a disk with a radius of two, the marker image will have the higher intensity black objects. The size and form of the dilation structuring element array was chosen as a disk to enhance the white all around for two units. Several values were tried for the value of the radius and were evaluated visually. The radius of two seemed to form an image capable of identifying the high-intensity objects without destroying them too much nor identify too much of them (if the radius is too big and enhances those objects too much, most of the information surrounding the object in the image will be overwritten).

Complement

The images created by the methods explained before are more white than black, a complement of the image was used to test if the fact that there is blacker (and so, more 0 values) in the image, will help the CNN to better differentiate images.

For that, the imcomplement [80] method from MATLAB was used.

4.3.5 – Classifier

As said before, this work is focused on using the combined work of multiple CNNs to try to predict a seizure. As such, this subsection will explain what are CNNs and what types were used throughout this work.

Convolutional Neural Networks

CNNs are a class of neural networks inspired by visual cortex connectivity patterns. They were originally designed for image processing and analysis [91], but its application was, throughout the years, extended to other areas, such as image classification, natural language processing, time series, etc. [92, 93]

These are regularized versions of multi-layer perceptrons, that take advantage of the hierarchical pattern in data and assemble more complex patterns from simpler ones in the data. So, they don't have a complexity nor connectivity as high as other methods of this kind [94].

They also need less pre-processing than other image processing methods, since they can automatically extract more discriminative features from raw inputs than the ones extracted manually [94].

A CNN consists in a set composed by an input layer, an output layer, and several hidden layers in between these two. There are several types of hidden layers, with the most important ones being the pooling layer and the convolution layer, which gives the name to the network. Some of the most important layers are:

- Image Input Layer – prepares the image for the network, may apply normalization.

- Convolutional Layer – composed by a series of filters that run through the layer's input, calculating the scalar product between the input and the filter. An example of a 3x3 convolutional layer filter can be seen in Figure 27. By applying this filter to the region shown to the left side of the same, the feature map that can be seen to the right side of the filter is formed. As the filter runs through the layer's input, it creates a feature map. Each of these maps is the result of a convolution using different weights and biases. So, the layer learns features of each image's region. Parameters like the number, size and step of the filters can be defined on each use of this layer.
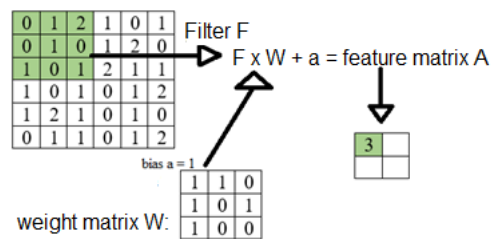
Figure 27 – Example of a 3x3 convolutional layer filter.

- Pooling Layer – Divides the input in regions, calculating the maximum/mean (depending on whether it is a Max Pooling Layer or an Average Pooling Layer) of each. Layers of this kind reduce the number of parameters to learn for the next layers and help to reduce overfitting. Figure 28 shows an example of applying a Max Pooling Layer with 2x2 filters and step 2.
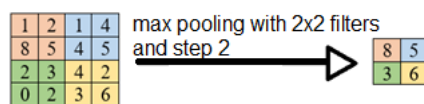
Figure 28 – Example of a Max Pooling Layer with 2x2 filters and a step of 2.

- Fully Connected Layer – combines all learned features in the preceding layers to identify patterns. In classification problems, the last fully connected layer combines the features to classify images. This layer's outputs are numeric real values, in equal number to the number of the classes, yet without any special meaning.

- Softmax Layer – the softmax function (equation 3) is applied to the output of the preceding layer, the fully connected layer. This function quantifies the probability of an image belonging to a certain class. The softmax function is given by the following equation:

$$\sigma(v)_i = \frac{e^{v_i}}{\sum_{n=1}^{N} e^{v_i}} \qquad (3),$$

Where:

- N is the number of classes.
- v is the resulting vector of the preceding layer (normally, a fully connected layer), needs to have dimension N.
- i is the class whose categorical probability needs to be calculated.
- σ is the function's output.
- e is the Neper's constant.

- Classification Layer – takes the values returned by the softmax function and, for classification problems with mutually exclusive classes, assigns each input to one of the mutually exclusive classes using the cross-entropy function (equation 4), given by:

$$\text{Loss} = -\sum_{i=1}^{K} \sum_{j=1}^{N} t_{ij} \ln y_{ij} \qquad (4),$$

Where:

- K is the number of images.
- N is the number of classes.
- t_{ij} is image i's label.
- y_{ij} is the value returned by the softmax function, which means that it is the probability that the network gave to the association of the image I to class j.

Equation 4 can also be used to evaluate the quality of the network in training/validation.

CNNs used in this work

The first CNN used in this work was an 81x81 image input one, created for this work.

It has the following composition:

- First, an image input layer that receives images with the size 81x81.

- A 2 dimensions Convolution Layer with 8 3x3 filters, followed by a Batch Normalization layer, a ReLu Layer and a 2x2 Max-pooling Layer, with a step of 2.

- Another 2 dimensions Convolution Layer with 16 3x3 filters, followed by a Batch Normalization layer, a ReLu Layer and a 2x2 Max-pooling Layer, with a step of 2.

- Yet another 2 dimensions Convolution Layer with 32 3x3 filters, followed by a Batch Normalization layer, a ReLu Layer and a 2x2 Max-pooling Layer, with a step of 2.

- One last 2 dimensions Convolution Layer with 64 3x3 filters, followed by a Batch Normalization Layer, a ReLu Layer and a 2x2 Max-pooling Layer, with a step of 2.

- A Fully Connected Layer.

- A Softmax Layer that provides the necessary information for the Classification Layer to decide.

- Classification Layer.

The second and final CNN used in this work was AlexNet. AlexNet is a CNN architecture designed by Alex Krizhecsky et al. [81]. It contains 22 layers and needs image inputs with the size of 227x227. This work used the MATLAB Deep Learning Toolbox alexnet [82] method to apply it. The original network can distinguish between 1000 objects, but in this work, it will only need to distinguish between two, to identify if an image is or is not from the class it will be specialized in.

So, the adapted AlexNet used the first 22 layers as they are originally, as can be seen in Figure 29.

```
1    'data'     Image Input                  227x227x3 images with 'zerocenter' normalization
2    'conv1'    Convolution                  96 11x11x3 convolutions with stride [4  4] and padding [0  0  0  0]
3    'relu1'    ReLU                         ReLU
4    'norm1'    Cross Channel Normalization  cross channel normalization with 5 channels per element
5    'pool1'    Max Pooling                  3x3 max pooling with stride [2  2] and padding [0  0  0  0]
6    'conv2'    Grouped Convolution          2 groups of 128 5x5x48 convolutions with stride [1  1] and padding [2  2  2  2]
7    'relu2'    ReLU                         ReLU
8    'norm2'    Cross Channel Normalization  cross channel normalization with 5 channels per element
9    'pool2'    Max Pooling                  3x3 max pooling with stride [2  2] and padding [0  0  0  0]
10   'conv3'    Convolution                  384 3x3x256 convolutions with stride [1  1] and padding [1  1  1  1]
11   'relu3'    ReLU                         ReLU
12   'conv4'    Grouped Convolution          2 groups of 192 3x3x192 convolutions with stride [1  1] and padding [1  1  1  1]
13   'relu4'    ReLU                         ReLU
14   'conv5'    Grouped Convolution          2 groups of 128 3x3x192 convolutions with stride [1  1] and padding [1  1  1  1]
15   'relu5'    ReLU                         ReLU
16   'pool5'    Max Pooling                  3x3 max pooling with stride [2  2] and padding [0  0  0  0]
17   'fc6'      Fully Connected              4096 fully connected layer
18   'relu6'    ReLU                         ReLU
19   'drop6'    Dropout                      50% dropout
20   'fc7'      Fully Connected              4096 fully connected layer
21   'relu7'    ReLU                         ReLU
22   'drop7'    Dropout                      50% dropout
```

Figure 29 – Image of the first 22 layers of the AlexNet. Taken from [82], on July 29th.

The last 3 layers, to fully adapt the network to this work's problem, in a transfer learning approach were:

- A Fully Connected Layer with 2 outputs, the same number of classes of each network (being of class and not being of class).
- A Softmax Layer that provides the necessary information for
- a Classification Layer that will decide if a certain image is or isn't of the class the trained network is specialized in.

Transfer learning allows to reuse knowledge gained from a previously used machine learning model. As it was not yet tried before in seizure prediction, and the task could potentially benefit from it, experiments were done to see if it showed better performance than the 81x81 network.

Between all the options to do transfer learning for this work, AlexNet was chosen because its input size of 227x227x3 was the most adequate for the first experiment done. Because the signal is from 27 channels, for the first experiment, it was only needed to add padding of 100 lines.

4.3.6 – Outputs

The result of the application of the whole architecture to a patient are a set of trained networks, each of which specialized in identifying if a certain image is from the seizure cycle stage it is trained in. Besides saving the trained networks, it is also needed to save the required data to transform the raw EEG signal into an image suitable for the trained networks. As such, it is also needed to save the signal pre-processing data, which is simply the value obtained by the sum of the mean of the patient's training raw EEG signal added to multiplication of the standard deviation with the multiplier selected in subsection 4.3.1 for the patient.

Of course, it is also important that all the techniques applied in the creation of the images with which the networks were trained with, are used to create the images that the networks will be tested with.

4.4 - Techniques Used in Testing of the Predictor

In this section, techniques used in each step of the testing architecture will be described in detail. Again, each technique will be used at least in one of the experiments presented in future chapters.

To create the images for each experiment's test, the 30% of the signal selected for testing is processed in the same way as it was for its training. So, in the testing architecture, all signal pre-processing, image creation and image processing techniques are the same as in training.

The only differences in the testing architecture up to classification, are that the testing signal is normalized using the training data, and that there is no image selection. The testing signal is turned into a sequence of images, which will then be classified by each network developed in training.

4.4.1 – Classification, Decision Making and Regularization

One of the outputs of the training phase is the set of trained networks. Each of those trained networks will be specialized in deciding whether a certain image is or isn't of the class it is trained for.

So, the series of trained network will classify each image of the testing sequence, and each network will give an output with the class (between two) they deem the image to be.

This means that, for each image, there are three outputs. So, a decision mechanism is needed so that these outputs are joined into a final decision, saying what state the patient is at that moment.

But each network simply saying if the image is or isn't from the class they are specialized in, is not enough information to make a good decision. By looking at the composition of a CNN, if in the softmax layer, the network has 65% of probability of being from the class it is specialized in, the output would normally be 1 (meaning it is from the class). So, it was decided to look at the certainty the CNN has of the image being from the class, instead of simply looking at the binary output.

As seen in Figure 30, these probability values are still of a very wide range, and make it very hard to devise on a threshold or another method to decide which state the patient is at any moment. So, it was decided to consider the mean of the last 10 seconds, the last 45 images. As it can be seen by the black line in Figure 31, representing the mean of the last 10 seconds of images, it gives a much more readable line (even if not perfect), that can more easily be analysed to make a decision. In both images, the light blue represents inter-ictal instances, while green represent pre-ictal, red ictal instances and yellow post-ictal instances. The magenta line is an example of a threshold, and will be used to explain the concept in a few paragraphs.

Even though only the last 45 images were tested in this work, results will surely vary with other numbers of images, and should be looked at in further work.
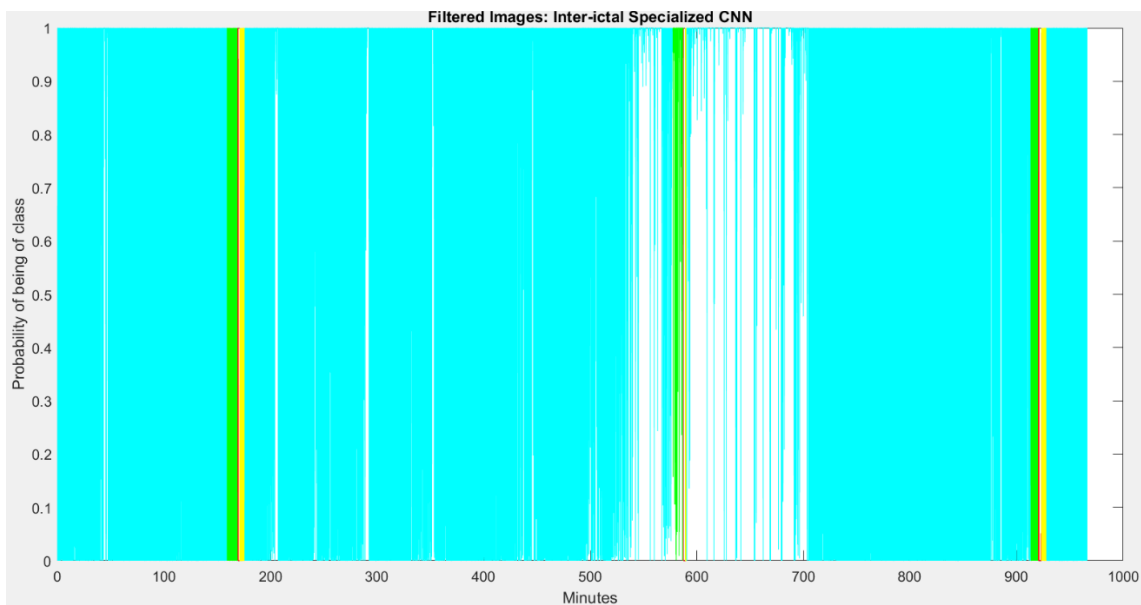
Figure 30 – Probability values an inter-ictal specialized network gives to a testing set.
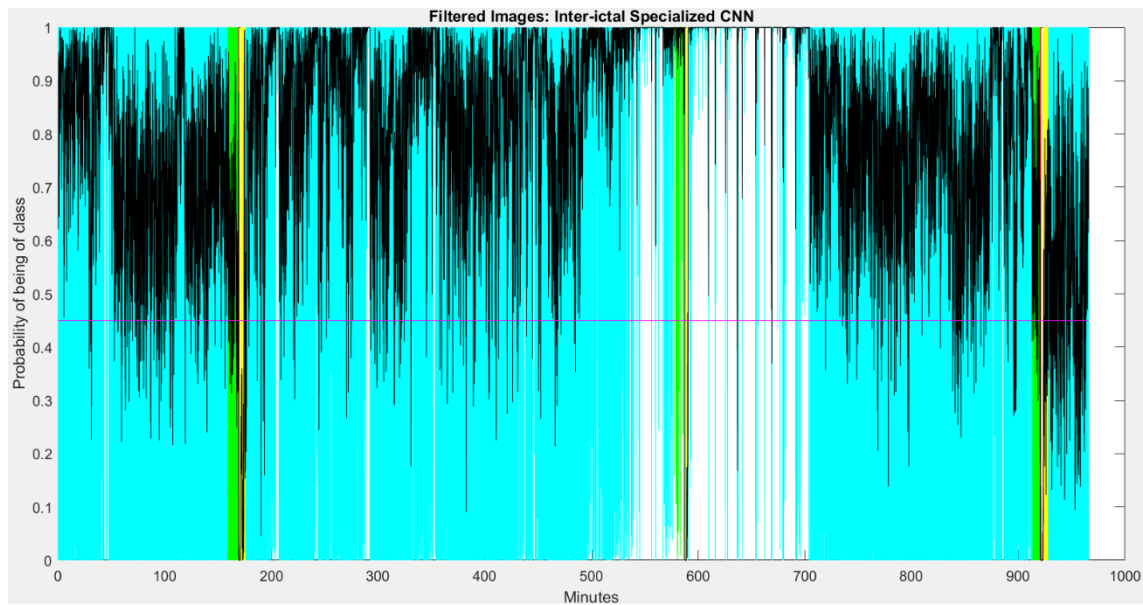
Figure 31 - Probability values with mean of the last 10 seconds (in black) that an inter-ictal specialized network gives to a testing set.

So, to decide which class an image belongs to, the algorithm created to make a decision simply checks three thresholds, if the mean of probabilities of being inter-ictal is below a certain threshold and if the mean of probabilities of being pre-ictal is above another threshold. In this last case there may be one or two thresholds, depending on the trained networks. For some experiments, two types of pre-ictal networks were trained, one that decides if an image is pre-ictal or not, and another that decides if an image is pre-ictal or inter-ictal. Different thresholds are needed for both of them.

An image is classified as pre-ictal if the mean of the probabilities of the last 10 seconds given by the specialized networks for being inter-ictal is below the inter-ictal threshold, if the probability of an image being pre-ictal against all other classes is above another threshold, and if the probability of an image being pre-ictal against inter-ictal is above another threshold. In Figure 31, an example of a threshold is also shown. So, as the figure represents the output of an inter-ictal specialized network, every black point that is below the magenta line can be counted as pre-ictal, as long as the same happens in the inter-ictal specialized network and the inter-ictal versus pre-ictal network (in these two cases, the black line must be above the magenta line).

The ideal value of those thresholds are found by running the prediction for several values, and then finding the combination of values that gives the best performance

results. These values were tested for each patient and each pre-ictal time, in order to find the best combination of thresholds for each of these.

While predicting, outputs will be regularized by the Firing Power method. So, it is only considered that the patient entered pre-ictal stage, if the Firing Power threshold is surpassed. So, it only happens when the number of instances (the mean of the last 10 seconds certainty) that are classified as pre-ictal in the last x minutes, with x being the pre-ictal time for the experiment, surpasses that threshold.

Unfortunately, because of time constraints for the conclusion of this work, only the probability threshold values were exhaustively tested. In total there are 7 values that need to be experimented, and all of them can take a lot of values. So, to test them all, it would be needed to run the prediction thousands or even millions of times, thus taking too much time. As such, the Firing Power threshold, the number of past images to be in the mean of the probability, and the SOP and SPH values were not tested exhaustively. Instead, the value adopted for each was found by visually analyzing the result of some values for those variables. The SPH was always 2 minutes, so there is always some time to act before a seizure may happen. The SOP and the Firing Power threshold depends on the pre-ictal time chosen, and can be seen in Table 7. In the table, the number of last images considered is the approximation of the amount of images needed to check the last x minutes of prediction (x being the pre-ictal time). So, for example, to check the last 5 minutes of images (5 minutes are 300 seconds), with each image having 227 instances and a sampling frequency of 1024 Hz (1024 samples per second), we need to check the last 300*1024/227 images, which are approximately 1350 images. The firing power threshold means that an alarm will be fired if that number of images presented in that column of the table are declared as pre-ictal over the last x number of images (x corresponding to the pre-ictal time images). The SPH time is always 2 minutes (541 images), as said before.

Table 7 – Firing Power threshold, SPH time and SOP time values used.

Pre-ictal time (minutes)	Number of last images considered	Firing Power Threshold	SPH Time	SOP Time
5	1350	500	541	2707
10	2707	700	541	5413
15	4060	1500	541	8120
30	8120	3000	541	10826
40	10826	4500	541	10826

There was also an extra method implemented in the prediction. Sometimes, the amplitude of the signal becomes very low, and that phenomenon becomes visible in the prediction graphics, as can be seen right before the 600 minute mark in Figure 31. To detect a pre-ictal period when such happens (and predict a seizure), a script was specially created to predict in those circumstances.

The prediction algorithm is by default in a normal state, but when it notices that the difference between the predictions of the inter-ictal specialized network and the pre-ictal specialized one is over 0.85, it assumes that the signal is having a very low amplitude (when inter-ictal prediction is too high, and pre-ictal prediction is too low). The algorithm then tries to identify when the difference between the predictions of the two networks is reduced, by being below that threshold (0.85) for a certain amount of time. The threshold used was of 0.85, which means that when the difference between the inter-ictal and pre-ictal predictions is higher than 0.85, the algorithm stays alert for when it stops to be. When it stops to be for an amount of time like the Firing Power threshold, it fires an alarm. This method isn't perfect and, in some cases, will create a false alarm at the end of the low amplitude period, if the signal amplitude gets back to normal without a seizure occurence. Nevertheless, it helped improve sensitivity without worsening FPR/h too much in some patients.

4.4.2 – Performance Evaluation and Validation

To find the best combination of the thresholds presented in the preceding subsection, the Sensitivity and FPR/h metrics were obtained for each of the combinations tested. When the best metrics were found for a patient, validation was applied to it, to find if it performed better than a random predictor. For that, a method based on Schelter et al. [39, 80] was used.

After running the prediction, the number of total alarms generated was used to create the probability of the alarm being fired at random at each instance. This probability is given by equation 5.

$$Probability\ of\ firing\ at\ any\ point = \frac{Number\ of\ total\ alarms}{Number\ of\ instances\ of\ the\ signal} \quad (5)$$

Then, 100 runs of the random predictor were done. What happens in each run is that an array of the same size of the test image vector is iterated through, and at each instance of that array, the probability of the alarm being fired is equal to the result of equation 5. Each time the alarm is fired, the SOP+SPH period happens, and in the end, the result vector (with the random predictions) is compared to the original target. The sensitivity is calculated over the 100 runs and, in the end, if the predictor created in this work has better sensitivity than the random predictor (over the same FPR/h), is better than a random predictor.

Chapter 5
Experiments

In this chapter, the experiments done to test the algorithms created in this work will be presented and explained.

Only a small description of the results will be given in this chapter, as the next one intends to better discuss the results of the different experiments and take conclusions about them.

5.1 - 81x81 Network versus AlexNet

The first experiments done in this work used an 81x81 network created for this work. This network was supposed to be a simple one, based on the example given on MATLAB's *'Create Simple Deep Learning Network for Classification'* [84]. After testing this network, it was decided to look at AlexNet and its already proven potential as a classifier. Even though it is popular as a classifier, it hasn't yet been applied to the problem of this work. This experiment had the aim of checking how applying it to the problem could improve the results shown by the first 81x81 network or had the potential to improve them.

These experiments were done to all the 6 patients considered in this study (whose information can be seen in Table 8), and tested for 5, 10 and 15 minutes of pre-ictal period. No image processing was applied, and the raw signal was processed equally for both networks, with the signal processing methods explained in the preceding chapter. As for the multi-classification, for each experiment, two networks were trained: inter-ictal vs non-inter-ictal and pre-ictal vs non-pre-ictal.

All networks were trained with 50 epochs, fewer than the next rounds of experiments, as this was mainly of a preliminary experiment. It was also trained with an initial learning rate of 0.001 and a mini batch size of 64, values chosen based on MATLAB

documentation [96]. The time it took to train each network depended on various factors, namely on the number of images selected for training. As some patients had more recorded seizures than others, they would have more images selected for training and would take more time to train.

Table 8 - Information about the patients used.

Patient Number	Patient ID in EPILEPSIAE	Gender	Age	Number of Seizures	Hours of recordings	Minutes for testing
1	200	F	53	10	84:03	958
2	1200	F	40	24	62:20	911
3	1500	M	50	10	62:05	602
4	2900	F	21	21	67:56	1024
5	6100	F	27	24	103:17	1148
6	6200	F	37	11	105:08	645

5.1.1 - 81x81 CNN

For the training of this architecture, the signal was processed by applying a 1-256 Hz bandpass filter, a 50 Hz notch filter and then normalization. The method explained in the 4.3.2 subsection was used to create the images. Two groups of images would then be selected, the first to distinguish between inter-ictal and non-inter-ictal images, and the other to distinguish between pre-ictal and non-pre-ictal images. These images would then be used to train the 81x81 network explained in the 4.3.5 subsection.

To test the networks, the testing set was processed in the same way as the training one was and given to the trained networks. After obtaining their predictions, the technique explained in subsection 4.4.1 was applied to process these predictions.

In Figure 32 (inter-ictal specialized) and Figure 33 (pre-ictal specialized), the training progress of one of the 81x81 networks can be seen.
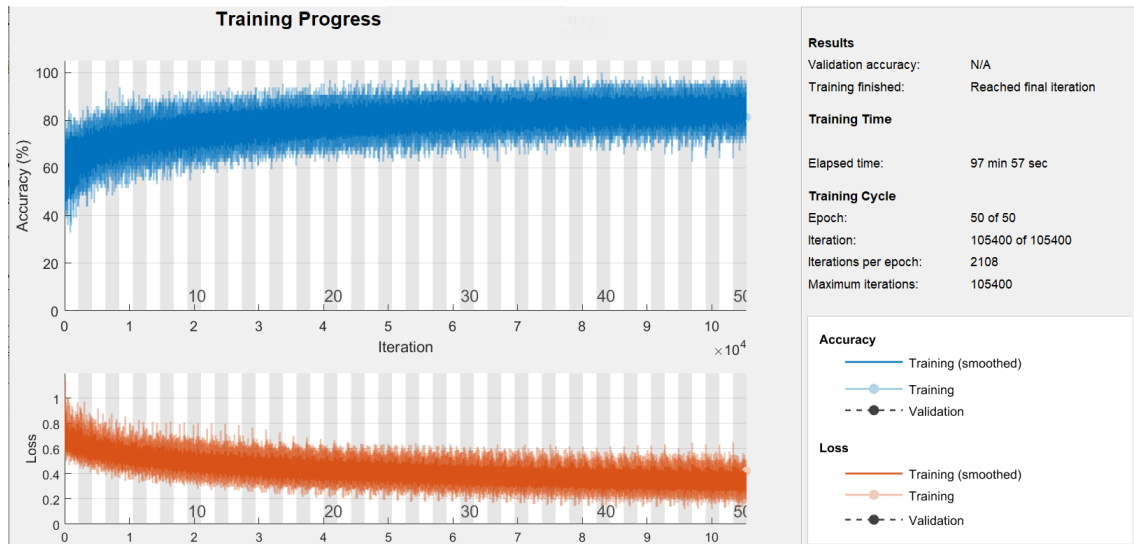
Figure 32 - Training progress of the inter-ictal specialized 81x81 network.
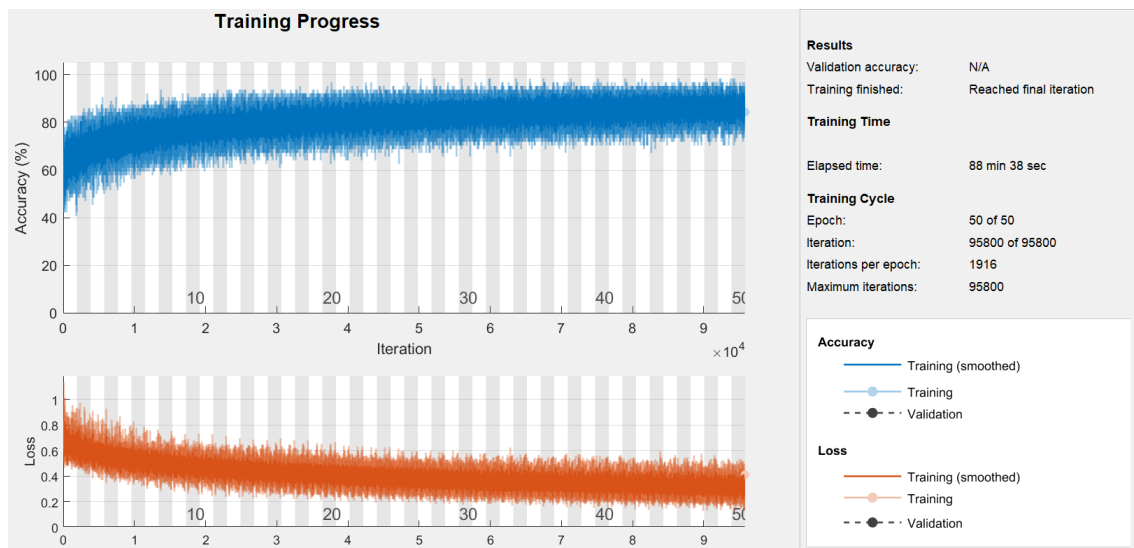
Figure 33 - Training progress of the pre-ictal specialized 81x81 network.

5.1.2 - AlexNet

The second architecture used in this first experiment was the AlexNet, which is highly regarded as a classifier (the authors participated as team Supervision in [86]).

The signal was processed by applying a 1-256 Hz bandpass filter, a 50 Hz notch filter and then normalized. After dividing the signal in the needed time windows, each with 227

63

instances, the padding method explained in the 4.3.2 subsection was used to create the images, by simply adding 100 rows of 0's on the top and bottom of the image obtained from the signal.

These images were then selected for the two classification problems of this experiment, that is, distinguish between inter-ictal and non-inter-ictal images and distinguish between pre-ictal and non-pre-ictal images. The selected images would then be used to train the AlexNet network explained in the 4.3.5 subsection.

Finally, in testing, the dedicated signal was processed in the same way as the training one was, to create similar images. Those images were then given to the trained networks for classification. After obtaining their predictions, the technique explained in subsection 4.4.1 was applied to process these predictions and obtain the performance metrics.

In Figure 34 (inter-ictal specialized) and Figure 35 (pre-ictal specialized), the training progress of one of the padded images AlexNet networks can be seen.
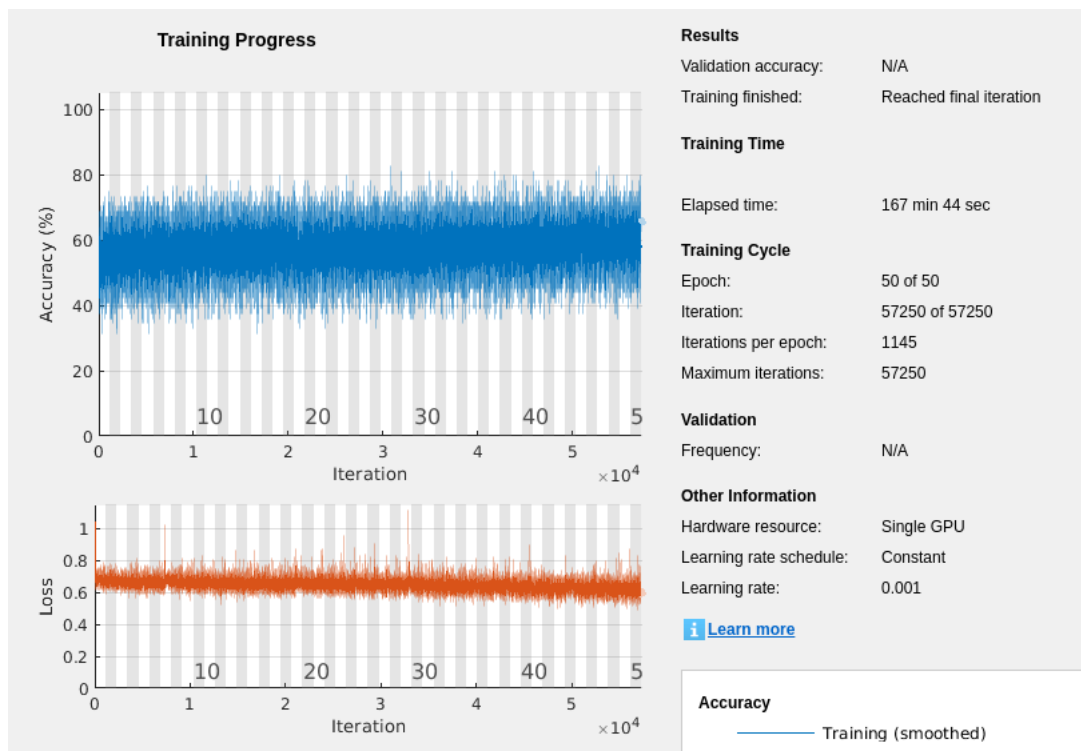
Figure 34 - Training progress of the inter-ictal specialized padded image AlexNet network.
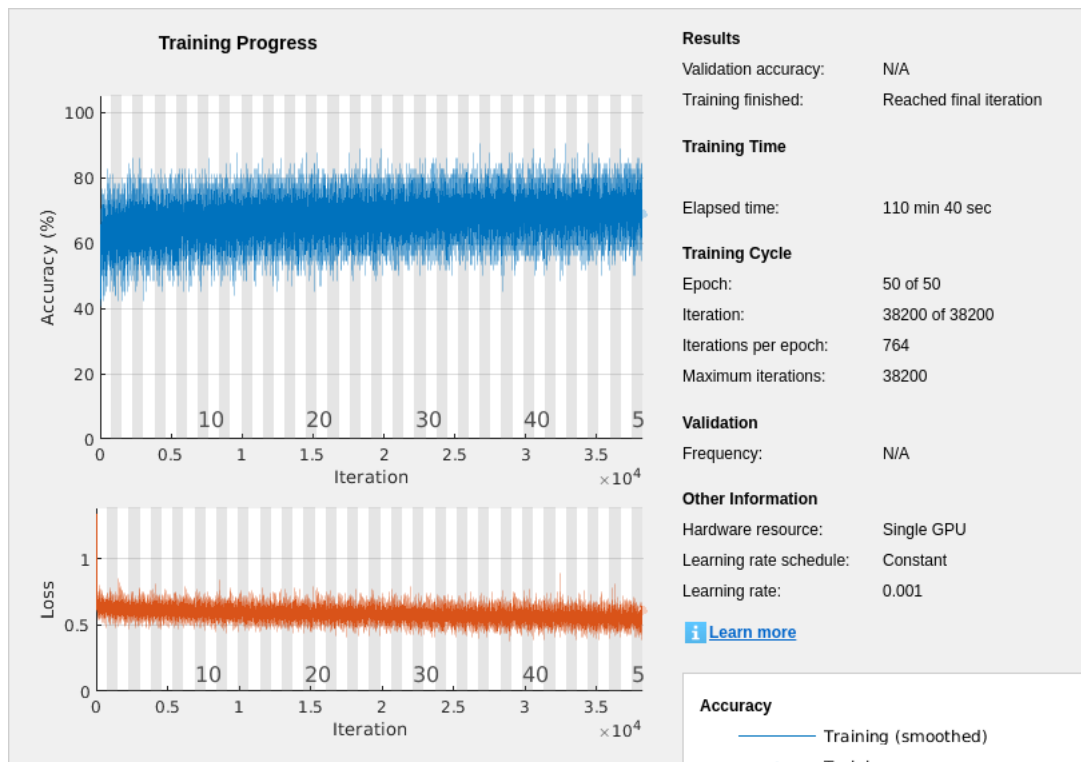
Figure 35 - Training progress of the pre-ictal specialized padded image AlexNet network.

5.1.3 – Results

In Table 9, the results obtained from the training and testing of these two types of networks are presented. Trained networks will give, for each image, two probabilities: the probability of being of the inter-ictal period and the probability of being of the pre-ictal period. So, only when the two threshold conditions are fulfilled - that is to say, an image is classified as having less probability than the inter-ictal threshold by the inter-ictal specialized network, and also as having more probability than the pre-ictal threshold by the pre-ictal specialized network, can the image be counted for the firing power technique and, therefore, count for the raising of an alarm. So, the results in the table can be achieved by using the presented inter-ictal and pre-ictal thresholds together for each combination of experiment (type of network + patient + pre-ictal time).

In-depth discussion will be given in the next chapter.

The duration of the test for each patient can be found in Table 8.

Table 9 – Results of the 81x81 network and AlexNet network experiments.

Patient Number	Pre-Ictal Time	81x81				AlexNet			
		Sensitivity	FPR/h	Inter-ictal threshold	Pre-Ictal threshold	Sensitivity	FPR/h	Inter-ictal threshold	Pre-Ictal threshold
1	5	0.66	0.11	0.59	0.62	0.66	0.11	0.38	0.72
	10	0.66	0.26	0.52	0.67	0.66	0.14	0.49	0.7
	15	0.66	0.67	0.65	0.47	0.66	0.47	0.51	0.4
2	5	0.43	0.28	0.7	0.46	0.43	0.42	0.59	0.62
	10	0.57	0.31	0.55	0.65	0.71	0.4	0.62	0.61
	15	0.57	0.8	0.7	0.55	0.71	0.83	0.61	0.61
3	5	0.66	0.41	0.63	0.7	1	0.66	0.5825	0.51
	10	1	0.9	0.57	0.65	0.66	0.5	0.57	0.497
	15	0.66	0.49	0.6	0.59	0.33	0.52	0.53	0.5
4	5	0.5	0.62	0.39	0.5	1	0.5	0.49	0.51
	10	0.66	0.63	0.49	0.4	0.66	0.66	0.5	0.46
	15	0.66	0.75	0.54	0.45	0.66	0.91	0.47	0.532
5	5	0.57	0.59	0.6	0.5	0.71	0.57	0.6	0.58
	10	0.57	0.45	0.62	0.58	0.42	0.59	0.54	0.54
	15	0.57	0.51	0.61	0.52	0.57	0.66	0.52	0.55
6	5	0.66	0.41	0.49	0.66	1	0.44	0.515	0.55
	10	0.66	0.29	0.45	0.56	0.66	0.23	0.495	0.58
	15	0.66	0.64	0.71	0.4	0.66	0.47	0.505	0.55

5.2 - AlexNet Dynamic Images vs Mean Images

For the second round of experiments, it was decided to try and improve the AlexNet classification architecture built for the first experiment.

As in the first experiment AlexNet 227x227 images were built by simply adding padding to the image taken from the signal, it meant that only around 12% of the space of the 227x227 image that the AlexNet needs was being used.

As such, in this second experiment, an attempt to improve classification of the AlexNet in this problem, by increasing the useful space in the image, was done.

This experiment was applied to all the six patients, and tested on 5, 10 and 15 minutes, and with three specialized CNNs (one more than the first round of experiments): one to distinguish between inter-ictal and non-inter-ictal, another to distinguish between pre-ictal and non-pre-ictal, and the last one, to classify an images into inter-ictal and pre-ictal.

All networks were trained with 100 epochs, an initial learning rate of 0.001 and a mini batch size of 64. Again, the time it took to train each network depended on various

factors, namely on the number of images selected for training. As some patients had more recorded seizures than others, they would have more images selected for training and would take more time to train.

5.2.1 – Dynamic Images

For this experiment, the signal was again processed by applying a 1-256 Hz bandpass filter, a 50 Hz notch filter and then normalized. Then, after dividing the signal in the needed time windows, each with 227 instances, the dynamic images method explained in the 4.3.2 subsection was used to create the images. So, the first 5 lines and the last 6 are all 0's, because the algorithm only needs 216 lines (8 times 27). Starting in the 8th image, an image is created using the preceding 7 images, in order from top to bottom, and on the last 27 lines before the bottom padding, the current image.

After all images are created, selection is done to balance their number for the training of each of the three CNNs (Inter vs Non-inter; Pre vs Non-pre; and Inter vs Pre) are trained. The selected images would then be used to train the AlexNet network explained in the 4.3.5 subsection.

Finally, while in testing, the dedicated signal was processed the same way the training one was, to create similar images. Those images were then given to the trained networks for classification. After obtaining their predictions, the technique explained in subsection 4.4.1 was applied to process these predictions and obtain the performance metrics.

In Figure 36 (inter-ictal specialized), Figure 37 (pre-ictal specialized) and Figure 38 (inter-ictal vs pre-ictal network), the training progress of one of the dynamic images AlexNet networks can be seen.

# Seizure Prediction with Specialized Classifiers and Image Processing
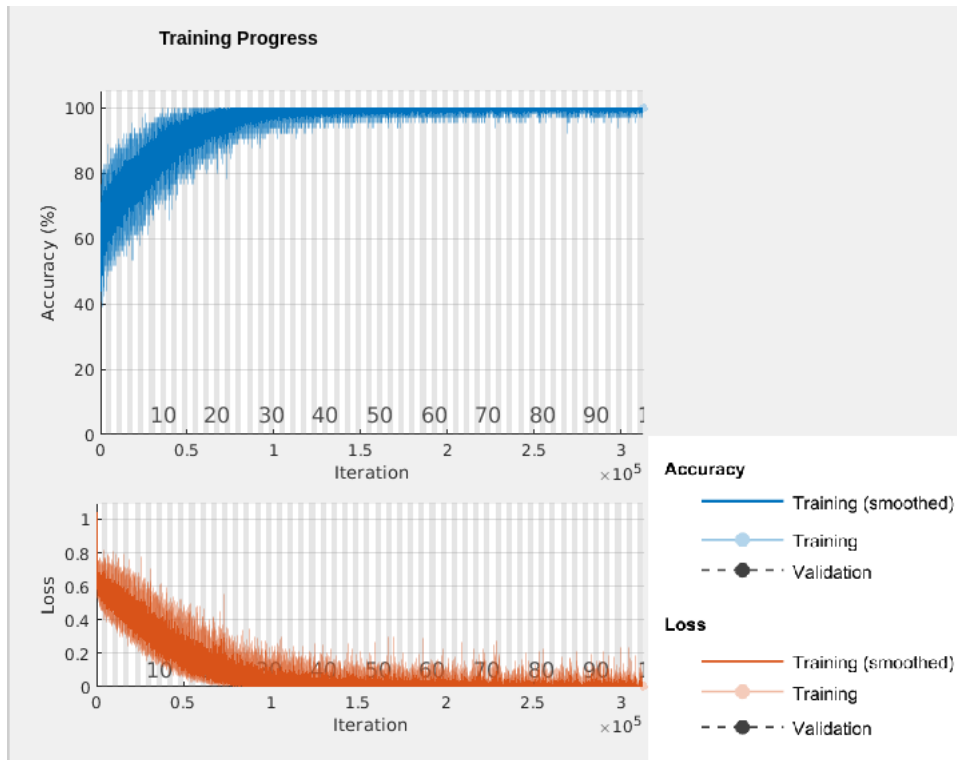
Figure 36 - Training progress of the inter-ictal specialized dynamic image AlexNet network.
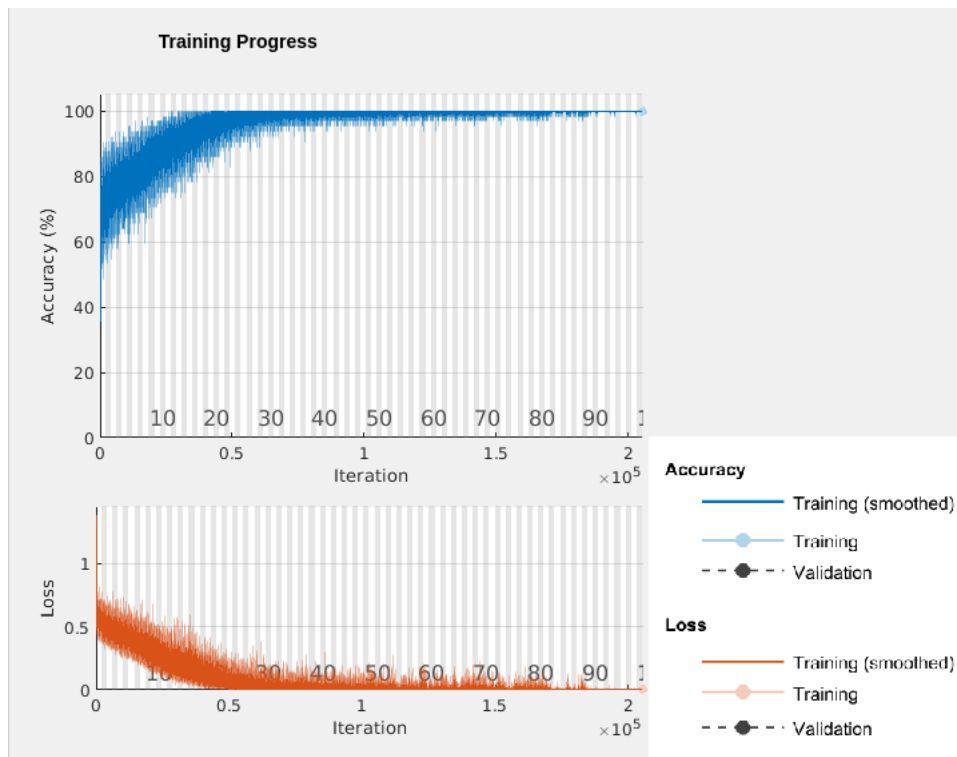
Figure 37 - Training progress of the pre-ictal specialized dynamic image AlexNet network.
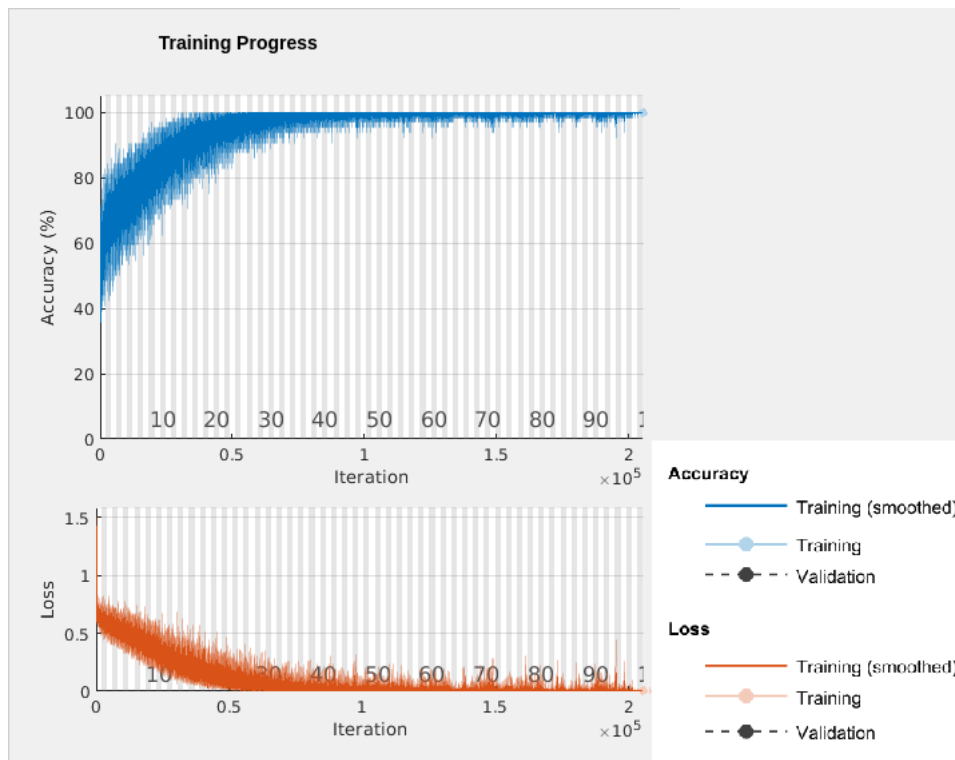
Figure 38 - Training progress of the inter-ictal vs pre-ictal dynamic image AlexNet network.

5.2.2 – Mean Images

The second experiment inside this round was another attempt to fill in the 227 lines of the 227x227 image required for the AlexNet. The dynamic images are a big improvement in useful space usage in that image, with only 11 lines being occupied by 0's. To get to 100%, with all 227 lines filled, mean images were thought of, that use the current and the 226 preceding images.

So, to create them, the signal was again processed by applying a 1-256 Hz bandpass filter, a 50 Hz notch filter and then normalized. Then, after dividing the signal in the needed time windows, each with 227 instances, the mean images method explained in the 4.3.2 subsection was used to create the images. So, the current and the last 226 images' mean of each of the 227 columns was calculated, forming 227 1x227 images. These images were then joined with older ones to current from top to bottom (older ones on top, newer on bottom). The last line is the mean of all the lines of the current image.

After that, selection is done to balance the number of images with which the training of each of the three CNNs (Inter vs Non-inter; Pre vs Non-pre; and Inter vs Pre) will be trained. The selected images would then be used to train the AlexNet network explained in the 4.3.5 subsection.

Finally, in testing, the testing signal was processed the same way the training one was, to create similar images. Those images were then given to the trained networks for classification. After obtaining their predictions, the technique explained in subsection 4.4.1 was applied to process these predictions and obtain the performance metrics.

In Figure 39 (inter-ictal specialized), Figure 40 (pre-ictal specialized) and Figure 41 (inter-ictal vs pre-ictal network), the training progress of one of the dynamic images AlexNet networks can be seen.

Training of this types of networks was done with only 10 epochs, since it converged quickly to 100% training accuracy. This shows the advantage of transfer learning.
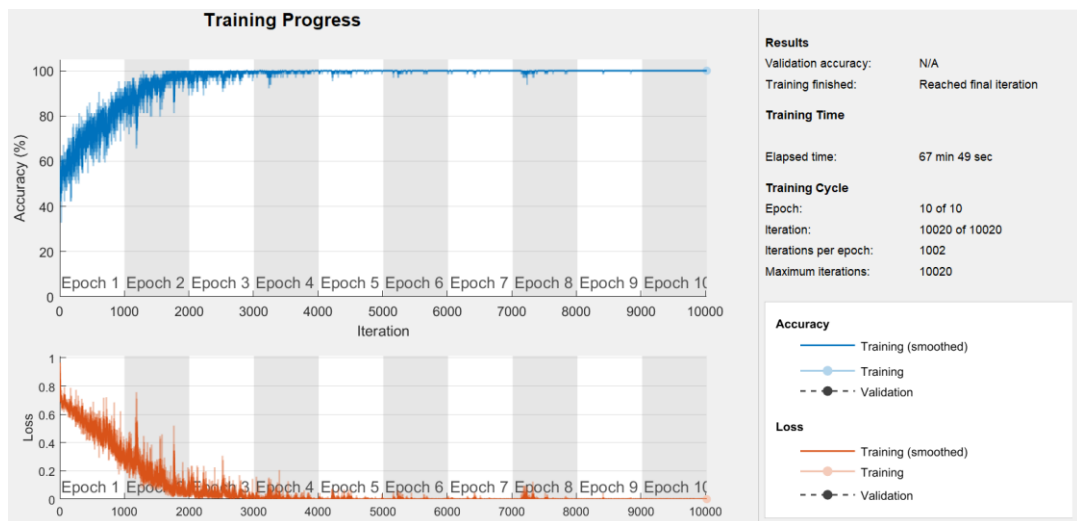
Figure 39 - Training progress of the inter-ictal specialized mean image AlexNet network.
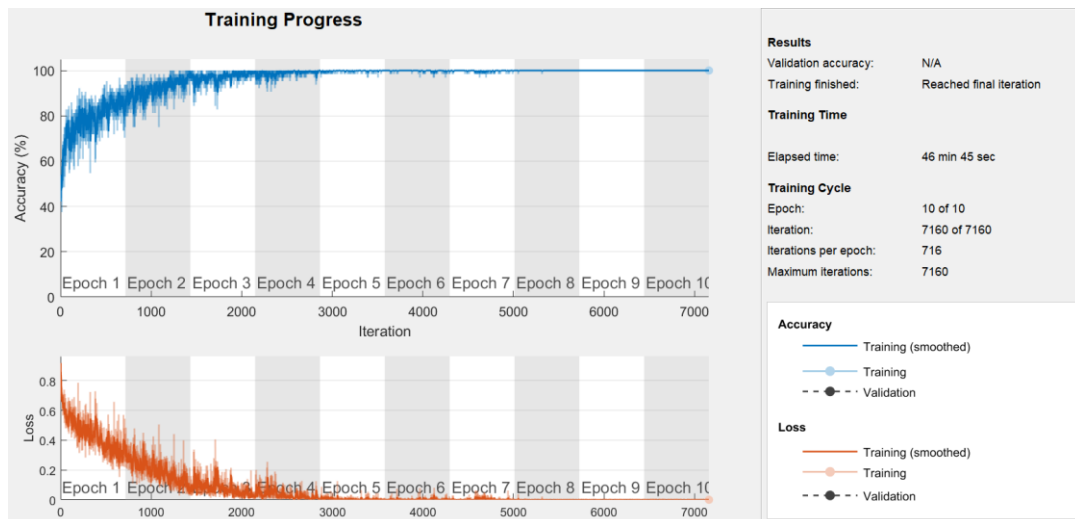
Figure 40 - Training progress of the pre-ictal specialized mean image AlexNet network.
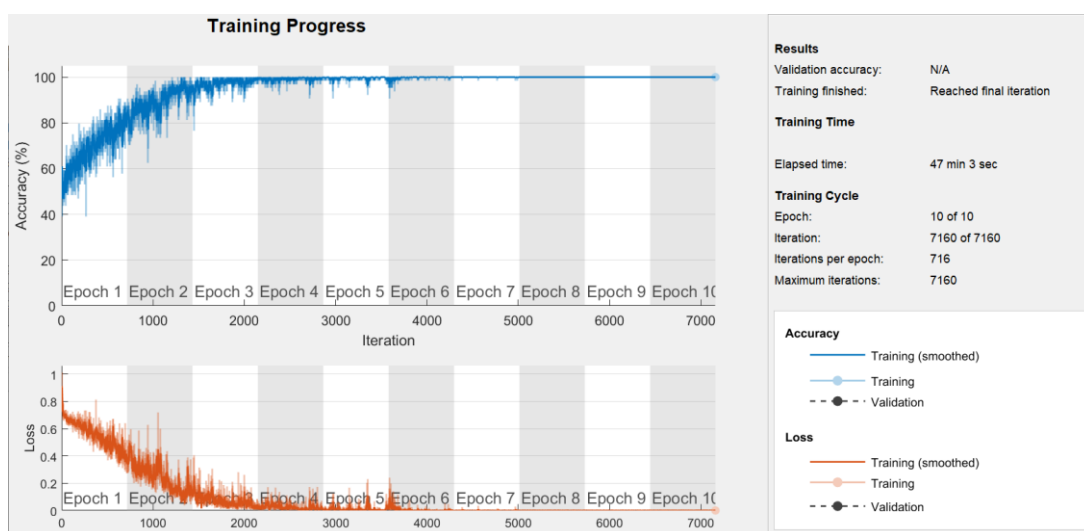
Figure 41 - Training progress of the inter-ictal vs pre-ictal mean image AlexNet network.

5.2.3 – Results

In Table 10, the results of the dynamic networks test are presented. Mean images proved themselves to not be able to predict. As can be seen in Figure 42, Figure 43 and Figure 44, the spikes in probability of being of each class are not distinguishable in any of the different stages. As such, this experiment was dropped, and it was decided to continue with the dynamic images for the next round of experiments.

The duration of the test for each patient can be found in Table 8.

Seizure Prediction with Specialized Classifiers and Image Processing

Table 10 – Results of testing with dynamic images in all six patients, with pre-ictal times of 5, 10 and 15 minutes.

Patient Number	Pre-ictal Time	Sensitivity	FPR/h	Inter-ictal Threshold	Pre-ictal Threshold	Inter vs Pre Threshold
1	5	0.66	0.19	0.675	0.7	0.55
	10	1	0.12	0.65	0.6	0.45
	15	1	0.31	0.85	0.5	0.2
2	5	0.43	0.22	0.8	0.15	0.4
	10	0.43	0.28	0.6	0.15	0.45
	15	0.43	0.44	0.65	0.15	0.35
3	5	0.66	0.38	0.8	0.3	0.35
	10	0.33	0.11	0.8	0.5	0.5
	15	0.66	0.47	0.75	0.3	0.3
4	5	0.5	0.51	0.6	0.2	0.2
	10	0.33	0.44	0.7	0.35	0.35
	15	0.5	0.56	0.9	0.4	0.2
5	5	0.57	0.33	0.65	0.25	0.2
	10	0.57	0.47	0.85	0.45	0.35
	15	0.57	0.31	0.65	0.3	0.45
6	5	1	0.36	0.8	0.25	0.1
	10	1	0.43	0.75	0.45	0.1
	15	1	0.41	0.8	0.25	0.1
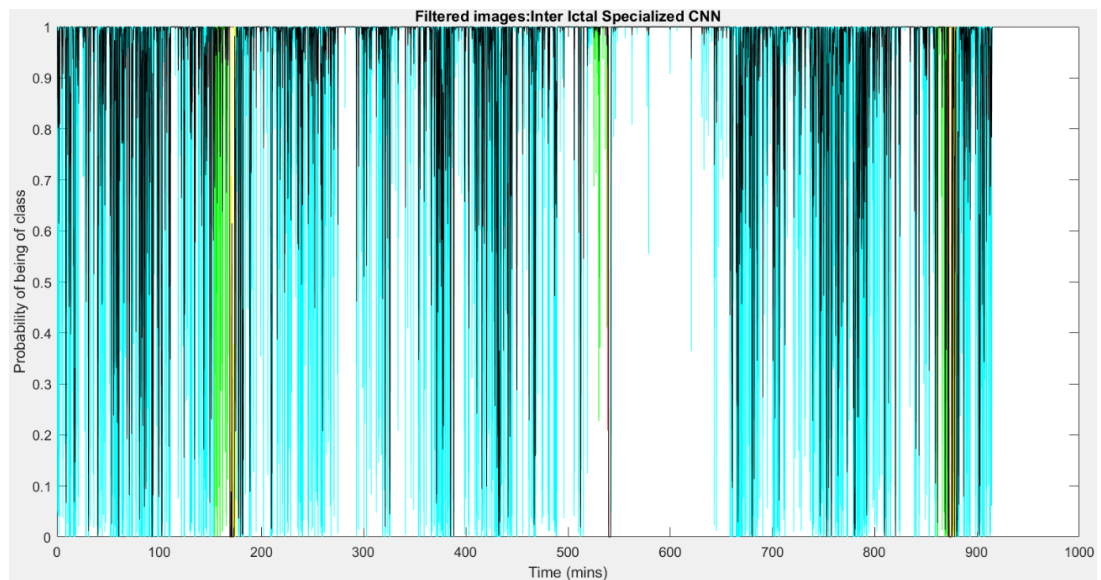
Figure 42 – Prediction of the inter-ictal specialized mean images network.
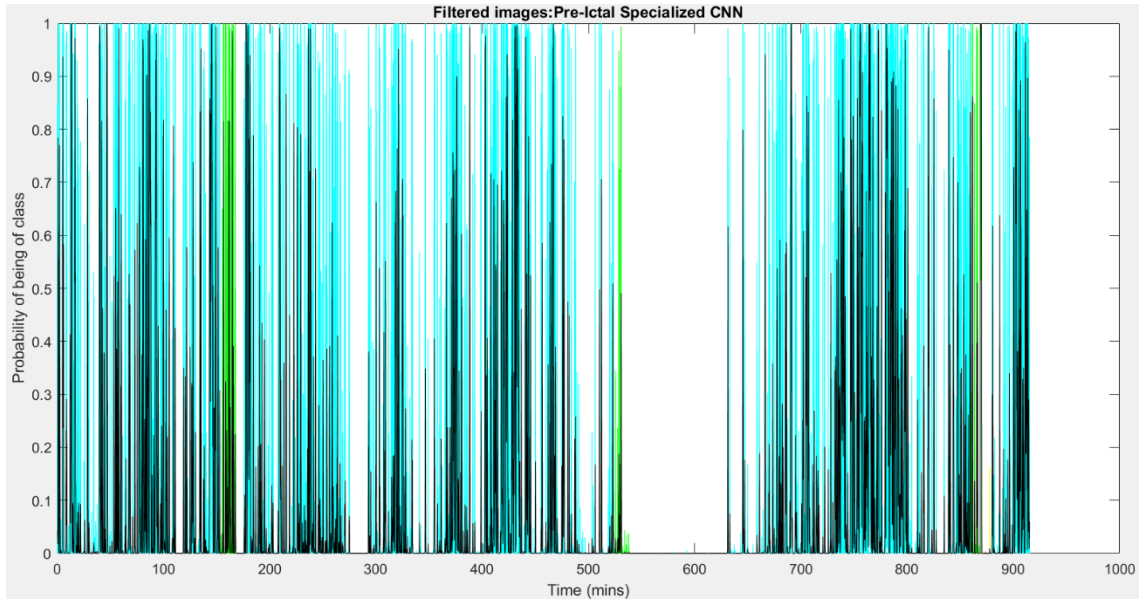
Figure 43 - Prediction of the pre-ictal specialized mean images network.
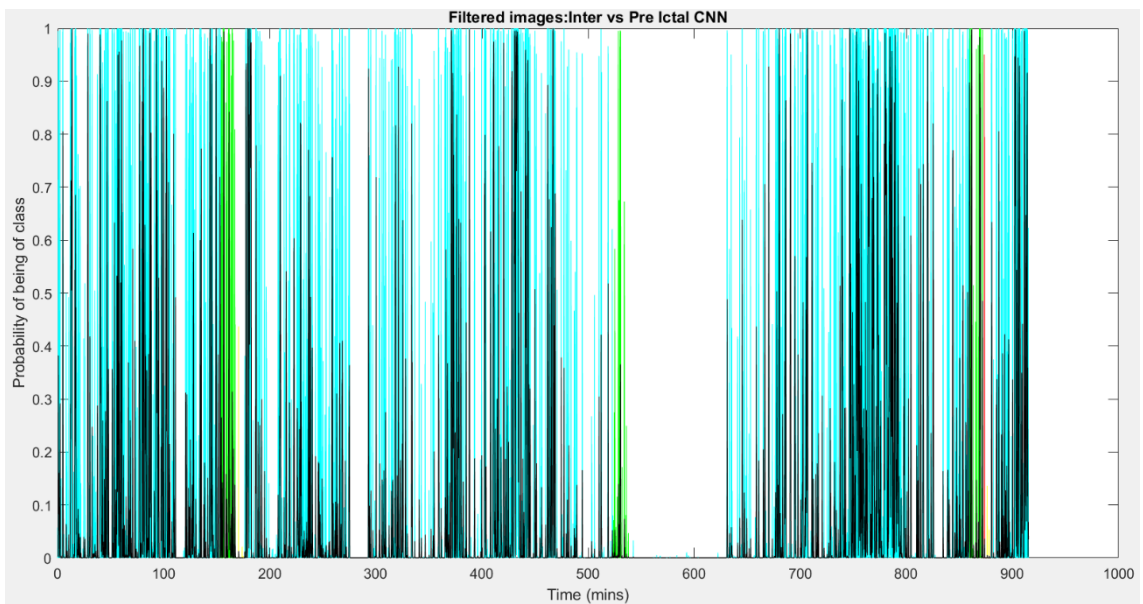
Figure 44 - Prediction of the inter-ictal vs pre-ictal mean images network.

5.3 - Final Experiment – Image Processing

To try and further improve the AlexNet classification of images created from the raw signal, in the final round of experiments, processing was applied to the dynamic images. As shown in the preceding experiments, mean images showed no capacity to predict, so dynamic images were the chosen ones to be the base of this final experiment. In fact, normal dynamic images are also included in this experiment, not only for comparison, but also because the pre-ictal times were expanded to also include 30 and 40 minutes. So, in this experiment, normal dynamic images, contrast dynamic images and reconstructed dynamic images were the ones used. Each willl be better explained in the following subsections.

These experiments were done to all six patients and, as already stated, the pre-ictal times tested were extended to 40 and 30 minutes, beyond the usual 5, 10 and 15 minutes done in the preceding experiments. Finally, 3 CNNs were trained: one to classify between inter-ictal and non-inter-ictal, another to distinguish between pre-ictal and non-pre-ictal and the last one, to classify images into inter-ictal and pre-ictal. In this third network, ictal and post-ictal instances are not considered in training, hoping to better differentiate between inter-ictal and pre-ictal. In testing, those instances will be classified into one of inter-ictal or pre-ictal, which will obsviously be wrong. But working together with two other specialized networks capable of making that distintion will help the whole system overcome that fact. So, this last network will try to improve the other two, by trying to make a more certain distintion between ictal and pre-ictal than the other networks can make.

All networks were trained with 100 epochs, an initial learning rate of 0.001 and a mini batch size of 64. Again, the time it took to train each network depended mainly on the number of images selected for training. As some patients had more recorded seizures than others, they had more images selected for training and, therefore, took more time to train.

5.3.1 – Dynamic Images

The dynamic images used for this experiment are exactly the same as the last experiment (explained in 5.2.1). The only difference between this and 5.2.1 was that here, networks were also trained for 30 and 40 minutes of pre-ictal, in addition to the 5,10 and 15 from last experiment.

5.3.2 – Contrast Images

First, the signal was processed by applying a 1-256 Hz bandpass filter, then a 50 Hz notch filter and then normalized. After that, the signal was divided in the needed time windows, each with 227 instances, and the dynamic images method explained in the 4.3.2 and 5.2.1 subsections was used to create the images. The contrast method explained in subsection 4.3.4 was then used to apply contrast and finalize the creation of the images for this experiment.

With the images created, a balanced set of images was selected to train each of the three CNNs (Inter vs Non-inter; Pre vs Non-pre; and Inter vs Pre). Those selected images would then be used to train the AlexNet network explained in the 4.3.5 subsection.

Finally, in testing, the testing signal was processed the same way the training one was, to create similarly contrasted images. Those images were then given to the trained networks for classification to obtain their predictions. The technique explained in subsection 4.4.1 was then applied to process these predictions and obtain the performance metrics. In Figure 45 (inter-ictal specialized), Figure 46 (pre-ictal specialized) and Figure 47 (inter-ictal vs pre-ictal network), the training progress of one of the dynamic images AlexNet networks can be seen.
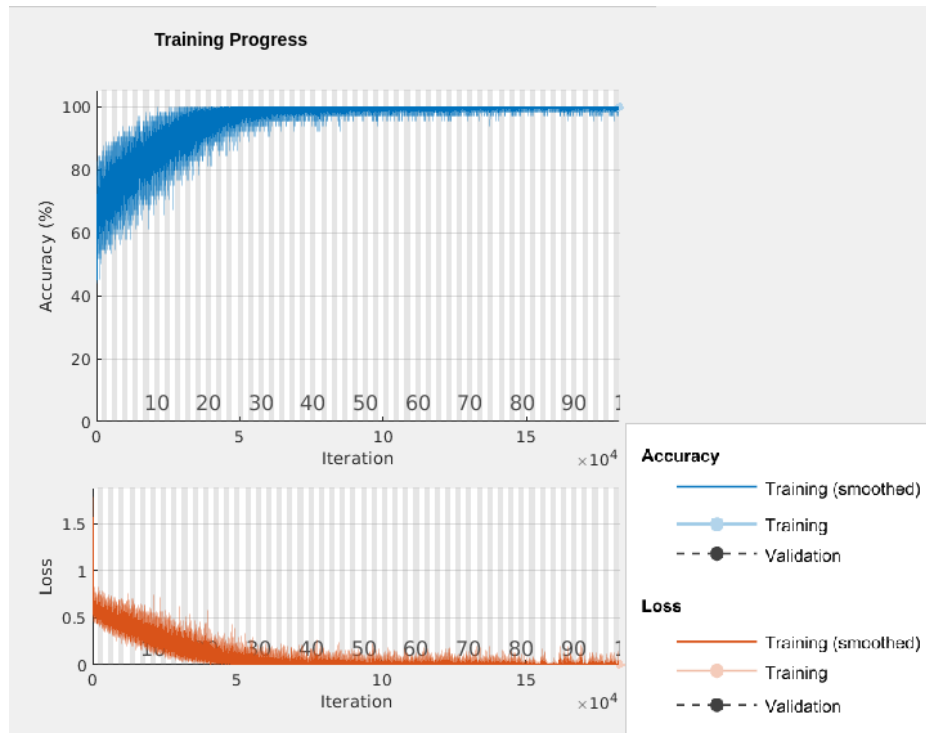
Figure 45 - Training progress of the inter-ictal specialized contrast enhanced dynamic image AlexNet network.
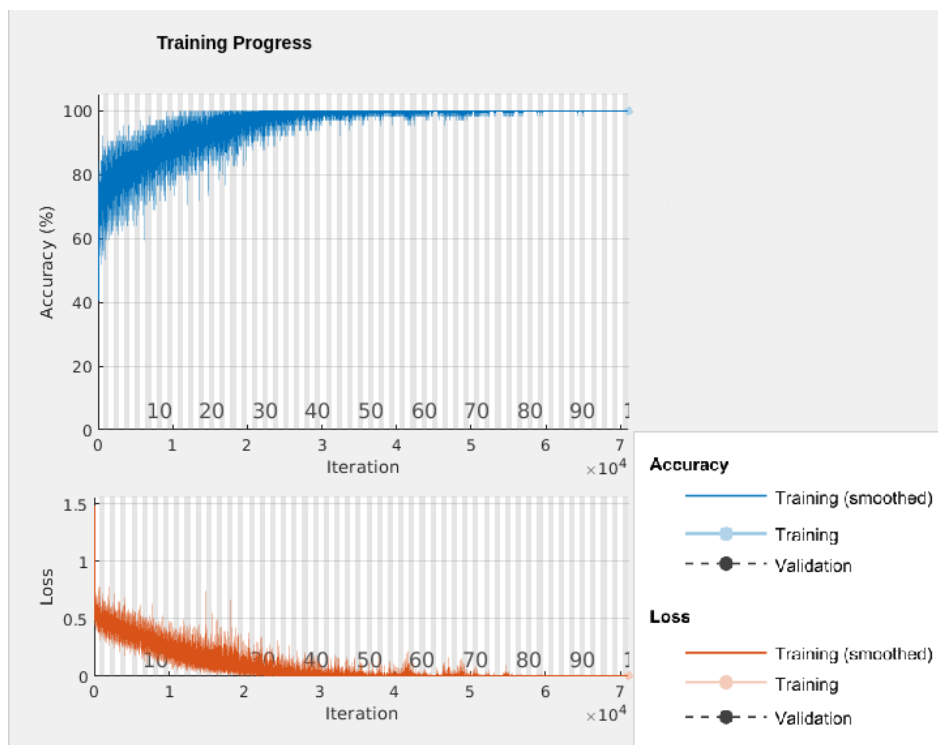
Figure 46 - Training progress of the pre-ictal specialized contrast enhanced dynamic image AlexNet network.
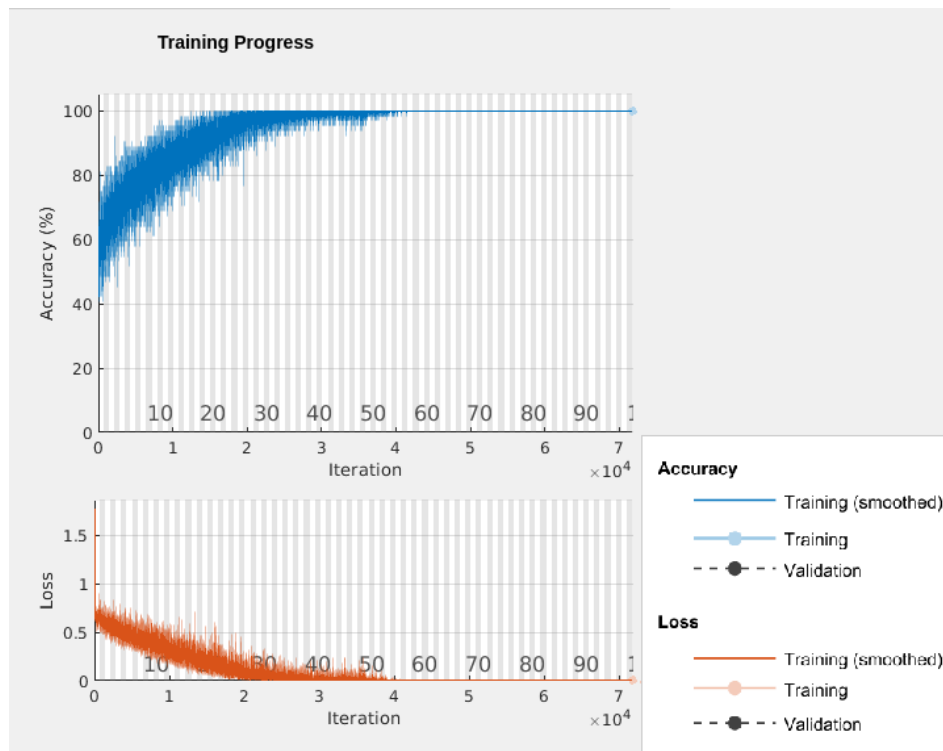
Figure 47 - Training progress of the inter-ictal vs pre-ictal contrast enhanced dynamic image AlexNet network.

5.3.3 – Reconstructed Images

The last experiment had the objective of checking the performance of applying several different image processing methods to the normal 227x227 dynamic image.

So, after processing the signal with a 1-256 Hz bandpass filter, a 50 Hz notch filter, normalizing it, and dividing it in the needed time windows, each with 227 instances, the dynamic images method explained in the 4.3.2 – 227x227 images and 5.2.1 subsections was used to create the images.

These images were then processed. This process started by applying contrast enhancement to the base image. Then, the possible image objects' edges were enhanced with sharpening. This operation is followed by the reconstruction explained in subsection 4.3.4. Finally, MATLAB Image Processing Toolbox's *imcomplement* method was applied, to make the image predominantly darker.

This last method was applied to make the images more distinct from the other sets and, attempt to improve classification by having a predominantly darker image. Because of

the nature of the filters (Figure 27) in a CNN, 0's may have more influence than a whiter (with more 1's) image.

After that, three balanced sets of images were selected to train each of the specialized AlexNet network explained in the 4.3.5 subsection.

Finally, in testing, the testing signal was processed the same way the training one was, to create similar images. Those images were then given to the trained networks for classification to obtain their predictions. The technique explained in subsection 4.4.1 was then applied to process these predictions and obtain the performance metrics.

5.3.4 - Results

In Table 11, Table 12 and Table 13, results from test of these three experiments are presented. The best result for each combination of patient + pre-ictal + type of image was selected using the technique explained in subsection 4.4.1. These results will be discussed in-depth in the next chapter.

The duration of the test for each patient can be found in Table 8.

Table 11 – Results of normal dynamic image AlexNet for 5, 10, 15, 30 and 40 minutes of pre-ictal.

Patient Number	Pre-ictal Time	Sensitivity	FPR/h	Inter-ictal Threshold	Pre-ictal Threshold	Inter vs Pre Threshold
1	5	0.66	0.19	0.675	0.7	0.55
	10	1	0.12	0.65	0.6	0.45
	15	1	0.31	0.85	0.5	0.2
	30	0.66	0.35	0.9	0.4	0.15
	40	0.66	0.46	0.8	0.35	0.2
2	5	0.43	0.22	0.8	0.15	0.4
	10	0.43	0.28	0.6	0.15	0.45
	15	0.43	0.44	0.65	0.15	0.35
	30	0.43	0.67	0.45	0.2	0.2
	40	0.29	0.47	0.5	0.45	0.45
3	5	0.66	0.38	0.8	0.3	0.35
	10	0.33	0.11	0.8	0.5	0.5
	15	0.66	0.47	0.75	0.3	0.3
	30	0.66	0.73	0.75	0.3	0.15
	40	0.33	0.36	0.65	0.1	0
4	5	0.5	0.51	0.6	0.2	0.2
	10	0.33	0.44	0.7	0.35	0.35
	15	0.5	0.56	0.9	0.4	0.2
	30	0.5	0.82	0.775	0.3	0.3
	40	0.5	0.87	0.6	0.3	0.25
5	5	0.57	0.33	0.65	0.25	0.2
	10	0.57	0.47	0.85	0.45	0.35
	15	0.57	0.31	0.65	0.3	0.45
	30	0.57	0.54	0.55	0.45	0.45
	40	0.57	0.53	0.8	0.45	0.35
6	5	1	0.36	0.8	0.25	0.1
	10	1	0.43	0.75	0.45	0.1
	15	1	0.41	0.8	0.25	0.1
	30	0.66	0.48	0.7	0.2	0.2
	40	0.66	0.44	0.6	0.3	0.4

Table 12 - Results of contrast enhanced dynamic image AlexNet for 5, 10, 15, 30 and 40 minutes of pre-ictal.

Patient Number	Pre-ictal Time	Sensitivity	FPR/h	Inter-ictal Threshold	Pre-ictal Threshold	Inter vs Pre Threshold
1	5	0.66	0.06	0.625	0.65	0.45
	10	1	0.12	0.75	0.775	0.525
	15	1	0.35	0.85	0.5	0.2
	30	0.66	0.3	0.8	0.5	0.15
	40	0.66	0.15	0.7	0.2	0.4
2	5	0.43	0.24	0.75	0.4	0.05
	10	0.43	0.37	0.6	0.25	0.25
	15	0.43	0.46	0.55	0.35	0.05
	30	0.43	0.54	0.6	0.65	0.2
	40	0.43	0.53	0.7	0.5	0.5
3	5	0.66	0.34	0.75	0.35	0.35
	10	0.33	0.16	0.7	0.65	0.3
	15	0.66	0.58	0.75	0.3	0.3
	30	0.66	0.82	0.75	0.2	0.15
	40	0.66	1	0.75	0.15	0.15
4	5	0.33	0.33	0.85	0.2	0.4
	10	0.5	0.27	0.7	0.35	0.35
	15	0.33	0.56	0.8	0.3	0.3
	30	0.66	1.12	0.8	0.2	0.2
	40	0.17	0.54	0.5	0.25	0.3
5	5	0.57	0.43	0.85	0.4	0.3
	10	0.57	0.37	0.55	0.15	0.15
	15	0.57	0.27	0.55	0.3	0.45
	30	0.57	0.54	0.6	0.15	0.5
	40	0.57	0.53	0.7	0.4	0.45
6	5	1	0.4	0.7	0.15	0.15
	10	1	0.35	0.85	0.35	0.3
	15	1	0.35	0.8	0.1	0.1
	30	0.33	0.16	0.5	0.2	0.3
	40	0.66	0.4	0.65	0.3	0.45

Table 13 - Results of reconstructed dynamic image AlexNet for 5, 10, 15, 30 and 40 minutes of pre-ictal.

Patient Number	Pre-ictal Time	Sensitivity	FPR/h	Inter-ictal Threshold	Pre-ictal Threshold	Inter vs Pre Threshold
1	5	0.66	0.11	0.7	0.55	0.375
	10	0.66	0.19	0.5	0.5	0.35
	15	0.66	0.23	0.7	0.45	0.35
	30	0.66	0.4	0.85	0.4	0.3
	40	0.66	0.61	0.55	0.2	0.2
2	5	0.29	0.23	0.6	0.2	0.4
	10	0.43	0.35	0.6	0.5	0.5
	15	0.43	0.37	0.9	0.15	0.5
	30	0.43	0.47	0.85	0.2	0.5
	40	0.43	0.67	0.8	0.5	0.3
3	5	0.33	0.02	0.5	0.15	0.1
	10	0.33	0.08	0.8	0.15	0.55
	15	0.66	0.39	0.55	0.6	0.25
	30	0.66	1	0.85	0.2	0.25
	40	0.66	0.64	0.7	0.35	0.25
4	5	0.5	0.42	0.65	0.5	0.3
	10	0.5	0.27	0.65	0.5	0.45
	15	0.33	0.21	0.65	0.6	0.45
	30	0.5	0.51	0.55	0.4	0.5
	40	0.5	0.93	0.5	0.35	0.5
5	5	0.57	0.54	0.85	0.45	0.3
	10	0.57	0.42	0.75	0.7	0.15
	15	0.57	0.35	0.55	0.55	0.5
	30	0.57	0.54	0.7	0.15	0.65
	40	0.57	0.58	0.4	0.25	0.2
6	5	1	0.4	0.7	0.05	0.1
	10	1	0.27	0.7	0.25	0.2
	15	1	0.36	0.75	0.075	0.125
	30	0.66	0.73	0.7	0.15	0.1
	40	0.66	0.4	0.8	0.1	0.1

Chapter 6
Discussion

In this chapter, the results obtained from the experiences presented in the last chapter will be discussed. There will also be a reflection about what was, what was not and what can be done in the future about this work and his topic.

6.1 - Result discussion

From the information given throughout chapter 5's result tables, the results from the tests of the methods were not good but leave a lot open to be done in the future to be improved. Except for shorter pre-ictal times in the first patient, none of the other patients, regardless of type of image used, or type of processing was applied to image, had 100% sensitivity with an FPR/h below 0.15 (which is a good maximum FPR/h suggested by Winterhalder et al. [10]).

6.1.1 – First round of experiments

The first round of experiments compared two different types of networks. Its main objective was to test if an already recognized network would improve a network created in this work.

Results analysis

The results from this experiment are presented in Table 9.

Looking at the table, it is very rare to be able to predict all seizures in each patient. When it can do so, it is done with very high FPR/h, regardless of the network.

For the first patient, both networks can only correctly predict 2 out of 3 seizures but, overall, AlexNet does so with lower FPR/h values. The best result, the prediction for 5 minutes of pre-ictal is the same for both, correctly predicting 2 out of 3 seizures with an

FPR/h of only 0.11. In the rest, though, AlexNets presents lower FPR/h for the same sensitivity, which makes it better overall.

As for the second patient, the results are mixed. Even though for 5 minutes, the 81x81 network predicts the same number of seizures with lower FPR/h, it is still a quite high value. For 10 mintues, AlexNet predicts 1 more seizure than the 81x81, but does so with 0.09 more FPR/h. Nevertheless, these FPR/h values are too high to be deemed acceptable.

In the third patient, AlexNet achieves 100% sensitivity with less FPR/h than the 81x81 network. The best result for both networks happen in different pre-ictal times, with 81x81 correctly predicting all seizures with 10 minutes of pre-ictal and AlexNet achieving 100% with 5 minutes. FPR/h is 0.3 less in AlexNet for the 100%, but the value with which it does so is too high.

For the fourth patient, AlexNet shows itself to be superior again, correctly predicting 100% of the seizures with an FPR/h of 0.5. None of the 81x81 network pre-ictal times get to 100% and even the best results they achieve have a higher FPR/h than the one AlexNet got.

In the fifth patient, the better network is debatable. While the 81x81 network predicts 4 out of 7 seizures while having an FPR/h of 0.45, AlexNet padded image network correctly predicts 5 out of 7 seizures with an FPR/h of 0.57. While AlexNet was able to predict more, it did so with 0.12 more in FPR/h. Whichever one considers to be best, the values are too high to be considered a success.

The same case as the last one occurs here, with 81x81 correctly predicting 2 out of 3 seizures with 0.29 FPR/h and AlexNet predicting all 3 with an FPR/h of 0.44. While 0.29 is not such a bad value compared to other ones, when considered that there are only 3 seizures to test this patient, it may still seem like a high value. 0.44 is clearly high when looked at it this way.

Considerations

So, in general, AlexNet predicts better and with less FPR/h than the 81x81 network. It is not an unexpected result, since AlexNet is a famous network already recognized by the community. Even so, the results when applied to seizure prediction images built the way

they were for this experiment are not at all satisfactory, with FPR/h values being too high, except for one patient.

As such, it was decided that in the next experiments AlexNet would be used as the main classifier. The way to try to improve the classification for the next experiment, would be by adding one more specialized network to work together with the two already in use in this first experiment and by figuring out better ways to build images.

Even though the 81x81 network was able to get the best result for the first patient, it happens just once, for a patient that has good results in almost all the possible combinations. In the rest of the patients, it could not achieve equal or better results than the AlexNet.

It could still be worth following through with the 81x81 network, though. Factors such as being able to change the size of image in use without needing to change the whole network's structure and, as such, try more ways to build images from the signal could be followed to try and improve results in it. The results of this experiment, allied with the fact that there is still no attempt to adapt the AlexNet to this problem and the yet unexplored different possibilities of building images to train the network outweighed the 81x81 network when it came to making the decision.

6.1.2 – Second Round of Experiments

The second round of experiments served to compare to different types of methods to build images from the signal, to train the AlexNet.

So, mean images were to be tested against dynamic images. When it came to predict mean images proved themselves not to be able to create distinguishing features in the pre-ictal stage, making it impossible to predict anything at all.

As for the dynamic images, the results can be found on Table 10, but because these tests were expanded to more pre-ictal times in the next round of experiments, its results will only be discussed in the next section of this chapter.

Mean images seemed to have suffered from overfitting in training. As can be seen by Figure 42, Figure 43 and Figure 44, their training quickly converged to 100%, but when applied to the testing data, it wasn't able to create and distinguishing at all. Various

factors could contribute to that, like the fact that, to make the black line in those figures, only the last 45 images mean was considered. As mean images are built with the last 257 images information, that number may be smaller than needed.

In the end, the fact that so much information about the 27x227 image was reduced to only 1x127, allied with these results, it was decided to follow to the next round of experiments using the dynamic images.

6.1.3 – Final Round of Experiments

This last round was the most important and had as its objective to verify if applying several image processing techniques to the images would improve classification and lead to better seizure prediction.

So, three types of images were tested - normal images with no processing at all; images with contrast enhanced; and reconstructed images.

Normal Dynamic Images

These images were the same as used in the second round of experiments but expanded for 30 and 40 minutes of pre-ictal, in addition to the 5, 10 and 15 used before.

In Table 11, the results of the test of this type of images can be found.

For the first patient, with 10 and 15 minutes of pre-ictal, normal dynamic images achieved 100% of sensitivity on this patient. But only with 10 minutes, it had a good FPR/h, of only 0.12. Overall that best result is quite good. It is noticeable that, as the pre-ictal time increases, the FPR/h also increases, even when sensitivity starts to decrease at 30 minutes.

For the second patient, the algorithm only predicted 3 out of 7 seizures, which is not a good result, even if it is done with a relatively acceptable FPR/h of 0.22 for pre-ictal time of 5 minutes. Again, it is noticeable the increase of FPR/h with the increase of pre-ictal time.

As for the third patient, the best result in this patient was achieved with 5 minutes of pre-ictal, with 2 out of 3 seizures being predicted. Nonetheless, it is done with 0.38 of FPR/h, which isn't a good value.

In the fourth patient, again, the best result is obtained with a pre-ictal time of 5 minutes, correctly predicting 3 out of 6 seizures with an FPR/h of 0.5, which is a high value.

The fifth patient had as its best result the correct prediction of 4 out of 7 seizures with an FPR/h of 0.31. This is still quite a high value, especially considering that it is only predicting 57% of the seizures. This result was obtained with 15 minutes of pre-ictal.

Finally, for the sixth patient, the predictor was able to predict all seizures on this patient with an FPR/h of 0.36, with 5 minutes of pre-ictal. Higher times for pre-ictal reduce the sensitivity of this types of images, with higher FPR/h.

So, it is evident that these types of images don't benefit from long periods of pre-ictal time, always achieving the best results with low values. It's also visible that the FPR/h is still quite high, even when relaxing the sensitivity a bit.

Contrasted Dynamic Images

These were images created by simply enhancing the contrast of the normal dynamic images, to test if such processing method helped the multiple AlexNet make a better prediction.

In Table 12, the results of the test of this type of images can be found.

For the first patient, the algorithm with this type of image correctly predicts all of the seizures with an FPR/h of 0.12, which is a good value. With too little (5 minutes) or too high pre-ictal time, the sensitivity decreases and not all seizures are predicted.

As for the second patient, all pre-ictal times find only 3 out of the 7 seizures. FPR/h, though, increases with the pre-ictal time, with 5 minutes being the lowest at 0.24. This would be quite an acceptable value if all the seizures were predicted. With only 43% being predicted, 0.24 of FPR/h doesn't seem promising.

In the third patient, the best result was obtained with 5 minutes of pre-ictal, with only 2 out of 3 seizures being correctly predicted. To add to that, the prediction was done with an FPR/h of 0.34, which is quite a high value for predicting only 66%.

In the fourth patient, with 10 minutes of pre-ictal time, 50% of the seizures were correctly predicted with 0.27 of FPR/h. Again, 0.27 is not a very high FPR/h, but only finding 3 out of 6 seizures with that much FPR/h may not be very good.

In the fifth patient, the same thing happens as the fourth. 4 out of 7 seizures are correctly predicted with an FPR/h of 0.27. This happens with a pre-ictal time of 15 minutes, and all the other times found 57% of the seizures with a worse FPR/h.

Finally, in the sixth patient, all of the seizures are correctly predicted with 5, 10 and 15 minutes of pre-ictal time. With 10 and 15 minutes, the lowest FPR/h for this patient is a 0.35. It is still a quite a high value, though.

Like the normal dynamic images, higher pre-ictal times were consistently worse than lower ones. Even though it has better results in 4 out of these 6 patients, those FPR/h are still high and would probably cause more harm than good when applied in real-time to a patient.

Reconstructed Dynamic Images

These types of images involved several image processing techniques joined together to create a type of image quite different from the original ones. The main method used was reconstruction with dilation, but contrast, sharpening, and complement were also used to enhance several aspects of the image.

In Table 13, the results of the test of this type of images can be found.

For the first patient, reconstruction couldn't correctly predict all the seizures, with 5 minutes of pre-ictal producing the best results - 66% sensitivity with an FPR/h of 0.11.

In the second patient, the best result came from 10 minutes of pre-ictal correctly predicting 3 out of 7 seizures with an FPR/h of 0.35. Having such a high 0.35 FPR/h with quite a low sensitivity makes it so that even this best result is a bad one.

For the third patient, very low pre-ictal times (5 and 10) could only predict 1 out of 3 seizures, but with a very low FPR/h. With 15 minutes, 2 out of 3 seizures were correctly predicted with an FPR/H of 0.39 which, again, is high for the 66% sensitivity achieved.

In the fourth patient, the algorithm with this type of reconstructed dynamic images found 50% of the seizures with an FPR/h of 0.27. Again, this might be too high of a value to only correctly predict 3 out of 6 seizures.

For the fifth patient, all the pre-ictal times correctly predicted 57% of the seizures. The lowest FPR/h was 15 minutes, with 0.35. Just like in the last patients, such a high value of FPR/h with only 4 out of 7 correctly predicted seizures is not a good result.

Finally, in the sixth patient, the algorithm correctly predicted all the seizures with 0.27 of FPR/h with 10 minutes of pre-ictal. Even though the FPR/h is still not ideal, predicting all the seizures with such a value is one of the best results obtained by this work.

So, the reconstructed images didn't improve the results obtained by the other networks with normal or simply contrast enhanced images. Reconstructed images only had a better results in the sixth patient. As with the other types of images, the reconstructed ones also had high FPR/h, even in cases where sensitivity had to be relaxed to try and decrease the FPR/h.

Overall

In Table 14, a summary of the best results for each patient and the type of image that was used to obtain it can be seen. Also, for each of the best results in each patient, validation was applied to check if the created algorithm performed better than a random predictor.

Table 14 - Summary of best results for each patient.

Patient	Pre-ictal Time	Type of Processing	Sensitivity	FPR/h	Better than random predictor?
1	10	Normal/Contrast	1	0.12	Yes
2	5	Normal	0.43	0.22	Yes
3	5	Contrast	0.66	0.34	Yes
4	10	Contrast/Reconstruction	0.5	0.27	Yes
5	15	Contrast	0.57	0.27	Yes
6	10	Reconstruction	1	0.27	Yes

So, overall, lower pre-ictal times (from 5 to 15 minutes) worked best with this kind of algorithms, with 30 and 40 minutes never having the best results in any patient.

Also, contrast was the processing method that produced most best results for each patient.

Even so, the only patients where a good prediction (with very high sensitivity and low FPR/h) was made was the first and the last one. The first patients results is clearly very good, predicting all seizures with only 0.12 FPR/h. The sixth patient had 100% sensitivity,

with a relatively good FPR/h, even though it is still 0.12 above the 0.15 maximum suggested by Winterhalder et al. [10]. The other patients all presented high FPR/h and few seizures they were predicted.

6.2 – Comparison with other methods from the state of the art

Table 15 presents the results of some algorithms that used DL methods to do seizure prediction presented in state of art, along with this works. This work's results are represented by the results obtained from Table 14 - equations 1 and 2 were used over all patient's testing data (over 5288 minutes) to obtain the sensitivity and FPR/h shown in Table 15.

Table 15 – Comparison of this work's results with other works that used DL to classify.

Work	Database	Classifier	Sensitivity	FPR/h
Mirowski et al.	Freiburg	CNN	71%	0
Khan et al.	MSSM and CHB-MIT	CNN	87.8%	0.14
Zhou et al.	CHB-MIT	CNN	62%	-
Daoud et al.	CHB-MIT	Bi-LSTM	99.72%	0.004
Abdelhameed et al.	Bonn	Bi-LSTM	99%	-
This Work	EPILEPSIAE	Multi-CNNs	62%	0.25

The results obtained from this work do not look promising when compared to other works like in Table 15. It should be noted, however, that this work was done with the best database available for seizure prediction, which provides more realistic experiments. While CHB-MIT is still a good dataset, it lacks the amount of continuous data EPILEPSIAE does.

One needs to be careful when comparing these works. Very likely, the algorithms were developed in different conditions. A clear difference that is very common is on the data quality (duration and continuity over time) used to develop predictors. A predictor developed and tested in short-term data cannot be compared with a predictor developed and evaluated in long-term data, i.e. in a more realistic scenario.

The fact that some authors don't calculate FPR/h also doesn't help in comparing the results.

Overall, the sensitivity obtained in this work is quite low compared with what others have achieved, and the FPR/h, when compared with those who calculated it, is higher. In this work FPR/h is not very good, since it is 0.1 above the maximum proposed as an example by Winterhalder et al. [10].

Because different works used different datasets, and sometimes use different performance measures, it is questionable how they can be compared. In any case it can be concluded that this work still has a long way to go to make this algorithm better and perform with clinical application. Seizure prediction with multi-classifiers and image processing still has rich improvement possibilities.

6.3 – Some perspectives for improvements

There is still a lot to discuss in relation to this approach. So, in this section, effects of various parts of the algorithms, that can still be improved, and other possible ways to explore seizure prediction on the raw signal with DL methods will be discussed.

This work tried to explore several options within the range of the very scarcely explored road of applying DL methods to predict seizures from the raw EEG signal. It tried to do so by combining several DL classifiers working together, which is something no other work in this area tried to do before, and even experimented using an already famous DL classifier as a basis to that cooperation. Furthermore, it tried to improve prediction using image processing methods to the images.

6.3.1 - Signal Pre-processing

Seizure prediction using the raw signal is hard, because the signal is full of noise and interference from other types of signals in the body. In this work, 2 types of filters and a normalization were applied to try and decrease its effects on the useful part of the signal. In relation to this, there is still a lot to be tried. For this, pre-processing of the signal with ICA is a promising concept, as it splits the signal in its various independent

components, allowing for the reconstruction of the signal without the components that represent outside interference. Problem with this approach is that the several independent components are not always outputted in the same order. Solving this problem can help improve the remotion of undesired interference on the signal.

Another possible way to follow and try different approaches in pre-processing the signal, is to try different values for the bandpass filter, or even other filters. Also, other ways of normalizing and reducing the spikes can and should be tried.

Signal pre-processing wasn't something that was deeply studied in this work. Some preliminary tests were done before any real experiment, to verify which could be most useful for this work. In the end, processing was done by the method explained in section 4.3.1.

6.3.2 - Multi-classification with DL methods

The use of several specialized AlexNets working together to improve classification was not tested against an architecture that predicted with only one classifier distinguishing the various stages. In this work's case, various combinations of specialized classifiers were tried. The several networks helped each other by filtering spikes in probability that only happened in one of the predictions of a network.

There was, however, a big problem with complexity of the experiments. Running the script to predict took, in average, 14 seconds. Also, in average, 10 values of each of the thresholds were tested (value range was chosen beforehand to not include the ones who would yield abnormally high FPR/h values or 0 sensitivity), sometimes more, sometimes less. So, to obtain the predictions for all these combinations, it took, in average, 14*10*10*10 seconds, which is around 3.88 hours (the combination test was done in a computer with an Intel Core i7-8565U 1.8GHz CPU). If, on top of that, SOP time, SPH time and Firing Power threshold were also tested (with an average of 10 values each time), this value would reach 3880 hours just to obtain the best possible prediction for one pre-ictal time of one patient of one experiment.

The solution found was to manually test some values to find ones that yielded good results, by running the program, manually changing the variables and checking the results until one that produces better results was found. This way, some values were

skipped, but a lot of time was spared. The chosen values can be found on Table 7. Of course, the probability of being ideal is very low, but by this way the test could focus on finding the right combination of probabilities.

There is also the problem of the the black line in Figure 31. Just like in last paragraph, it had to be manually tested, so it also may not be the ideal value. A better study of this value is also a potential way to enhance the performance of this method.

In the same Figure 31, an advantage of predicting with this method can also be seen. The black line gives some interpretability to the classification. DL methods are not known for ther interpretability, but predicting using the softmax layer values helps to improve that aspect.

Also in relation to the decision making process, other different techniques could be used. An example is the use of Dempster-Shafer theory [95] to combine the outputs of the specialized networks.

The fact that, from the already known CNN architectures, only AlexNet was tested in this case is also worthy of metntion in this section. There are several more CNN architectures [86] that have proved themselves to have very good performance in other areas, like GoogleNet [87] or ResNet [88]. It would be interesting to see how they would apply to this problem or if making several different kinds of CNN architectures working together with each other to predict seizures would be create a good predictor.

6.3.3 - Image Creation and Processing

This work's main experiments ended up being related to the image creation and enhancement. This was because one of the most important part of classification with CNNs is the image creation. As such, several ways to create the images and process them were experimented.

For the construction of the images, several methods were tried. In the end, the method who proved to be better was the dynamic image construction. It doesn't mean that there isn't a better method to create the images. A lot of work can still be tried and experimented, as there are a lot of possibilities for the construction of images, squared or rectangular.

An example of such, is the fact that, in the AlexNet, the 2 out of the 3 color channels weren't used. The first channel was simply copied from the first to the other two, to

avoid altering the AlexNet, and possibly causing it to lose performance. A possibility for the future is explore them, for example, by dividing the channels in groups and, in each image, distribute them through the color channels (for example, reducing 27x227 image to 9x227x3 image). Then use the dynamic image construction method to create dynamic images that can used 3 times more past images than the ones tried in this work. With the example given, 9x227x3 images would create a dynamic image of 227x227x3 with the current image, as well as the past 25 (and only 2 lines filled with 0's).

As for image processing, the results of the experiences showed that it helped to improve results, especially when comparing the contrast enhanced images to the normal ones. There is still a need to try more image processing methods to improve classification, as it is something that hasn't yet been tried in this area and will surely help it. Also, the image processing methods tried in this work focused on processing each image individually. Using data from all the images looks like a more promising to successfully apply image processing methods to the seizure prediction, since it will help make the different types of images more distinguishable.

6.3.4 - Other Remarks

Another limitation of this work also came from the complexity of the algorithms created and the limited time to finish the work.

Ideally, these algorithms would be tested on more patients. This would have provided even more realistic results to this work. With access to the EPILEPSIAE database, there were a lot of possible patients to test in but, unfortunately, the time to pre-process, train, test and find the best combination of values on a patient took more time than initially expected.

Ultimately, a lot of methods were thought of, especially in the image creation and processing part of the algorithm, but could not be experimented in this work. In the future, this is certainly a path that should be explored, as it still has a lot to be experimented, with methods and ideas that have proven themselves useful in improving other areas.

Chapter 7
Conclusion

This thesis aim was to develop a seizure predictor that helps in the improvement of the quality of life of patients with refractory epilepsy. As such, an approach was proposed that aimed to use the raw EEG signal without feature extraction as a basis to train several Convolutional Neural Networks in parallel.

Thus, a search was carried out for relevant works in the prediction of epileptic seizures to deepen the knowledge about the different techniques used there.

A more specific state of the art on seizure prediction from raw EEG signal without feature extraction was then presented. From it, it was concluded that there are few studies carried out in this area. Those who did, admitted that they had a limitation in data they had access to train and test the algorithm. This limitation means that, when applied to real-time data, with many hours or even days of continuous EEG recording, it has not been possible to reproduce the published performances so far.

Concerning novelty of this work, it was also observed that no work in this area tried to improve image quality before training the networks, and none tried to put several specialized CNNs working together to predict seizures.

With the availability of the EPILEPSIAE database, the largest and most complete database with EEG records of epileptic patients, some of the difficulties presented by the studies found in the state of the art of this approach can, in part, be overcome. With MATLAB and the several toolboxes it provides, new ways to predict seizures using DL methods on raw signal could also be tried.

So, several algorithms were developed to try different ways to build and process images, and use them to train several CNNs, who would later work together to predict seizures. All the algorithms were based on an architecture like the one presented in the state of the art, but modified to include image creation and processing methods, as well as several CNNs predicting in parallel.

The experiments to test the created algorithms were divided in three rounds.

In the first round of experiments, two types of CNNs were tested – an 81x81 created for this work, and the AlexNet, with padded images. Results showed that both networks presented too high FPR/h but, overall, AlexNet with padded images was able to outperform the 81x81 network.

In the second, several methods to create the images for the AlexNet were also tried, with the methods creating padded images, dynamic images, and mean images. Dynamic images improved the results from the padded images, and the mean images could not create a distinguishable pattern nor threshold when tested.

Finally, in the last experiment, some processing methods were applied to the images, to see if image processing helped improving prediction. Those methods were mainly contrast enhancement and reconstruction, which were compared to prediction with images without processing. This experiment showed that shorter pre-ictal times worked best with this algorithm, and that, even though not always the best, contrast enhanced images created the best results for patients more frequently than normal or reconstructed images.

All the best results outperformed a random predictor, but when compared to the result achieved by other works, the 62% sensitivity and 0.25 of FPR/h obtained by the algorithms in this work couldn't reach the level of the best ones. However, one needs to be careful when making comparisons as, very likely, the algorithms were developed in different conditions.

The proposed algorithm still needs more testing and development until it can reach its full potential. Time limitations of this work, allied with the complexity of the created algorithms, didn't allow deep testing to check the ideal value to all the variables used in the prediction, nor in more patients.

There is still a lot to be tried in connection with this methodology, from different signal processing techniques to different image creation methods or different network combinations. There is potential in this algorithm, and it is worth to keep trying more and more, so that it can one day be able to help patients in their daily lives.

References

[1] Fisher, RS; Acevedo, C; Arzimanoglou, A; Bogacz, A; Cross, JH; Elger, CE; Engel, J; Forsgren, L; French, JA; Glynn, M; Hesdorffer, DC; Lee, BI; Mathern, GW; Moshé, SL; Perucca, E; Scheffer, IE; Tomson, T; Watanabe, M; Wiebe, S. «ILAE official report: a practical clinical definition of epilepsy». In *Epilepsia*, 55(4):475–482, 2014 https://dx.doi.org/10.1111%2Fepi.12550

[2] WHO. "Epilepsy Fact sheet". Accessed August 2021. https://www.who.int/news-room/fact-sheets/detail/epilepsy

[3] Viglione, S; Ordon, V; Martin, W; Kesler, C. (1973). "Epileptic seizure warning system". https://patents.google.com/patent/US3863625A

[4] Kwan, P; Brodie, MJ. "Early identification of refractory epilepsy". In *New England Journal of Medicine*, 342(5):314-319, 2000. https://doi.org/10.1056/nejm200002033420503

[5] Lehnertz, K; Litt, B. "The First International Collaborative Workshop on Seizure Prediction: summary and data description". In *Clinical Neurophysiology*, 116(3):493-505, 2005. https://doi.org/10.1016/j.clinph.2004.08.020

[6] Towle, VL; Bolaños, J; Suarez, D; Tan, K; Grzeszczuk, R; Levin, DN; Cakmur, R; Frank, SA; Spire, JP. "The spatial location of EEG electrodes: Locating the best-fitting sphere relative to cortical anatomy". In *Electroencephalography and Clinical Neurophysiology*, 86(1):1-6, 1993. https://doi.org/10.1016/0013-4694(93)90061-Y

[7] Palmini, A. "The concept of the epileptogenic zone: A modern look at Penfield and Jasper's views on the role of interictal spikes". In *Epileptic Disord*, 10(2):191, 2008. https://pubmed.ncbi.nlm.nih.gov/17012068/

[8] Goldberger, A; Amaral, L; Glass, L; Hausdorff, L; Ivanov, PC; Mark, R; Stanley, HE. "PhysioBank; PhysioToolkit; and PhysioNet: Components of a new research resource for complex physiologic signals.". In *Circulation*, 101(23):215-220, 2020. https://doi.org/10.1161/01.cir.101.23.e215

[9] AboutKidsHealth; "Invasive electroencephalography (EEG) monitoring before epilepsy surgery"; accessed August 2021. https://www.aboutkidshealth.ca/article?contentid=2056&language=english

[10] Winterhalder, M; Maiwald, T; Voss, H; Aschenbrenner-Scheibe, R; Timmer, J; Schulze-Bonhage, A. "The seizure prediction characteristic: a general framework to assess and

compare seizure prediction methods". In *Epilepsy & Behaviour*, 4(3):318-325, 2003. https://doi.org/10.1016/s1525-5050(03)00105-7

[11] Schelter, B; Winterhalder, M; genannt Drentrup, HF; Wohlmuth, J; Nawrath, J; Brandt, A; Schulze-Bonhage, A; Timmer, J. "Seizure prediction: the impact of long prediction horizons". In *Epilepsy Research*, 73(2):213-217, 2007. https://doi.org/10.1016/j.eplepsyres.2006.10.002

[12] Bou Assi, E; Nguyen, DK; Rihana, S; Sawan, M. "Towards accurate prediction of epileptic seizures: A review". In *Biomedical Signal Processing and Control*, 34:144-157, 2017. https://doi.org/10.1016/j.bspc.2017.02.001

[13] Mormann, F; Kreuz, T; Rieke, C; Andrzejak, RG; Kraskov, A; David, P; Elger, CE; Lehnertz, K. "On the predictability of epileptic seizures". In *Clinical Neurophysiology*, 116(3):569-587, 2005. https://doi.org/10.1016/j.clinph.2004.08.025

[14] Mirowski, P; Madhavan, D; Lecun, Y; Kuzniecky, R. "Classification of patterns of EEG synchronization for seizure prediction". In *Clinical Neurophysiology*, 120(11):1927-1940, 2009. https://doi.org/10.1016/j.clinph.2009.09.002

[15] Winterhalder, M; Schelter, B; Maiwald, T; Brandt, A; Schad, A; Schulze-Bonhage, A; Timmer, J. "Spatio-temporal patient-individual assessment of synchronization changes for epileptic seizure prediction". In *Clinical Neurophysiology*, 117(11):2399-2413, 2006. https://doi.org/10.1016/j.clinph.2006.07.312

[16] Bandarabadi, M; Teixeira, CA; Rasekhi, J; Dourado, A. "Epileptic seizure prediction using relative spectral power features". In *Clinical Neurophysiology*, 126(2):237-248, 2015. https://doi.org/10.1016/j.clinph.2014.05.022

[17] Runarsson, TP; Sigurdsson, S. "On-line detection of patient specific neonatal seizures using support vector machines and half-wave attribute histograms". In *International Conference on Computational Intelligence for Modelling, Control and Automation and International Conference on Intelligent Agents, Web Technologies and Internet Commerce (CIMCA-IAWTIC'06)*, 2:637-677, 2005. https://doi.org/10.1109/CIMCA.2005.1631546

[18] Rana, P; Lipor, J; Lee H; Drongelen, WV; Kohrman, MH; Veen, BV. "Seizure detection using the phase-slope index and multichannel ECoG". In *IEEE Transactions on Biomedical Engineering*, 59(4):1125-1134, 2012. https://doi.org/10.1109/tbme.2012.2184796

[19] Alam, SMS; Bhuiyan, MIH. "Detection of seizure and epilepsy using higher order statistics in the EMD domain". In *IEEE Journal of Biomedical and Health Informatics*, 17(2):312-318, 2013. https://doi.org/10.1109/jbhi.2012.2237409

[20] Beniczky, S; Conradsen, I; Pressler, R; Wolf, P. "Quantitative analysis of surface electromyography: Biomarkers for convulsive seizures". In *Clinical Neurophysiology*, 127(8):2900-2907, 2016. https://doi.org/10.1016/j.clinph.2016.04.017

[21] Mporas, I; Tsirka, V; Zacharaki, E; Koutroumanidis, M; Megalooikonomou, V. (2014). "Online Seizure Detection from EEG and ECG Signals for Monitoring of Epileptic Patients". In: Likas A., Blekas K., Kalles D. (eds) Artificial Intelligence: Methods and Applications. SETN 2014. Lecture Notes in Computer Science, vol 8445. Springer, Cham. https://doi.org/10.1007/978-3-319-07064-3_37

[22] Qaraqe, M; Ismail, M; Serpedin, E; Zulfi, H. (2016). "Epileptic seizure onset detection based on EEG and ECG data fusion". https://doi.org/10.1016/j.yebeh.2016.02.039

[23] Mporas I., Tsirka V., Zacharaki E.I., Koutroumanidis M., Megalooikonomou V. (2014) Online Seizure Detection from EEG and ECG Signals for Monitoring of Epileptic Patients. In: Likas A., Blekas K., Kalles D. (eds) Artificial Intelligence: Methods and Applications. SETN 2014. Lecture Notes in Computer Science, vol 8445. Springer, Cham. https://doi.org/10.1007/978-3-319-07064-3_37

[24] Mormann, F; Andrzejak, RG; Kreuz, T; Rieke, C; David, P; Elger, CE; Lehnertz, K. "Automated detection of a preseizure state based on a decrease in synchronization in intracranial electroencephalogram recordings from epilepsy patients". In *Phys. Rev. E*, 67(2):021912, 2003. https://doi.org/10.1103/physreve.67.021912

[25] Bou Assi, E; Sawan, M; Nguyen, DK; Rihana, S. "A hybrid mRMR-genetic based selection method for the prediction of epileptic seizures". In *2015 IEEE Biomedical Circuits and Systems Conference (BioCAS)*, pages 1-4, 2015. https://doi.org/10.1109/BioCAS.2015.7348367

[26] Acharya, UR; Molinari, F; Sree, SV; Chattopadhyay, S; Ng, KH; Suri, JS. "Automated diagnosis of epileptic EEG using entropies". In *Biomedical Signal Processing and Control*, 7(4):401-408, 2012. https://doi.org/10.1016/j.bspc.2011.07.007

[27] Teixeira, C; Direito, B; Bandarabadi, M; Dourado, A. "Output regularization of SVM seizure predictors: Kalman Filter versus the Firing Power method". In *2012 Annual International Conference of the IEEE Engineering in Medicine and Biology Society*, pages 6530-6533, 2012. https://doi.org/10.1109/embc.2012.6347490

[28] Teixeira, C; Direito, B; Bandarabadi, M; Le Van Quyen, M; Valderrama, M; Schelter, B; Schulze-Bonhage, A; Navarro, V; Sales, F; Dourado, A. "Epileptic seizure predictors based on computational intelligence techniques: A comparative study with 278 patients". In *Computer methods and programs in Biomedicine*, 114(3):324-336, 2014. https://doi.org/10.1016/j.cmpb.2014.02.007

[29] Direito, B; Ventura, F; Teixeira, C; Dourado, A. "Optimized feature subsets for epileptic seizure prediction studies". In *2011 Annual International Conference of the IEEE Engineering in Medicine and Biology Society*, pages 1636-1639, 2011. https://doi.org/10.1109/IEMBS.2011.6090472

[30] Mount Sinai, "The Epilepsy Program", accessed December 2020, https://www.mountsinai.org/care/neurology/services/epilepsy-program

[31] Flint Hills Epilepsy Database, http://www.fhs.lawrence.ks.us/PublicECoG.html

[32] Bonn University Epilepsy, accessed December 2020, http://epileptologie-bonn.de/cms/front_content.php

[33] University of Freiburg, "Seizure Prediction Project Freiburg", accessed December 2020, http://epilepsy.uni-freiburg.de/freiburg-seizure-prediction-project/eeg-database

[34] European Epilepsy Database – EPILEPSIAE, accessed December 2020, http://epilepsy-database.eu/

[35] UPenn and Mayo Clinic's Seizure Detection Challenge, accessed December 2020, https://www.kaggle.com/c/seizure-detection/data

[36] Schulze-Bonhage, A; Feldwisch-Drentrup, H; Ihle, M. "The role of high-quality EEG databases in the improvement and assessment of seizure prediction methods". In *Epilepsy & Behaviour*, 22(1):88-93, 2011 . https://doi.org/10.1016/j.yebeh.2011.08.030

[37] Klatt, J; Feldwisch-Drentrup, H; Ihle, M; Navarro, V; Neufang, M; Teixeira, C; Adam, C; Valderrama, M; Alvarado-Rojas, C; Witon, A; Le Van Quyen, M; Sales, F; Dourado, A; Timmer, J; Schulze-Bonhage, A; Schelter, B. "The EPILEPSIAE database: An extensive electroencephalography database of epilepsy patients". In *Epilepsia*, 53(9):1669-1676, 2012. https://doi.org/10.1111/j.1528-1167.2012.03564.x

[38] D'Alessandro, M; Esteller, R; Echauz, J; Vachtsevanos, G; Hinson, A; Litt, A. "Epileptic Seizure Prediction Using Hybrid Feature Selection Over Multiple Intracranial EEG Electrode Contacts: A Report of Four Patients". In *IEEE Transactions on Biomedical Engineering*, 50(5):603-615, 2003. https://doi.org/10.1109/TBME.2003.810706

[39] Schelter, B; Winterhalder, M; Maiwald, T; Brandt, A; Schad, A; Schulze-Bonhage, A; Timmer, J. "Testing statistical significance of multivariate time series analysis techniques for epileptic seizure prediction". In *Chaos: An Interdisciplinary Journal of Nonlinear Science*, 16(1):013108, 2006. https://doi.org/10.1063/1.2137623

[40] Park, Y; Luo, L; Parhi,K; Netoff, T. "Seizure prediction with spectral power of EEG using cost-sensitive support vector machines". In *Epilepsia*, 52(10):1761-1770, 2011. https://doi.org/10.1111/j.1528-1167.2011.03138.x

[41] Valderrama, M; Alvarado, C; Nikolopoulos, S; Martinerie, J; Adam, C; Navarro, V; Le Van Quyen, M. "Identifying an increased risk of epileptic seizures using a multi-feature EEG-ECG classification". In *Biomedical Signal Processing and Control*, 7(3):237-244, 2012 https://doi.org/10.1016/j.bspc.2011.05.005

[42] Moghim, N & Corne, D. "Predicting epileptic seizures in advance". In *PLOS ONE*, 9:1-17, 2014. https://doi.org/10.1371/journal.pone.0099334

[43] Direito, B; Teixeira, C; Sales, F; Castelo-Branco, M; Dourado, A. "A Realistic Seizure Prediction Study Based on Multiclass SVM". In *International Journal of Neural Systems*, 27(3):1750006, 2017. https://doi.org/10.1142/s012906571750006x

[44] McSharry, PE; Smith, LA; Tarassenko, L. "Prediction of epileptic seizures: are nonlinear methods relevant?". In *Nat Med*, 9:241-242, 2003. https://doi.org/10.1038/nm0303-241

[45] Teixeira, C; Direito, B; Feldwisch-Drentrup, H; Valderrama, M; Costa, R; Alvarado-Rojas, C; Nikolopoulos, S; Le Van Quyen, M; Timmer, J; Schelter, B; Dourado, A. "EPILAB: a software package for studies on the prediction of epileptic seizures". In *Journal of Neuroscience Methods*, 200(2):257-271, 2011. https://doi.org/10.1016/j.jneumeth.2011.07.002

[46] MATLAB, accessed August 2021, https://www.mathworks.com/products/matlab.html

[47] Aarabi, A; Fazel-Rezai, R; Aghakhani, Y. "EEG seizure prediction: measures and challenges". In *2009 Annual International Conference of the IEEE Engineering in Medicine and Biology Society*, pages 1864-1867, 2009. https://doi.org/10.1109/iembs.2009.5332620

[48] Lehnertz, K; Andrzejak, R; Arnhold, J; Kreuz, T; Mormann, F; Rieke, C; Widman, G; Elger, G. "Nonlinear EEG analysis in epilepsy: its possible use for interictal focus localization, seizure anticipation, and prevention". In *Clinical Neurophysiology*, 18(3):209-222, 2001. https://doi.org/10.1097/00004691-200105000-00002

[49] Iasemidis, LD; Sackellares, JC; Zaveri,HP; Williams, WJ. "Phase space topography and the Lyapunov exponent of electrocorticograms in partial seizures". In *Brain Topography*, 2:187-201, 1990. https://doi.org/10.1007/bf01140588

[50] Le Van Quyen, M; Martinerie, J; Baulac, M; Varela, F. "Anticipating epileptic seizures in real time by a non-linear analysis of similarity between EEG recordings". In *NeuroReport*, 10(10):2149-2155, 1999. https://doi.org/10.1097/00001756-199907130-00028

[51] Hyvärinen, A; Oja, E. "Independent component analysis: algorithms and applications". In *Neural Networks*, 13(4-5):411-430, 2000. https://doi.org/10.1016/s0893-6080(00)00026-5

[52] Gupta, D; James, CJ; Gray, WP. "Phase synchronization with ICA for epileptic seizure onset prediction in the long-term EEG". In *4th IET International Conference on Advances in Medical, Signal and Information Processing*, pages 1-4, 2008. https://doi.org/10.1049/cp:20080427

[53] Iasemidis, LD; Shiau, DS; Pardalos, PM; Chaovalitwongse, W; Narayanan, K; Prasad, A; Tsakalis, K; Carney, PR; Sackellares, JC. "Long-term prospective on-line real-time seizure prediction". In *Clinical Neurophysiology*, 116(3):532-544, 2005. https://doi.org/10.1016/j.clinph.2004.10.013

[54] Bandarabadi, M; Teixeira, C; Direito, B; Dourado, A. "Epileptic seizure prediction based on a bivariate spectral power methodology". In *2012 Annual International Conference of the*

IEEE Engineering in Medicine and Biology Society, pages 5943-5946, 2012.
https://doi.org/10.1109/embc.2012.6347347

[55] Peng, H; Fulmi, L; Ding, C. "Feature selection based on mutual information criteria of max-dependency, max-relevance, and min-redundancy". In *IEEE Transactions on Pattern Analysis and Machine Intelligence*, 27(8):1226-1238, 2005.
https://doi.org/10.1109/TPAMI.2005.159

[56] Usman, S; Latif, S; Beg, A. "Principle components analysis for seizures prediction using wavelet transform". In *International Journal of ADVANCED AND APPLIED SCIENCES*, 6:50-55, 2019. https://doi.org/10.21833/ijaas.2019.03.008

[57] Ventura A., Franco J.M., Ramos J.P., Direito B., Dourado A. (2009) Epileptic Seizure Prediction and the Dimensionality Reduction Problem. In: Alippi C., Polycarpou M., Panayiotou C., Ellinas G. (eds) Artificial Neural Networks – ICANN 2009. ICANN 2009. Lecture Notes in Computer Science, vol 5769. Springer, Berlin, Heidelberg.
https://doi.org/10.1007/978-3-642-04277-5_1

[58] Aggarwal, G; Gandhi, T. (2017). "Prediction of Epileptic Seizures based on Mean Phase Coherence". https://doi.org/10.1101/212563

[59] Khan, H; Marcuse, L; Fields, M; Swann, K; Yener, B. "Focal onset seizure prediction using convolutional networks". In *IEEE Transactions on Biomedical Engineering*, 65(9):2109-2118, 2018. https://doi.org/10.1109/TBME.2017.2785401

[60] Abdelhameed, A; Daoud, H; Bayoumi, M. "Deep convolutional bidirectional lstm recurrent neural network for epileptic seizure detection". In *2018 16th IEEE International New Circuits and Systems Conference (NEWCAS)*, pages 139-143, 2018.
https://doi.org/10.1109/NEWCAS.2018.8585542

[61] Chisci, L; Mavino, A; Perferi, G; Sciandrone, M; Anile, C; Colicchio, G; Fuggetta, F. "Real-time epileptic seizure prediction using AR models and support vector machines". In *IEEE Transactions on Biomedical Engineering*, 57(5):1124-1132, 2010.
https://doi.org/10.1109/tbme.2009.2038990

[62] Bandarabadi, M; Rasekhi, J; Teixeira, C; Karami, M; Dourado, A. "On the proper selection of preictal period for seizure prediction". In *Epilepsy & Behaviour*, 46:158-166, 2015.
https://doi.org/10.1016/j.yebeh.2015.03.010

[63] Zhou, M; Tian, C; Cao, R; Wang, B; Niu, Y; Hu, T; Guo, H; Xiang, J. "Epileptic Seizure Detection Based on EEG Signals and CNN". In *Frontiers in Neuroinformatics*, 12:95, 2018.
https://dx.doi.org/10.3389%2Ffninf.2018.00095

[64] Daoud, H; Bayoumi, M. "Efficient Epileptic Seizure Prediction Based on Deep Learning".
In *IEEE Transactions on Biomedical Circuits and Systems*, 13(5):804-813, 2019.
https://doi.org/10.1109/TBCAS.2019.2929053

[65] Wei, Z; Zou, J; Zhang, J; Xu, J. "Automatic epileptic EEG detection using convolutional neural network with improvements in time-domain". In *Biomedical Signal processing and Control*, 53:101551, 2019. https://doi.org/10.1016/j.bspc.2019.04.028

[66] Rasekhi, J; Mollaei, M; Bandarabadi, M; Teixeira, C; Dourado, A. "Epileptic Seizure Prediction based on Ratio and Differential Linear Univariate Features". In *Journal of medical signals and sensors*, 5(1):1–11, 2015. https://pubmed.ncbi.nlm.nih.gov/25709936/

[67] Gómez, C; Arbeláez, P; Navarrete, M; Alvarado-Rojas, C; Le Van Quyen, M; Valderrama, M. (2020). "Automatic seizure detection based on imaged-EEG signals through fully convolutional networks". In *Scientific Reports*, 10:21833, 2020. https://www.nature.com/articles/s41598-020-78784-3

[68] European Commision, "Evolving Platform for Improving Living Expectation of Patients Suffering from IctAI Events", accessed January 2021. https://cordis.europa.eu/project/id/211713

[69] MATLAB, "Deep Learning Toolbox", accessed August 2021, https://www.mathworks.com/products/deep-learning.html

[70] MATLAB, "Signal Processing Toolbox", accessed August 2021, https://www.mathworks.com/products/signal.html

[71] MATLAB, "Image Processing Toolbox", accessed August 2021, https://www.mathworks.com/products/image.html

[72] MATLAB, "imadjust function", accessed August 2021, https://www.mathworks.com/help/images/ref/imadjust.html?s_tid=srchtitle_imadjust_1

[73] MATLAB, "imsharpen function", accessed August 2021, https://www.mathworks.com/help/images/ref/imsharpen.html?s_tid=doc_ta

[74] MATLAB, "imdilate function", accessed August 2021, https://www.mathworks.com/help/images/ref/imdilate.html?s_tid=doc_ta

[75] van den Boomgard, R, and R. van Balen, "Methods for Fast Morphological Image Transforms Using Bitmapped Binary Images," Computer Vision, Graphics, and Image Processing: Graphical Models and Image Processing, Vol. 54, Number 3, pp. 252-258, May 1992. https://doi.org/10.1016/1049-9652(92)90055-3

[76] MATLAB, "strel function", accessed August 2021, https://www.mathworks.com/help/images/ref/strel.html?s_tid=doc_ta

[77] Adams, R., "Radial Decomposition of Discs and Spheres," Computer Vision, Graphics, and Image Processing: Graphical Models and Image Processing, Vol. 55, Number 5, pp. 325–332, September 1993. https://doi.org/10.1006/cgip.1993.1024

[78] MATLAB, "imreconstruct function", accessed August 2021, https://www.mathworks.com/help/images/ref/imreconstruct.html?s_tid=doc_ta

[79] Vincent, L., "Morphological Grayscale Reconstruction in Image Analysis: Applications and Efficient Algorithms," IEEE Transactions on Image Processing, Vol. 2, No. 2, April, 1993, pp. 176-201. https://doi.org/10.1109/83.217222

[80] MATLAB, "imcomplement function", accessed August 2021, https://www.mathworks.com/help/images/ref/imcomplement.html?s_tid=doc_ta

[81] Krizhevsky, A; Sutskever, I; Geoffrey E. Hinton. "ImageNet classification with deep convolutional neural networks". In Communications of the ACM, 60(6):84-90, June 2017. https://doi.org/10.1145/3065386

[82] MATLAB, "alexnet", accessed August 2021, https://www.mathworks.com/help/deeplearning/ref/alexnet.html

[83] Schelter, B; Andrzejak, R; Mormann, F. "Can Your Prediction Algorithm Beat a Random Predictor?" In Seizure Prediction in Epilepsy (eds B. Schelter, J. Timmer and A. Schulze-Bonhage) ch. 18, 2008. https://doi.org/10.1002/9783527625192.ch18

[84] Matlab, "Create Simple Deep Learning Network for Classification", accessed Augutst 2021, https://www.mathworks.com/help/deeplearning/ug/create-simple-deep-learning-network-for-classification.html

[85] Oostenveld R.; Praamstra P. "The five percent electrode system for high-resolution EEG and ERP measurements", In Clinical Neurophysiology, Volume 112, Issue 4, 2001, Pages 713-719, ISSN 1388-2457. https://doi.org/10.1016/S1388-2457(00)00527-7

[86] Russakovsky, O.; Deng, J.; Su, H.; et al. "ImageNet Large Scale Visual Recognition Challenge." In International Journal of Computer Vision (IJCV). Vol 115, Issue 3, 2015, pp. 211–252. https://doi.org/10.1007/s11263-015-0816-y

[87] Szegedy C.; Liu W.; Jia Y.; Sermanet P.; Reed S.; Anguelov D.; Erhan D.; Vanhoucke V.; Rabinovich A. "Going deeper with convolutions," In 2015 IEEE Conference on Computer Vision and Pattern Recognition (CVPR), 2015, pp. 1-9, https://doi.org/10.1109/CVPR.2015.7298594

[88] He K.; Zhang X.; Ren S.; Sun J. "Deep Residual Learning for Image Recognition," In 2016 IEEE Conference on Computer Vision and Pattern Recognition (CVPR), 2016, pp. 770-778. https://doi.org/10.1109/CVPR.2016.90

[89] Alhussein M.; Muhammad G. "Automatic Voice Pathology Monitoring Using Parallel Deep Models for Smart Healthcare" In IEEE Access, vol. 7, pp. 46474-46479, 2019. https://doi.org/10.1109/ACCESS.2019.2905597

[90] Lu ,D.; Weng ,Q. "A survey of image classification methods and techniques for improving classification performance", In International Journal of Remote Sensing, 2007, 28:5, 823-870. https://doi.org/10.1080/01431160600746456

[91] Valueva, M.V.; Nagornov, N.N.; Lyakhov, P.A.; Valuev, G.V.; Chervyakov, N.I. "Application of the residue number system to reduce hardware costs of the convolutional neural network implementation", In Mathematics and Computers in Simulation, Volume 177, 232-243. 2020. https://doi.org/10.1016/j.matcom.2020.04.031

[92] Collobert R.; Weston, J. "A unified architecture for natural language processing: deep neural networks with multitask learning." In Proceedings of the 25th international conference on Machine learning (ICML '08). Association for Computing Machinery, New York, NY, USA, 160–167. 2008. https://doi.org/10.1145/1390156.1390177

[93] Tsantekidis, A.; Passalis, N.; Tefas, A.; Kanniainen, J.; Gabbouj, M.; Iosifidis, A. "Forecasting Stock Prices from the Limit Order Book Using Convolutional Neural Networks," In 2017 IEEE 19th Conference on Business Informatics (CBI), pp. 7-12. 2017. https://doi.org/10.1109/CBI.2017.23

[94] Saha, S. "A Comprehensive Guide to Convolutional Neural Networks — the ELI5 way" In Towards Data Science. 2018. Accessed in August 2021. https://towardsdatascience.com/a-comprehensive-guide-to-convolutional-neural-networks-the-eli5-way-3bd2b1164a53

[95] Sentz, K.; FERSON, S. "Combination of Evidence in Dempster-Shafer Theory". United States. 2002. https://doi.org/10.2172/800792

[96] Joe Hicklin, "Deep Learning with MATLAB: Transfer Learning in 10 Lines of MATLAB Code", MATLAB. 2017. Accessed March 2021. https://www.mathworks.com/videos/deep-learning-with-matlab-transfer-learning-in-10-lines-of-matlab-code-1487714838381.html